

Multicomponent Reactions and Photo/Electrochemistry Join Forces: Atom Economy Meets Energy Efficiency

Guglielmo A. Coppola ^{#a}, Serena Pillitteri ^{#a}, Erik V. Van der Eycken ^{*a,b}, Shu- Li You ^{*c}, Upendra K. Sharma ^{*a}

^a*Laboratory for Organic & Microwave-Assisted Chemistry (LOMAC), Department of Chemistry, University of Leuven (KU Leuven), Celestijnenlaan 200F, B-3001, Leuven, Belgium.*

^b*Peoples' Friendship University of Russia (RUDN University), 6 Miklukho-Maklaya Street, Moscow 117198, Russia.*

^c*State Key Laboratory of Organometallic Chemistry, Shanghai Institute of Organic Chemistry, Chinese Academy of Sciences, 345 Lingling Lu, Shanghai 200032, China.*

GAC and SP contributed equally and share first authorship.

erik.vandereycken@kuleuven.be, slyou@sioc.ac.cn, upendrakumar.sharma@kuleuven.be

Abstract: Visible-light photoredox catalysis has been regarded as an extremely powerful tool in organic chemistry, bringing the spotlight back to radical processes. The versatility of photocatalyzed reactions has already been demonstrated to be effective in providing alternative routes for cross-coupling as well as multicomponent reactions. The photocatalyst allows the generation of high-energy intermediates through light irradiation rather than using highly reactive reagents or harsh reaction conditions. In a similar vein, organic electrochemistry has experienced a fruitful renaissance as a tool for generating reactive intermediates without the need for any catalyst. Such milder approaches pose the basis towards higher selectivity and broader applicability. In photocatalyzed and electrochemical multicomponent reactions the generation of the radical species acts as a kickstart of the cascade of events. This allows for diverse reactivity and the use of reagents usually not covered by classical methods. Owing to the availability of cheaper and more standardized photo- and electrochemical reactors, as well as easily scalable flow-setups, it is not surprising that these two fields have become the area of increased research interest. Keeping these in view, this review is aimed to provide an overview of the synthetic approaches in the design of MCRs involving photoredox catalysis and/or electrochemical activation as a crucial step with a particular focus on the choice of difunctionalized reagent.

Table of Contents

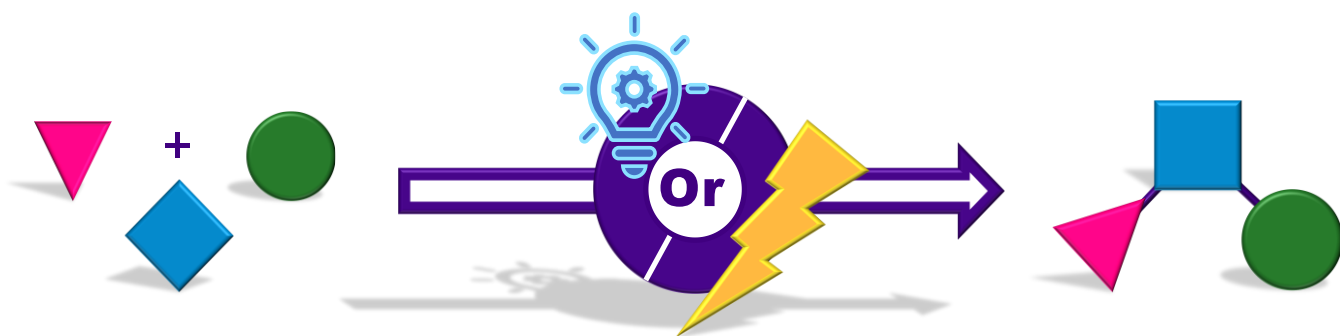
| | |
|--|----|
| 1. Introduction | 3 |
| 1.1 Photoredox catalysis | 5 |
| 1.2 Electrocatalysis | 7 |
| 2. Unsaturated bonds difunctionalization | 8 |
| 2.1. Alkenes | 8 |
| 2.1.1. Styrenes | 8 |
| 2.1.2. Activated and unactivated alkenes | 32 |
| 2.2. Alkynes | 39 |
| 2.3. Carbonyl compounds | 48 |
| 2.3.1. Functionalization of the carbonyl group | 48 |
| 2.3.2. α -Functionalization of <i>in situ</i> formed imines | 50 |
| 2.3.2.2. Generation of α -amino radicals from imines | 54 |
| 3. Carbonylation | 57 |
| 4. Sulfur dioxide insertion | 62 |
| 4.1. Aryldiazonium salts | 63 |
| 4.2. Trifluoroborates | 66 |
| 4.3. Hantzsch esters | 67 |
| 4.4. Diaryl iodonium salts and alkyl iodides | 68 |
| 4.5. <i>O</i> -Acyl oximes | 69 |
| 4.6. Miscellaneous | 70 |
| 4.7. SO ₂ fixation through electrochemical methods | 72 |
| 5. Installation of bicyclo[1.1.1]pentane (BCP) | 72 |
| 6. Conclusions | 74 |
| 7. Author contributions | 74 |
| 8. Conflicts of interest | 75 |
| 9. Acknowledgements | 75 |
| 10. References | 75 |

1. Introduction

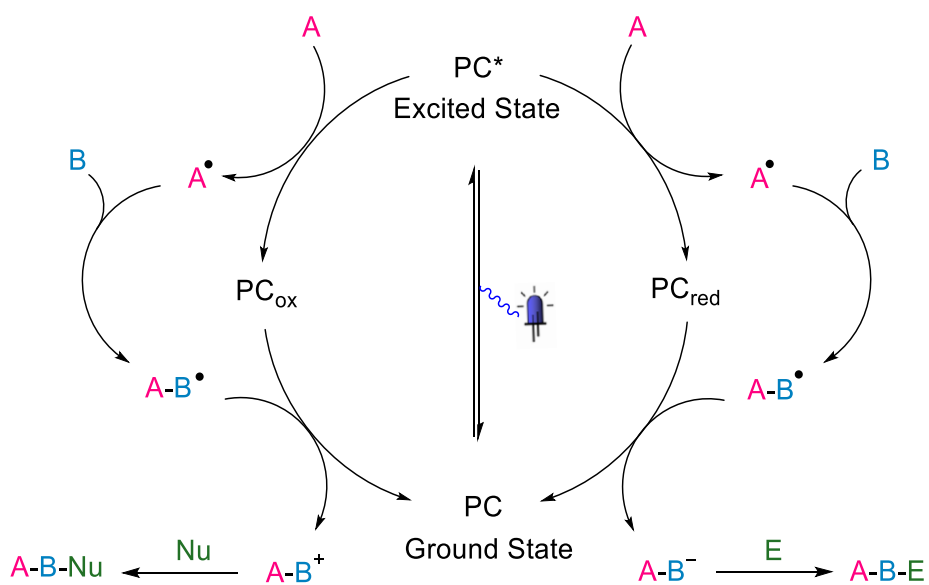
Sustainability has become the key objective to address the environmental issues that involve the whole society. Chemists have embraced this cause providing guidelines that gave rise to the era of Green Chemistry.¹ Ever since the twelve principles of Green Chemistry were enunciated,^{2,3} chemists answered the call to play their part in generating more sustainable syntheses. Analyzing the efficiency of a chemical process, one of the first values that come to mind is the E-factor, defined as the ratio between the mass of side products over the desired ones.⁴

In addition, to match the ever-evolving structural complexity of nature's toolbox, chemists need to bet on modern synthetic platforms to produce compounds that mimic the complexity of such bioactive natural-products with minimum effort and high efficiency. Multicomponent reactions (MCRs) therefore appear as an excellent solution.⁵⁻⁹ MCRs involve more than two components in a one-pot reaction and incorporate most or all the atoms of the reactants in the final product, therefore becoming a perfect example of the atom and step economy.⁴ Moreover, a vast literature has been produced showing the power of MCRs as well as post-MCR modifications, in simplifying the synthetic design and yet obtaining high complexity and diversity in the construction of privileged structures. From a medicinal chemistry point of view, the exploration of the chemical space is fundamental to explore novel binding modes in different biological targets. In this context, MCRs provide the tools to generate chemical diversity and to functionalize complex molecular scaffolds.^{5,10}

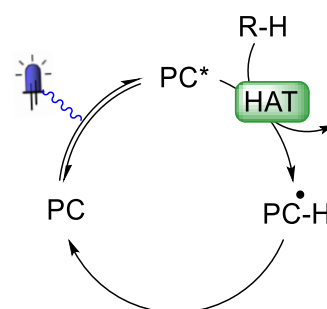
Great effort has been devoted in the design of MCRs based on cascade reactions involving two-electron interactions between electrophiles and nucleophiles. Notable chemists owned everlasting fame exploring this novel reactivity concept: Strecker, Ugi, Passerini, to name a few.¹¹⁻¹⁵ Recently, the broader applicability of MCRs has surfaced with the renaissance of radical chemistry. In this regard, both photoredox catalysis and electrochemistry provided a substantial breakthrough and have inspired chemists to explore novel pathways and expand the chemical space exploiting reactivity patterns that have previously been elusive. The key feature of photo- and electrochemistry is the use of photons and electrons, respectively, as traceless reagents. Both techniques share the ability to generate highly reactive intermediates with great selectivity and efficiency while employing low-hazard chemicals and mild reaction conditions. Furthermore, these synthetic tools are getting more accessible since cost-effective light sources with narrow and precise wavelengths as well as more standardized electrochemical set-ups are now available. Finally, the use of visible light and electrons to kickstart cascade reactions, especially in the frame of MCRs, fits perfectly in the aforementioned green chemistry principles, increasing the efficiency of the energy input.¹⁶



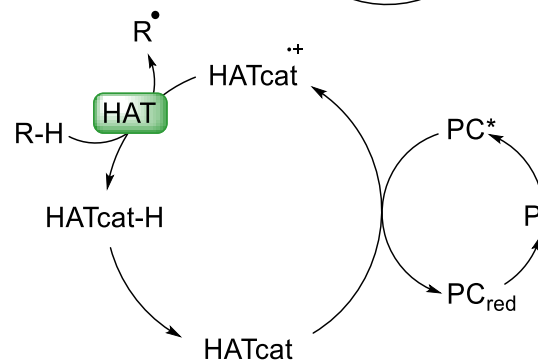
II Oxidative and reductive quenching pathways



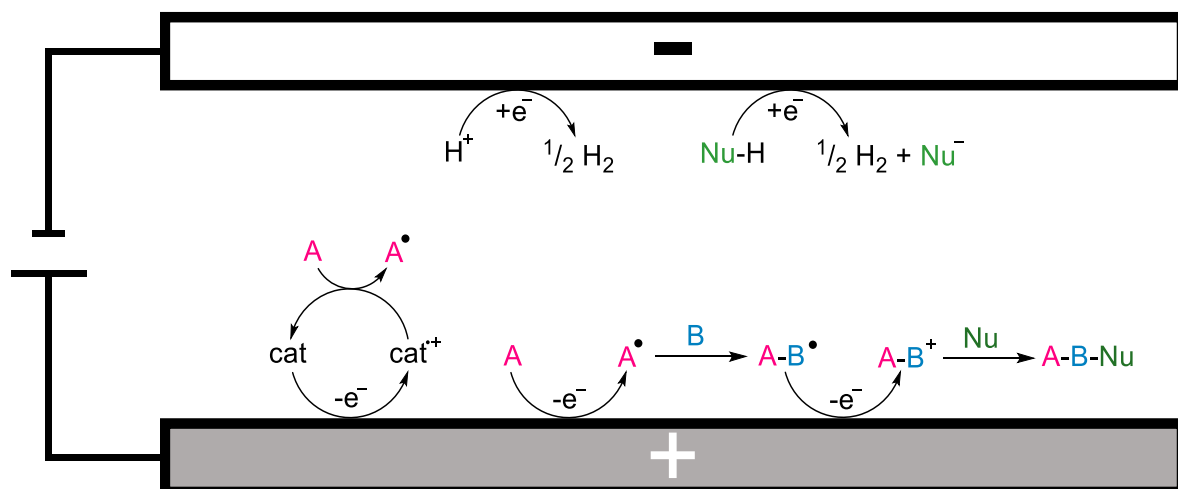
Direct HAT



Indirect HAT



IV Anodic oxidative activation/coupling sequence



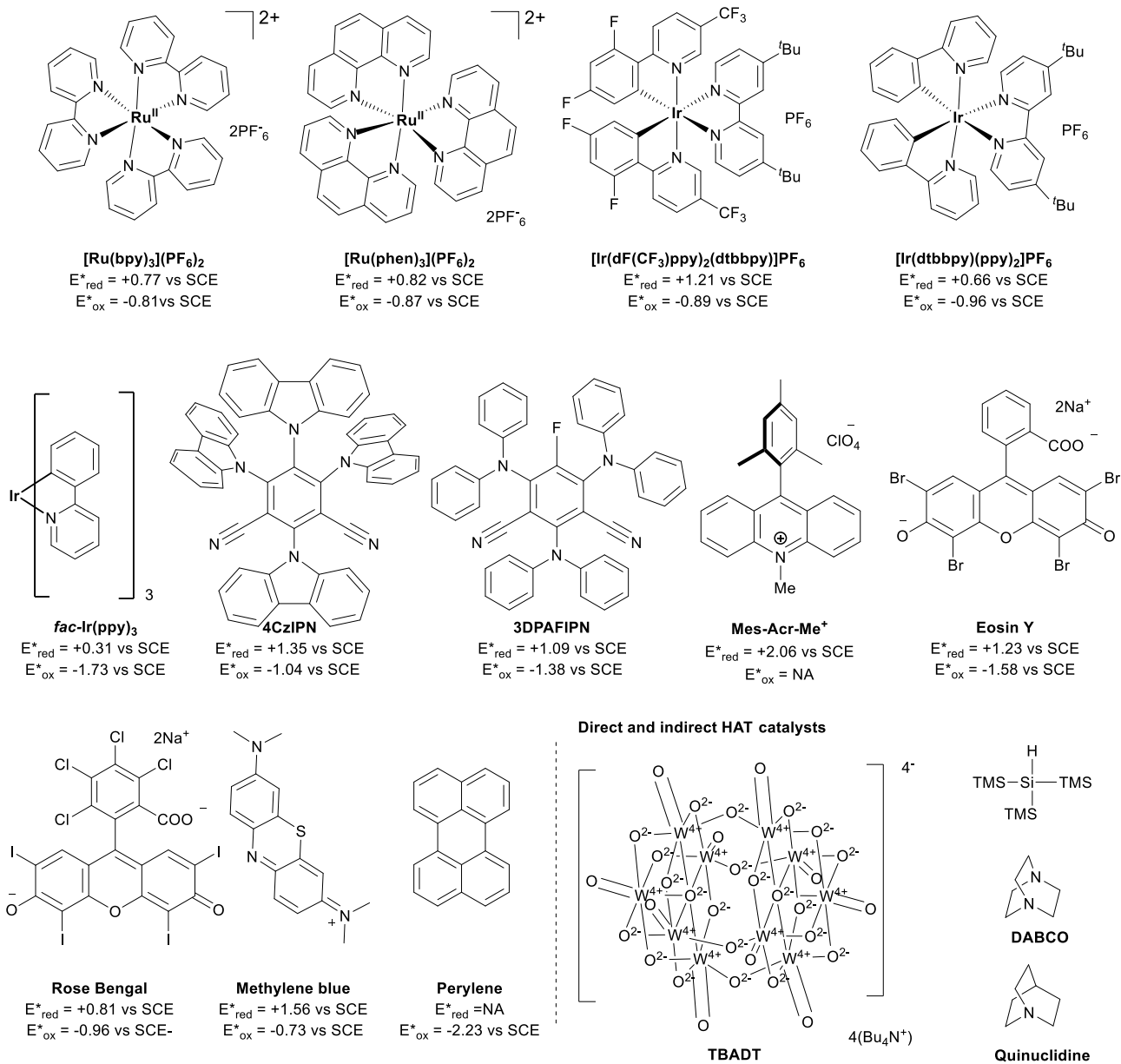
Scheme 1. Commonly reported reaction mechanisms.

1.1 Photoredox catalysis

For the sake of clarity, we will summarise here the main mechanistic scenarios involved in the transformations included in this review, providing insights to help the reader navigate through the examples discussed in the following sections.

In the realm of photoredox catalyzed reactions, the excitation of a photocatalyst is the key step that enables the catalytic cycle to start. In the past decade, the number of photoredox catalysts has increased exponentially, as a result of the need for a wide window of redox potentials useful to obtain selective radical generation. Besides Ir and Ru-based polypyridine complexes, many organic dyes have been introduced as well, as a result of increased sustainability, cost efficiency and availability of starting materials. The fine-tuning of the electronic properties of ligands and functionalities on the catalyst core allowed the synthesis and characterization of many photoredox catalysts. In Figure 1, a selection of photocatalysts is presented, taking into account the frequency of utilization in the works included in this review.^{17,18}

Commonly employed photocatalysts



Commonly employed electrodes materials

| | |
|--|--|
| <p>Graphite OER = 0.50 HER = -0.47 $\eta = 0.0003$</p> <p>RVC HER = -1.13 $\eta = 0.02-0.10$</p> <p>BDD OER = 1-2 HER = -1.5 $\eta = 0,000001-0,002$</p> | <p>Pt OER = 1.11 HER = -0.27 $\eta = 10.42$</p> <p>Fe OER = 0.41 HER = -0.40 $\eta = 11.67$</p> <p>Ni OER = 0.61 HER = -0.32 $\eta = 16.23$</p> |
|--|--|

Commonly employed electrolytes:

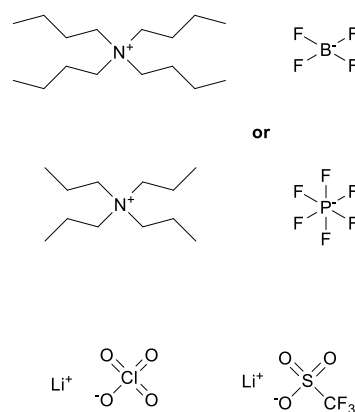


Figure 1. Selection of photocatalysts, electrodes and electrolytes.

Mechanistically, most of the examples here presented comprise single electron transfer (SET) processes, which involve the excitation of the photocatalyst by visible light, then followed by the single-electron oxidation or single electron reduction of the radical source. The radical intermediate thus generated is then often involved in an addition reaction on unsaturated bonds (namely alkenes, alkynes, imines, etc.), leading to the formation of a radical intermediate. At this stage, different scenarios can be devised, as shown in Scheme 1 (II, III):¹⁷

1. In a redox-neutral mechanism, a second single-electron oxidation/reduction of the radical intermediate generates a formal positive/negative charge, that leaves the scene open for further functionalization by reaction with nucleophiles/electrophiles.
2. Alternatively, a second radical generation step is responsible for the catalyst regeneration, and a radical coupling between radical intermediates can occur, supposing that a longer-lived radical and a transient radical are formed at similar rates.¹⁹
3. The involvement of a metal catalyst to afford cross-coupling products also accounts for a consistent number of reports.

In addition to these strategies, hydrogen atom transfer (HAT) also represents a convenient approach to access radical formation from strong aliphatic C-C bonds. In this case, two mechanistic scenarios can be involved, where the hydrogen abstraction is operated by a direct HAT catalyst (such as tetra-n-butylammonium decatungstate, TBADT) or where the hydrogen abstraction is mediated by an indirect HAT catalyst in combination with a photocatalyst (quinuclidine as an example). In both cases, the bond dissociation energy (BDE), and not the redox potential, must be taken into account.²⁰

Less represented in this review are the Proton Coupled Electron Transfer (PCET) and the Energy Transfer (ET) mechanisms. In the first case, the co-presence of a photocatalyst and a proton acceptor/donor enables the formal transfer of a hydrogen atom, but in a non-concerted process. The latter, on the other hand, involves the excitation of a substrate through the mediation of the photocatalyst, without electron transfers.

1.2 Electrocatalysis

In electrocatalytic processes, the application of electric potential at the electrodes triggers SET events with the substrates in solutions. Oxidation (reduction) of the substrate will occur at the anode (cathode) when the Fermi level of the electrode will lay at lower (higher) energy than the HOMO (LUMO) of the substrate. A clear parallel can be drawn with the interactions between the photocatalyst's excited state and the reagents. Nonetheless, the possibility for a continuous increment of the electrode's potential appears already as an obvious advantage over photocatalyzed processes, as this allows to match the redox potential of the substrates leading to high selectivity. Conversely in photocatalysis, the availability of a finite number of photocatalysts only allows for a discrete potential increment which can result in undesired interactions with other chemical species in solution.

Moreover, the window of achievable redox potentials is wider in both oxidation and reduction direction and its limitation mainly depends on the choice of solvent and electrolytes.

Operatively two main approaches are possible while conducting electrolysis, as explained in Scheme 1 (IV):

- Constant current, where the potential is allowed to vary and will adjust to let current flow in the solution by generating redox events at both electrodes.
- Constant potential, where the potential is kept stable with the aid of a reference electrode.

In galvanostatic conditions (constant current) the first substrates to be oxidized or reduced are the ones with the least positive or least negative potential respectively. As these substrates react, and therefore their concentration lowers, the potential will adjust in order to oxidize or reduce the next reagent in order of potential. Potentiostatic conditions avoid side reactions to occur since the potential is always kept at the optimal value for the desired substrate to react selectively. Nonetheless, the literature review clearly shows a generalized preference for constant current electrolysis and, as a matter of fact, in the preparation of this manuscript only a few cases of a reaction run at constant potential have been screened. This trend is mainly due to easier setup and tolerance to possible side reactions.

Constant potential electrolysis is inherently a less practical approach as the redox potential of the reagents must be known and the need for a reference electrode comes with some more technical challenges. Finally, the reaction times are longer in potentiostatic electrolysis compared to constant current.

Electrocatalytic reactions can involve several electron transfer events, leading to the activation of the substrates or quenching of radical intermediates. In the frame of electro catalyzed MCRs, sequential anodic oxidations alternated with chemical reactions represent the most common manifold.

This approach has the advantage to rely on rapid quenching of the open-shell reactive intermediates as the reaction occurs near the electrode surface where the radicals are generated. The occurrence of different mechanisms, as paired electrolysis, will be pointed out during the discussion.

Shifting our focus on the reactions occurring at the cathode there are several ways to close the flow of electrons in the system. Sacrificial reduction of protons to hydrogen is the most common mechanism. In some cases, the reaction involves protic solvents or

other nucleophiles which get activated by deprotonation. The newly formed anions can trap cationic species generated by anodic oxidation. The cathodic reduction has also been exploited in the activation of oxygen and SO₂ to the respective radical anions and in the formation of Se radicals from diselenides.

Finally, we cannot conclude this brief introduction without mentioning the importance of electrode materials and electrolytes as they can greatly affect reaction yields and selectivity. In Figure 1 we report the most common electrodes as well as a list of commonly used electrolytes. Carbon-based anodes as graphite rods, graphite felt and RVC (reticulated vitreous carbon) are the most widely represented. The use of platinum and magnesium has also been reported. On the other hand, platinum is usually the metal of choice for the cathode, as it shows good stability and a lower risk of passivation. Stainless steel can be employed as a cheaper solution as well as carbon electrodes. Regardless of the choice of electrodes, the addition of supporting electrolytes is in most cases necessary to ensure a sufficient conductivity of the reaction medium. The solvent used will be a crucial discriminant as the salt requires high solubility and dissociation to work properly. In addition, upon application of potential, positive and negative ions will be attracted towards the surface of the cathode and anode respectively. The accumulation of charges will in turn attract counter ions leading to the formation of a double layer in close proximity with the electrode surface. The nature of the double layer will influence the interaction between substrates or intermediates with the electrode and therefore the reaction outcomes.

In the attempt to find a *fil rouge* throughout the several publications we collected, we decided to classify the reactions on the basis of the functional group that, engaging the multicomponent reaction, is difunctionalized. Such a classification will help to spot uncovered fields as well as provide a comprehensive overview in terms of possible coupling partners, catalysts, and reaction conditions. Photocatalyzed and electrochemical examples will be discussed pairwise to allow a straightforward comparison between the two approaches. This review is therefore not only meant to summarize the achievements on the topic but mainly to underline the potential of its synthetic applications attracting greater attention and providing useful guidelines to researchers in the field. Photoinduced processes as well as the use of radical initiators will not be included in this review.

To date, the only review on visible-light promoted multicomponent reactions *sensu stricto* has been compiled in 2016 by Basso and co-workers²¹. Their excellent work contributed greatly to define this research area; still, no similar reviews have followed. As a matter of fact, although visible-light catalyzed difunctionalizations have been already partially covered by other reviews in the past years, they were focused solely on one class of compounds, often including other radicals. Moreover, in many cases, there is no clear distinction between multicomponent reactions and other difunctionalizations (functional groups migration, intramolecular reactions, two components reactions). A selection of reports will be therefore presented to avoid unnecessary overlap with previous works.

2. Unsaturated bonds difunctionalization

Unsaturated bonds have been extensively used in classical MCRs exploiting the change in hybridization to make orbitals and electron pairs available for the formation of new bonds with multiple functional groups. The multicomponent reaction will follow a cascade functionalization through sequential activation and coupling events resulting in the selective installation of new functional groups. Moreover, the concomitant increase in saturation allows the exploration of the surrounding tridimensional space with strong implications concerning chemical properties and bioactivity profile.^{22–24} Nonetheless, mild reaction conditions associated with highly specific reactivity manifolds can become crucial for the success of these transformations. This chapter will provide an overview of the photocatalyzed and electrochemical synthetic strategies involving unsaturated bonds disentangling the topic *via* dedicated sections and subsections.

2.1. Alkenes

Alkenes are undoubtedly the most represented compounds among unsaturated functionalities in the frame of photo-electro-difunctionalization. Several strategies have been undertaken providing a wide range of possible coupling partners, catalysts and reaction conditions.²⁵ Therefore, we will dedicate more space to this section being, in our opinion, the ideal substrate for the description of the heterogeneity in the field of photo- and electrocatalytic MCRs. Moreover, further classification has been made grouping the reactions according to the radical entity which attacks first the unsaturated bond.

2.1.1. Styrenes

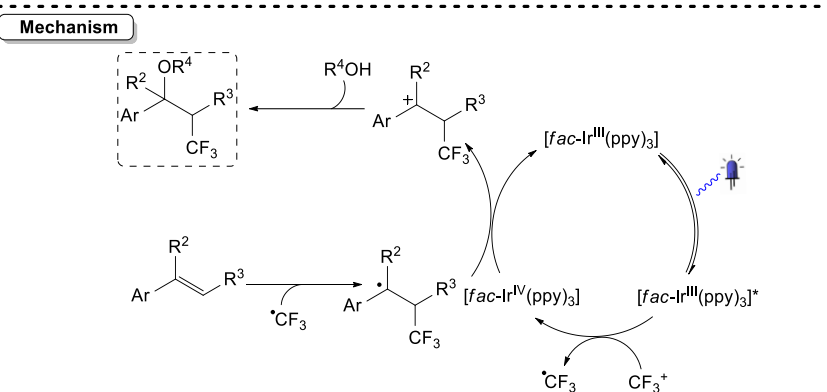
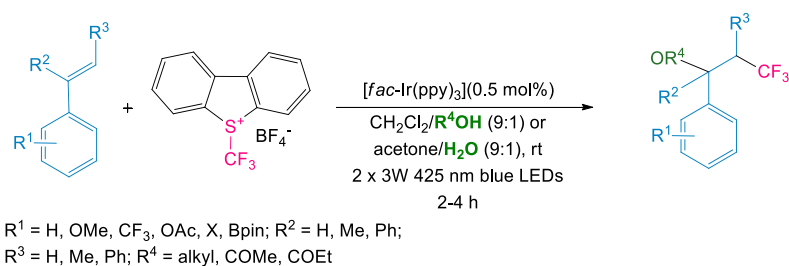
Vinyl arenes have proven to be particularly suitable for visible-light photocatalyzed and electro catalyzed MCRs and styrene has become a common benchmark to test the reactivity of alternative coupling partners as well as the feasibility of novel reaction pathways. As a result, vast literature is available on styrenes difunctionalization and they have been described reacting *via* each of the mechanisms we summarized in the previous chapter. More space will be therefore dedicated in this first chapter to allow the exhaustive description of the several combinations of activation mechanisms and coupling reagents.

2.1.1.1. Oxidative pathway

Transformations involving catalyst oxidative quenching or anodic oxidation for radical precursor activation and formation of the vinyl cation followed by a nucleophilic attack, are by far the most represented. Outstanding results have been obtained exploring various combinations of radical precursors and nucleophiles. The following subsections will orderly enumerate the numerous reports grouping them according to the radical source.

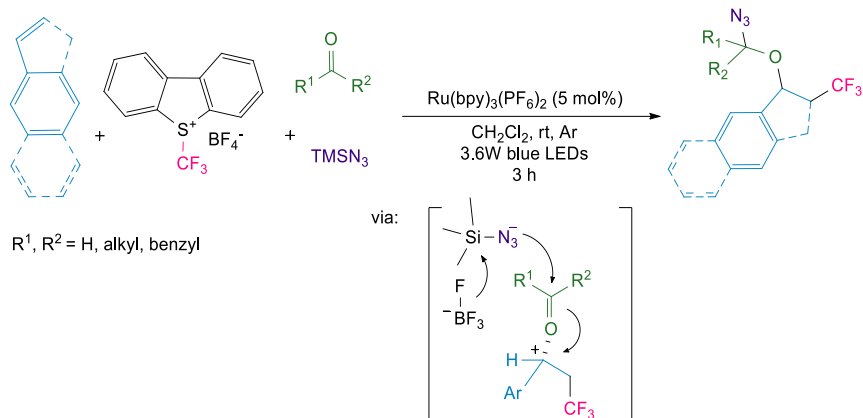
2.1.1.1.1. Fluoroalkyl radicals

The introduction of fluorinated functionalities has been widely explored for the strategical modulation of drug pharmacokinetics and pharmacodynamics properties. Fluorine combines higher electronegativity and lipophilicity than hydrogen with a relatively small Van der Waals radius²⁶ and this allows for significant changes in physicochemical properties without perturbing the interaction with the active site severely. In the frame of radical MCRs, trifluoromethylation and difluoroalkylation played a primary role in the hetero-difunctionalization of unsaturated C-C bonds, especially vinyl arenes. Based on the seminal work from MacMillan^{27,28} on the addition to unsaturated systems of CF₃ radicals, formed *via* electrophilic CF₃ sources, Akita's group kickstarted the fruitful investigation of styrene difunctionalization through photocatalyzed multicomponent processes. One of these early examples is the reaction reported in 2012 by Yasu *et al.* where the photocatalytic generation of CF₃ radical was applied in the three-component oxytrifluoromethylation of styrenes.²⁹ The choice of a trifluoromethyl radical source landed over Umemoto reagent and they employed [fac-Ir(ppy)₃] as photocatalyst. Nonetheless, [Ru(bpy)₃](PF₆)₂ could also deliver the desired product in similar yields. As depicted in Scheme 1 the iridium photocatalyst is excited upon irradiation with visible light. [fac-Ir^{III}(ppy)₃]* undergoes oxidative quenching *via* SET with CF₃⁺ to form CF₃ radical. Subsequent addition of ·CF₃ to the allyl position generates a benzyl radical intermediate readily oxidized to cation by the reduced photocatalyst [fac-Ir^{IV}(ppy)₃]. Finally, nucleophilic attack from the alcohol on the carbocation gives the desired three-component product. The authors have investigated the use of both water and alcohols as nucleophiles obtaining hydroxylated and alkoxyated products in good to excellent yields and with good tolerance towards functional groups. However, the presence of strongly electron-withdrawing substituents as CF₃ on the phenyl ring caused a drop in yield (Scheme 2).



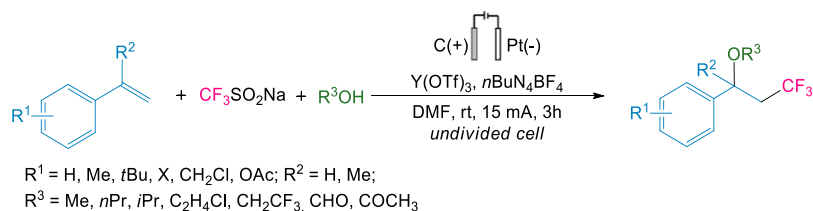
Scheme 2. Photoredox catalyzed oxytrifluoromethylation of styrenes.

Similar reaction conditions have been recently adopted by Levitre *et al.* in the elegant design of a four-component reaction.³⁰ In this case, the alcoholate involved in the final nucleophilic attack is formed *in situ*, from the reaction between TMSN₃ and a carbonyl compound (Scheme 3).



Scheme 3: 4-Component alkoxy trifluoromethylation of styrenes.

Trifluoromethyl alkoxylation of styrenes proved to be effective also in electrochemical conditions as reported by Zhang *et al.* in 2018. Langlois' reagent was employed to generate trifluoromethyl radicals by anodic oxidation. Then the reaction follows the same steps described in Scheme 2 with the exception that the vinyl cation is obtained by anodic oxidation of the corresponding radical while the alcohol is reduced at the cathode with the evolution of hydrogen gas. Optimal reaction conditions were found applying a constant current of 15 mA with C (+)|Pt(-) electrodes and $n\text{Bu}_4\text{NBF}_4$ as electrolyte. $\text{Y}(\text{OTf})_3$ was added to act as Lewis acid coordinating the double bond adjuvating the radical addition (Scheme 4).³¹ A library could be obtained employing methanol as solvent and nucleophile. Moreover, other alcohols were amenable to this reaction and also formic acid and acetic acid successfully trapped the cationic intermediate.

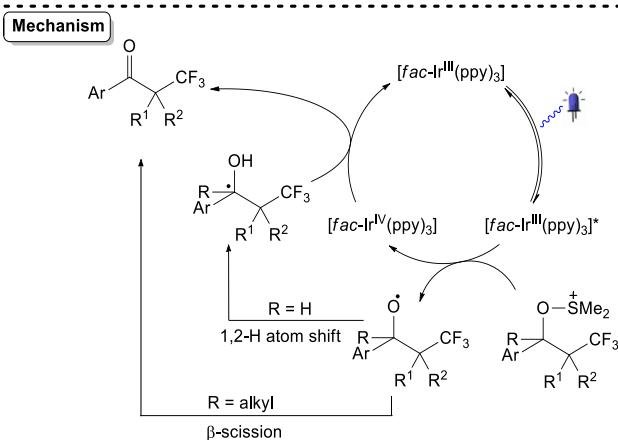
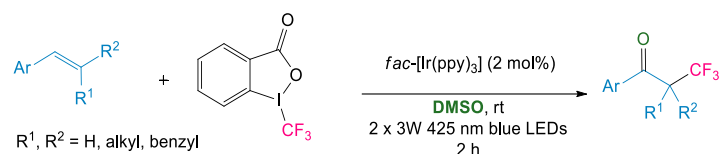


Scheme 4: Electrocatalytic trifluoromethyl alkoxylation of styrenes.

In 2018 Jud *et al.* obtained trifluoromethyl benzyl alcohols applying similar electrocatalytic conditions in the presence of water. To this goal, a series of organic solvent/water mixtures was tested. THF/water and acetone/water gave the best results delivering the desired products in moderate to excellent yields. Graphite and stainless-steel electrodes gave the best results employing $n\text{Bu}_4\text{NBF}_4$ or Et_4NBF_4 as electrolytes. As expected, when alcohol/water mixtures were employed a mixture of alkoxy and hydroxyl derivatives were obtained with the benzyl ether as the major product. Interestingly, the ratio between the two products lowered at the increase of the alcohol chain length (for MeOH 10:1, EtOH 7:1, *i*PrOH 3:1) probably as a consequence of a decrease in nucleophilicity.³² Later Huang *et al.* expanded the scope to the preparation of trifluoromethylated acetamides choosing acetonitrile as a solvent and nucleophile.³³

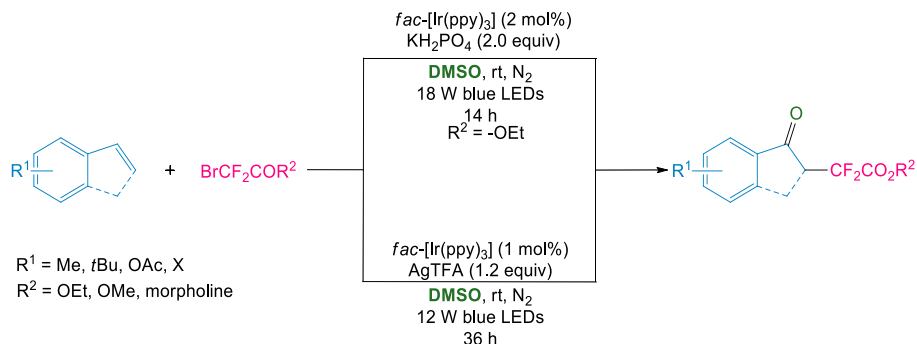
As we have described above, the exploitation of a photocatalyst oxidative quenching for the generation of radical species results in the formation of fairly reactive and versatile carbocation species, by oxidation of the radical intermediate, as the photocatalyst closes the catalytic cycle. In the context of styrene functionalization, this allowed for fast production of numerous publications focused on the expansion of the scope of both nucleophiles and radical sources.

In 2014, Tomita *et al.* employed DMSO as an oxygen source toward the preparation of trifluoromethylated ketones providing a novel example of Kornblum-type oxidation.³⁴ Upon the formation of the benzyl cation, DMSO acts as a nucleophile with the formation of a C-O bond. Base promoted abstraction of the α -H of the newly formed adduct and consequent cleavage of the S-O bond gives the final product. Notably, the authors proved that the use of a strongly reducing iridium catalyst allowed for reductive cleavage of the alkoxy-sulfonium intermediate and consequent oxidation to ketone either *via* 1,2-H atom shift/oxidation sequence or *via* direct β -scission without the addition of base. The latter hypothesis is supported by the reaction of α -alkyl styrene which could be transformed in the corresponding ketone through loss of an alkyl substituent (Scheme 5). The reaction tolerated a variety of substituents providing the products with moderate to good yields. Styrenes bearing electron-withdrawing substituents showed lower yields due to the formation of β -trifluoromethylstyrene derivatives as side products. A similar reaction was also reported by Li *et al.* employing electron-rich styrenes.³⁵



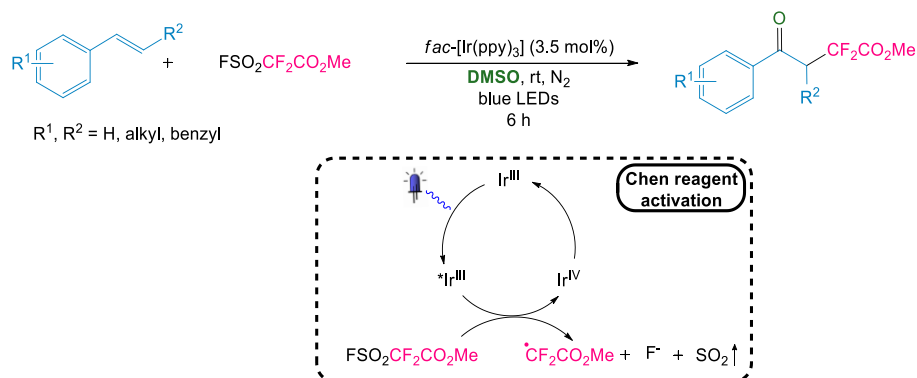
Scheme 5: Photocatalyzed synthesis of trifluoroketones *via* Kornblum-type oxidation.

On the wave of Akita's work, other examples of photocatalyzed fluoroalkylation processes have been reported involving the use of DMSO as an oxidant. In 2019, the independent works from Xia *et al.* and Li *et al.* showed the use of bromodifluoro esters as radical source^{36,37}. The α -Br- F_2 -ester undergoes SET with the photocatalyst's excited state and consequent homolytic cleavage of the C-Br bond to give the difluoroalkyl radical. Notably, in the latter report, the addition of a silver salt was found necessary for the reaction to proceed. In both cases, fragmentation of the alkoxy-sulfonium intermediate is adjudicated by the presence of a base, as for the classical Kornblum oxidation (Scheme 6).



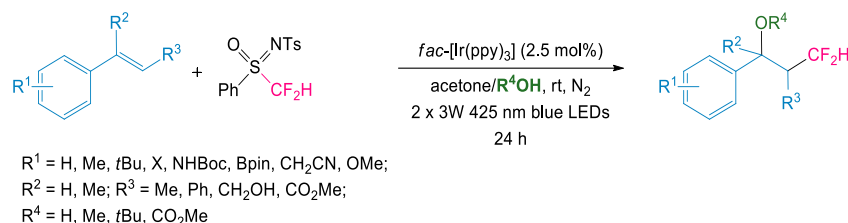
Scheme 6: Photoredox catalyzed oxydifluoroalkylation of styrenes.

The same year Luo *et al.* extended the scope of radical sources to $FSO_2CF_2CO_2Me$ (Chen reagent) and obtained the desired γ -ketoesters without the need of any additive or base, thus confirming again the reducing ability of $[fac\text{-}Ir^{III}(ppy)_3]^*$ (Scheme 7).³⁸



Scheme 7: Photoredox catalyzed preparation of γ -ketoesters.

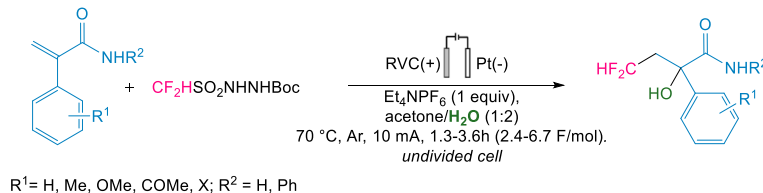
In 2016, Arai *et al.* reported the synthesis of CF₂H-containing alcohols *via* unprecedented use of *N*-tosyl-*S*-difluoromethyl-*S*-phenylsulfoximine (Hu's reagent) in photocatalytic conditions in the presence of water. This was the first example of photocatalyzed difluoromethylation of styrene.³⁹ The reaction demonstrated to be strongly influenced by both the photocatalyst and the source of the CF₂H radical and the product could be obtained in good yield only employing *fac*-Ir^{III}(ppy)₃ and Hu's reagent. Nonetheless, in the optimized conditions, styrenes bearing a variety of functional groups on the phenyl ring provided the desired products in moderate to good yields. When an alcohol (MeOH, *t*BuOH) or a carboxylic acid (AcOH) were used instead of water, the corresponding difluoromethylated ethers and esters were obtained (Scheme 8).



Scheme 8: Synthesis of CF₂H-containing alcohols and ethers.

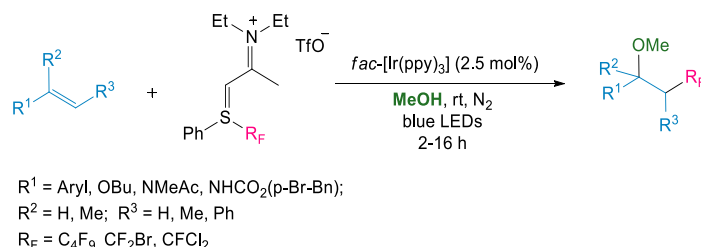
The same year Ran *et al.* employed difluoromethyltriphenylphosphonium bromide as the radical source, followed by trapping with water or alcohols. In both cases, best results were obtained by using [*fac*-Ir(ppy)₃], which has a strong reducing excited state ($E_{1/2}^{IV/*III} = -1.73$ V vs SCE) required for the activation of the radical source.⁴⁰

Xu *et al.* reported an example of oxidative difluoromethylation of phenyl acrylamides in electrocatalytic conditions. The authors employed an in-house developed precursor of CHF₂ radicals⁴¹ CF₂HSO₂NHNBoc.⁴² Optimal conditions were found using RVC/Pt electrodes at constant current with Et₄NPF₆ electrolyte and a 1:2 acetone/water solvent mixture. Heating to 70°C was required for the reaction to proceed, due to the low solubility of the reagents in the aqueous solution at room temperature. Also, a reduced amount of water would cause a drop in current efficiency. The reaction was strongly influenced by the nature of the anode and good results could only be obtained with the RVC electrode, whilst the use of both graphite and glassy carbon plates resulted in poor to no conversion. Tertiary amides could not afford the desired difunctionalized product and delivered solely the corresponding CF₂H-substituted acrylamides (Scheme 9).



Scheme 9: Synthesis of CF₂H-containing alcohols *via* electrocatalysis.

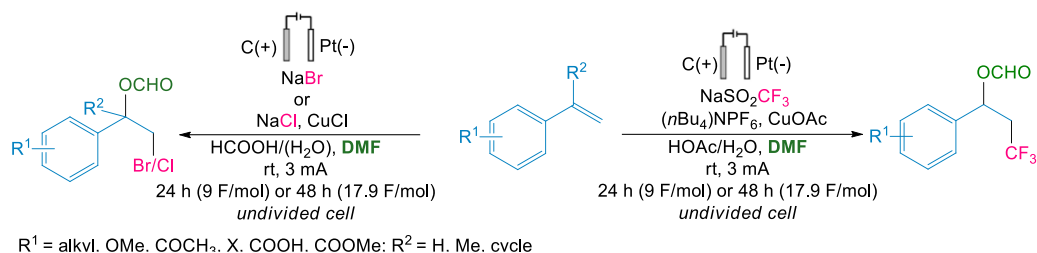
In 2017, a report from Daniel *et al.* contributed to the expansion of the scope of perfluoroalkyl radicals by employing an in-house developed *S*-perfluoroalkyl sulfilimino iminium as the radical source.⁴³ This allowed the introduction of C₄F₉, CF₂Br, and CFC₂ groups unexplored by previous methodologies. Notably, the nature of the radical did not strongly affect the reaction and the products were obtained in comparable moderate to good yields. Nonetheless, in the case of internal and cyclic alkenes, d.r. values were influenced by the steric hindrance of the fluorinated radical resulting in higher selectivity following the order: C₄F₉ > CF₂Br > CFC₂. On a side note, the scope of the nucleophile was left uncovered and limited to methanol (Scheme 10).



Scheme 10: Methoxy perfluoroalkylation of styrenes.

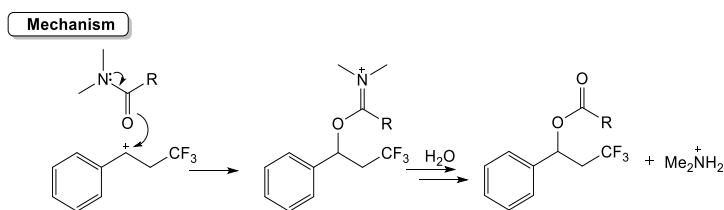
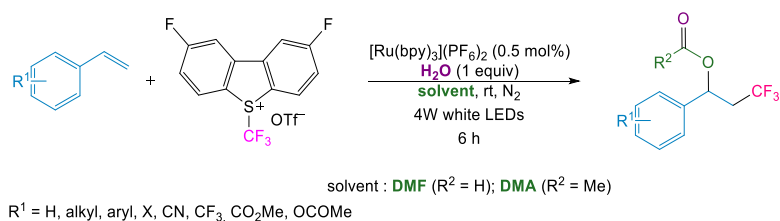
Sun *et al.* reported an interesting approach to oxidative trifluoromethylation of styrenes employing dimethylformamide as *O*-nucleophile in electrocatalytic conditions. Langlois reagent was chosen as the source of trifluoromethyl anions which could undergo copper-mediated anodic oxidation to trifluoromethyl radicals. Attack to the double bond was followed by oxidation to benzyl cation, trapped by DMF. Hydrolysis of the newly formed imine intermediate afforded the acetoxyl product with the release of dimethylamine. Anodic oxidation of the latter was prevented by the addition of an acid. Aqueous acetic acid performed best. The

authors easily applied to bromo and chloro-formyloxylation reactions by simple substitution of Langlois reagent with sodium bromide and chloride. In all cases, vinyl arenes di-substitution proceeded in good to excellent yields (Scheme 11).⁴⁴



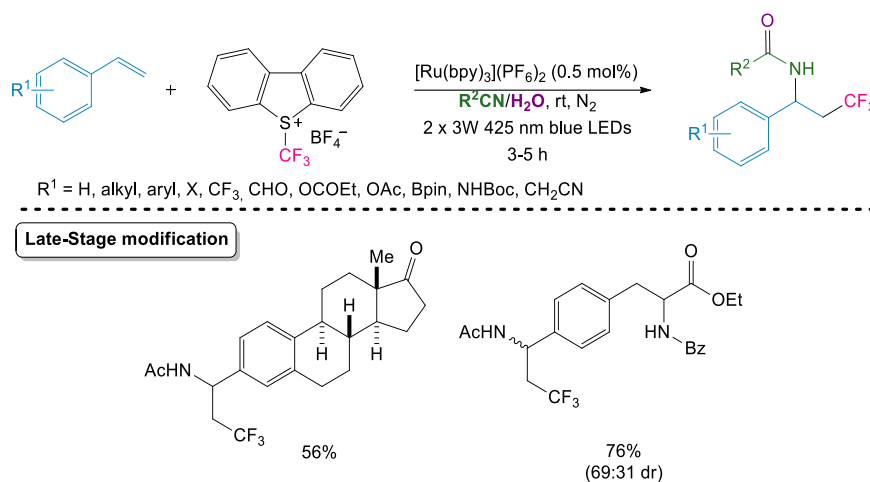
Scheme 11: Electrocatalytic trifluoromethyl- and halo-formyloxylation of styrenes.

Finally, as the last example of the trifluoromethylation/C-O bond formation sequence, it is worth mentioning the work of Zhou *et al.* from 2019⁴⁵. DMF or DMA was employed as nucleophiles to trap the photocatalytically generated trifluoromethyl phenyl cation leading to the formation of an imine intermediate. Subsequent hydrolysis to ester concluded the four component acyloxy-trifluoromethylation of aryl alkenes. As for previous reports, the generation of the trifluoromethyl benzyl cation intermediate remains the key reaction step, and the electronic effect of substituents on the aryl ring did not strongly affect the yields. The authors attempted to expand the scope to 2-vinylpyridine without success probably due to the lower stability of the corresponding cation (Scheme 12).



Scheme 12: Four-component synthesis of trifluoromethyl alkyl esters.

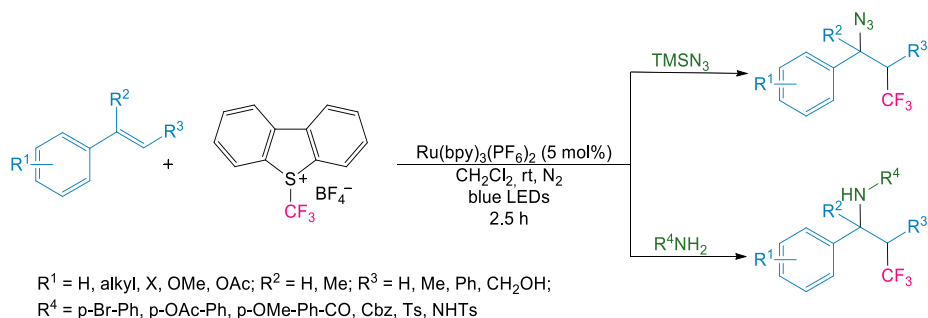
A similar approach was already presented in an early work from Akita and co-workers where they extended the scope of nucleophiles towards C-N bond formation.⁴⁶ In this report, the vinyl cation intermediate is trapped by nitriles used as solvents in a Ritter-type reaction⁴⁷ where a further nucleophilic attack by a water molecule and tautomerization results in the formation of an amide residue. In this work, $[\text{Ru}(\text{bpy})_3](\text{PF}_6)_2$ catalyst could afford similar yields as *fac*- $\text{Ir}^{\text{III}}(\text{ppy})_3$ and was therefore chosen as a cheaper alternative. Umemoto's reagent was employed as $^+\text{CF}_3$ reagent, as Togni's reagents were found unable to afford the desired product (Scheme 13). The reaction conditions provided the desired products in high yields with substrates bearing both electron-donating and electron-withdrawing substituents. Moreover, the mild reaction condition could be smoothly applied to late-stage modification of steroid and amino acid scaffolds.



Scheme 13: Four-component synthesis of trifluoromethyl alkyl amides.

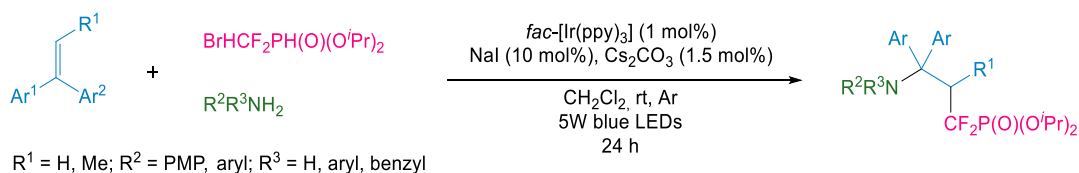
Later, the same authors explored the use of perylene as a metal-free photocatalyst, successfully obtaining the trifluoromethyl- and difluoromethyl- acetamides employing the corresponding *S*-(fluoroalkyl)sulfonium salts. Interestingly, perylene outperformed iridium catalyst allowing for considerably lower reaction times.⁴⁸

In 2014, Dagousset *et al.* reported the trapping of trifluoromethylated vinyl cations by both azide and amine nucleophiles.⁴⁹ In this paper, based on previous work from the same authors on the difunctionalization of enecarbamates, the electrophile was generated through radical trifluoromethylation/SET oxidation sequence employing Umemoto's reagent and ruthenium photocatalyst (Scheme 14). Small libraries of both trifluoromethyl amines and azides could be prepared in moderate to good yields without intervention in the reaction conditions, demonstrating once again the robustness of this synthetic strategy.



Scheme 14: Photoredox catalyzed trifluoromethyl amination/azidation.

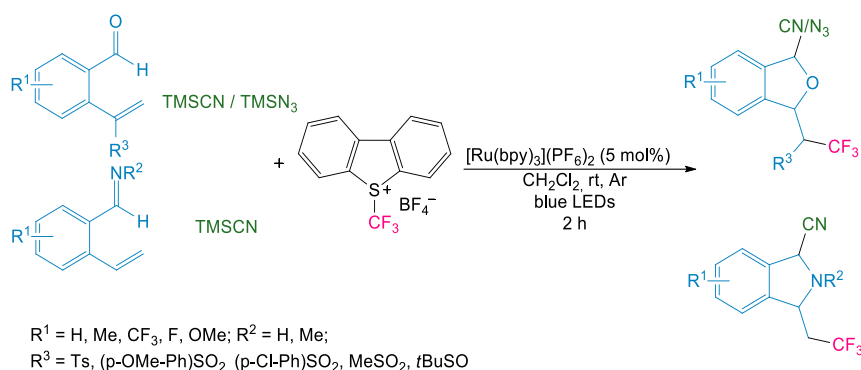
Further, research on C-N bond formation was carried by Yang *et al.*, who reported in 2018 the aminodifluoromethylphosphonation of 1,1-diarylethylenes.⁵⁰ They used difluoromethylphosphonate to introduce a phosphate group exploiting the photocatalytic formation of difluoromethyl radicals which effectively add to vinyl arenes. The cationic vinyl intermediate, obtained upon oxidation, was trapped by aromatic amines. The addition of NaI resulted in an improvement in yield and the authors suggest it could be associated with additional stabilization of the cationic intermediate by iodide. The substrate scope was limited to 1,1-diphenylethylenes as with styrene no product was obtained. Nonetheless, internal alkenes ($R^1 = \text{CH}_3$) were also found amenable to these reaction conditions (Scheme 15).



Scheme 15: Aminodifluoromethylphosphonation of 1,1-diarylethylenes.

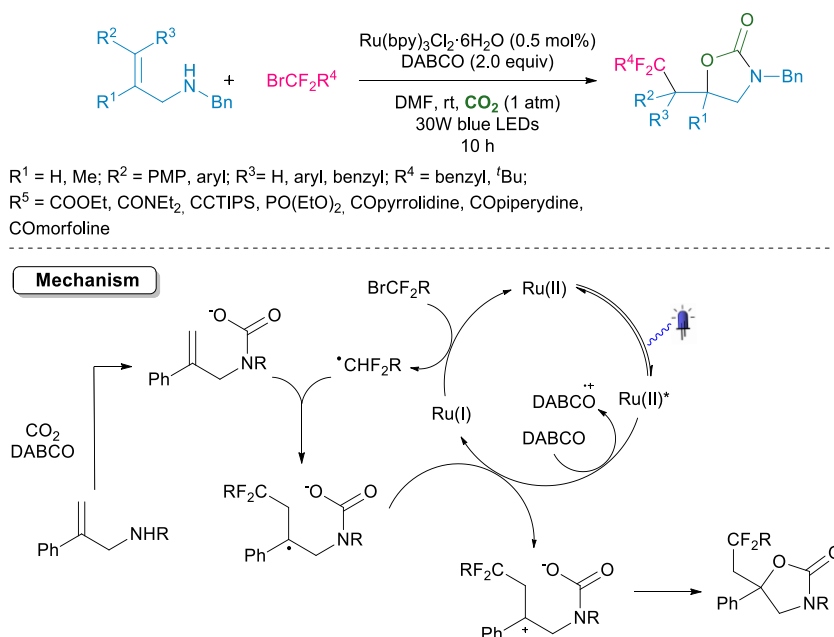
Finally, Jarrige *et al.* reported in 2016 an elegant O and N nucleophilic trapping of benzyl cations in an intramolecular fashion using *ortho* vinyl phenylaldehydes or imines as substrates.⁵¹ The multicomponent reaction consisted of a tandem intermolecular nucleophilic addition/cyclization. Both cyanide or azide nucleophiles could efficiently kickstart the process by addition to the aldehyde or imine to form the corresponding α -hydroxy or α -amino cyanides and azides. Follows the photocatalyzed trifluoromethylation/oxidation of the double

bond to give a benzyl cation amenable of intramolecular nucleophilic attack by the hydroxyl or amino residue. The overall reaction results in the formation of functionalized CF₃-containing phthalans and isoindolines in moderate to good yields in a restively short reaction time (2h). Notably, the reaction conditions well-performed varying both the substrate and the nucleophile without the need of further optimization (Scheme 16).



Scheme 16: Synthesis of di-hydro isobenzofurans and di-hydro isoindoles.

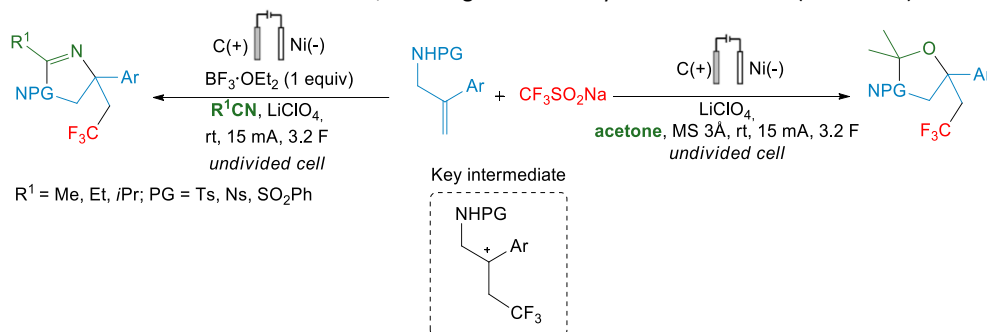
In 2017 Yin *et al.* reported a variation on the theme of intermolecular nucleophilic addition/cyclization presenting the incorporation of CO₂ in a tandem fashion between arylallylamines and bromodifluoroalkyl compounds to give 2-oxazolidinones with functionalized difluoroalkyl groups.⁵² Carbon dioxide as one of the most common waste products of natural and human activities represents the ideal feedstock material: cheap, abundant, and sustainable. In addition, it is associated with the low chemical hazards. These factors stimulated extensive research toward the design of synthetic strategies able to activate and trap CO₂. Tasks inherently challenging due to low reactivity associated with high thermodynamic stability and poor kinetic properties. Pioneering works in CO₂ valorization involved either highly reactive coupling partners or harsh conditions. Organometallic catalysis helped mitigate the reaction conditions but still required high reaction temperature.⁵³ Visible light photocatalyzed processes offer an alternative allowing for CO₂ fixation in mild conditions. In this report, the authors presented an elegant approach where allylamines act as bifunctional reagents. As depicted in Scheme 17, the amine group reacts with CO₂ to form a carbamate, subsequently, the double bond traps the fluoroalkyl radical to give a biofunctionalized intermediate which upon oxidation by the photocatalyst undergoes cyclization to the oxazolidinone. The reaction conditions provided the products in moderate to good yields with a variety of substituents on the phenyl ring. Substitution on the amine was limited to benzyl and *n*-butyl as common protecting groups as Boc and tosyl as well as the free amine could not afford the corresponding oxazolidinones. The scope of difluoroalkyl reagents included esters, amides, alkynes, and phosphonates.



Scheme 17: Synthesis of 2-oxazolidinones.

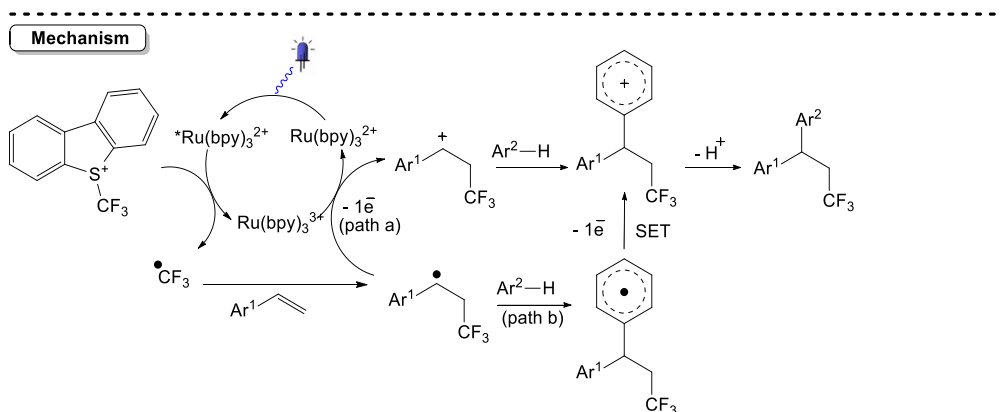
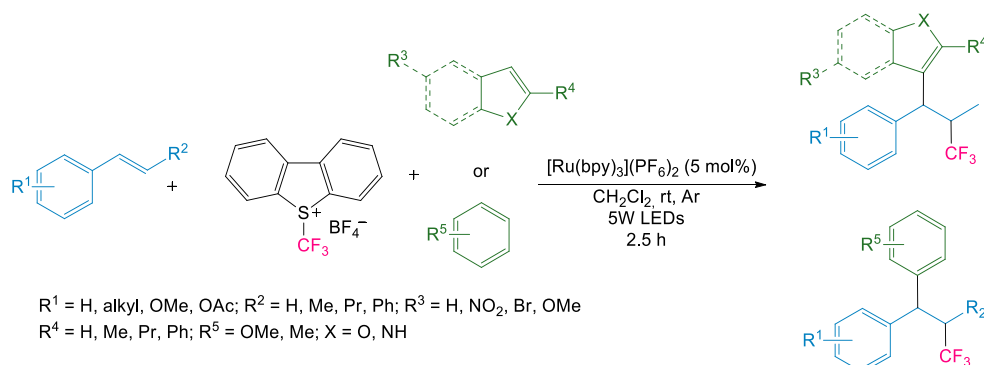
Recently, Claraz *et al.* further explored the use of allylamines as precursors in the synthesis of heterocycles in electrocatalytic conditions.⁵⁴ Based on their previous experience in electrochemical trifluoromethylation with Langlois reagent, the authors

envisioned the formation of a key dipolar intermediate able to react with nitriles or acetone, used as solvents, to give the corresponding imidazolines and oxazolines. Best yields were obtained running the reaction at a constant current of 15mA using graphite anode and nickel cathode with LiClO₄ as supporting electrolyte. When nitriles were employed the addition of a Lewis acid, BF₃·OEt₂, was required in order to suppress the competing formation of aziridine by cyclization of the dipolar intermediate. In the reaction with acetone, no aziridine was formed, nevertheless, amino alcohol was obtained as a major side product. This was easily solved by the removal of water with molecular sieves, resulting in increased yields of oxazolines (Scheme 18).



Scheme 18: Electrocatalytic synthesis of imidazolines and oxazolines.

In 2014, Masson's group demonstrated that carbon nucleophiles could also successfully be employed as terminal nucleophiles in photocatalytic difunctionalization following the oxidative quenching pathway.⁵⁵ In this work they showed an example of three-component aryl- and heteroaryl-trifluoromethylation of styrene with the generation of two C-C bonds. This was obtained employing Umemoto's reagent as CF₃ radical source and methoxy-benzene or heteroarenes as nucleophiles. The proposed mechanism is depicted in Scheme 19 and two alternative pathways have been suggested for the arylation step. Nonetheless, the authors propose Friedel-Crafts-type alkylation by the trifluoromethylated cationic intermediate (Scheme 19, path a) to be the most reasonable mechanism, as supported by the unreactivity of electron-deficient arenes as well as the regioselective addition on the C3-position of the indoles, both not justifiable by a radical process (Scheme 19, path b).

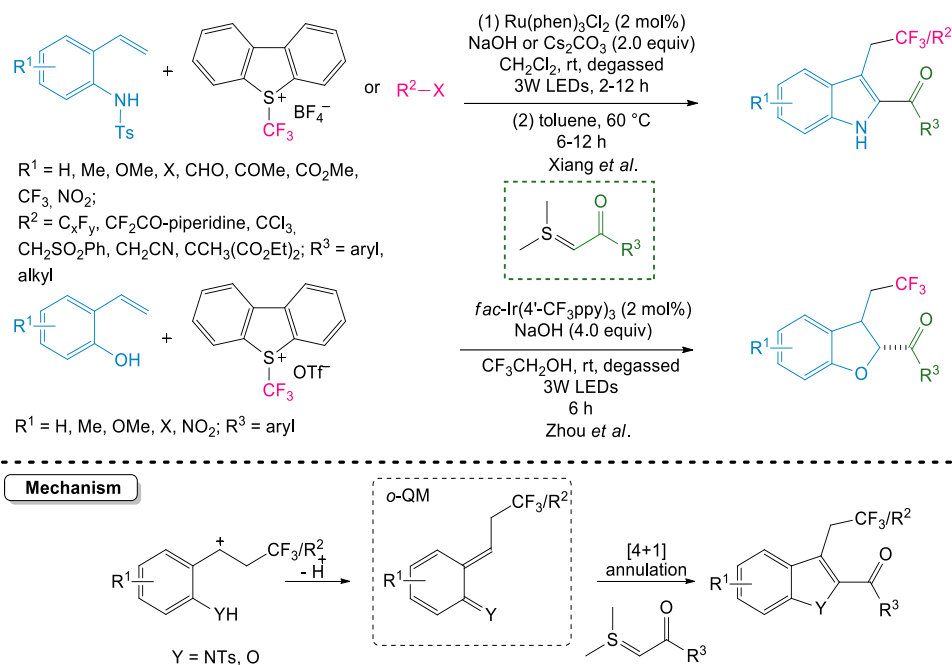


Scheme 19: Friedel-Crafts-type alkylation of (hetero)arenes.

The same strategy was later employed by Duan *et al.* extending the scope of radical precursors to α -carbonyl difluoroalkyl bromides in a three-component reaction involving styrenes and indoles.⁵⁶

In an interesting contribution from 2017, Liu *et al.* exploited a trifluoromethylation/oxidative quenching sequence for the preparation of a key aza-*ortho*-quinone methide (aza-*o*-QM) intermediate starting from *ortho*-*N*-tosyl styrene and Umemoto's reagent.⁵⁷ The newly formed reactive intermediate readily reacted with sulfur ylide *via* a [4+1] annulation to *N*-tosyl-indole. As depicted in Scheme 20, the aza-*o*-QM is

formed upon deprotonation and tautomerization of the benzyl cation intermediate. Desulfonation/aromatization was obtained in the same flask by the solvent swap from CH₂Cl₂ to toluene and increase of temperature to 60°C. Although the use of Umemoto's reagent did not require any photocatalyst when other radical sources were employed, these reaction conditions proved to be ineffective. Implementation of a photocatalytic cycle for the activation of the radical source solved the issue allowing the use of a variety of haloalkyl substrates. The catalytic system of choice was Ru(phen)₃Cl₂ in the presence of NaOH. A following paper from the same group extended the scope to 2-vinyl phenols providing a new route for the synthesis of 2,3-dihydrobenzofurans through *ortho*-quinone methide intermediate.⁵⁸



Scheme 20: Synthesis of 2,3-dihydrobenzofurans and indoles.

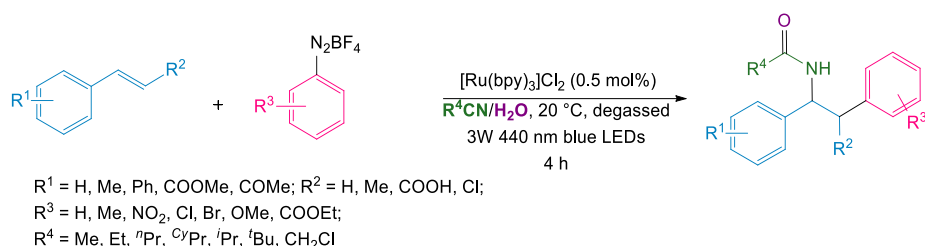
2.1.1.1.2. Other C-centered radicals:

To conclude this first subsection, we will go over a few more C-centered radical sources other than fluoroalkyl substrates, which have been successfully employed in styrene difunctionalization. Back in 2013, Fumagalli *et al.* investigated the adoption of diaryliodonium tetrafluoroborates as a source of aryl radicals. These were able to engage SET with Ir^{III}(ppy)₃* *via* oxidative quenching, and generate sp² radicals which could add to styrene. Vinyl cation intermediates were formed following a similar pathway, as in Scheme 1, and delivered the desired alkoxyated and aminated products by reaction with *O*- or *N*-nucleophiles.⁵⁹ Addition of Zn(OAc)₂ increased the reaction efficiency further allowing to reduce the photocatalyst loading to 1 mol%. Styrenes bearing electron-donating or withdrawing substituents were well tolerated, except *m*-NO₂-styrene and vinyl pyridines. In the case of diaryliodonium tetrafluoroborates, among the several substitution patterns tested, only electron-donating groups at the *para*-position, *viz.* *p*-NHAc and *p*-MeO, lead to a drop in yield. Finally, both *O*- and *N*-nucleophiles were amenable to the reaction conditions (Scheme 21).



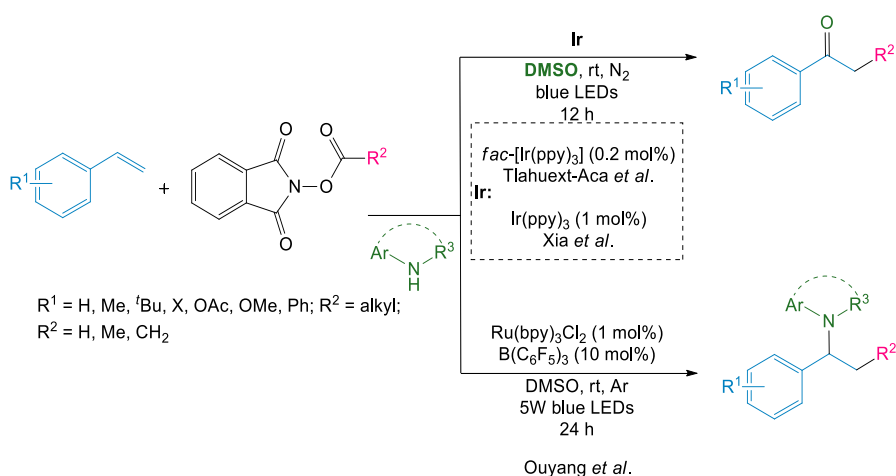
Scheme 21: *O/N*-aryl difunctionalization of styrenes.

Aryl diazonium salts represent another class of widely employed radical precursors.⁶⁰ Facile preparation from the corresponding anilines and relatively low redox potential concurred to the success of aryl diazonium salts, started with the seminal contributions from Pschorr and Meerwein.⁶¹ The latter reported the installation of aryls onto double bonds through the initial addition of both the aryl residue halogen atom followed by elimination of halogenidric acid to restore the unsaturation. In 2014, Hari *et al.* exploited the Meerwein type mechanism in a photocatalyzed difunctionalization/Ritter-type amination of styrene, using diazonium salts as radical sources and nitriles as nucleophiles.⁶² The reaction follows the same mechanism as presented in Scheme 3 and could deliver the aryl aminated products in good to excellent yields.



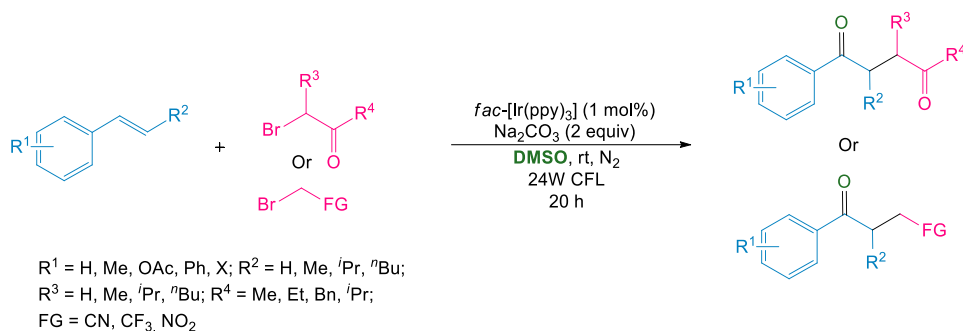
Scheme 22: Aryl diazonium salts as radical source.

More recently, alkyl *N*-hydroxyphthalimide ester's ability to be selectively cleaved under photocatalytic conditions allowed for the *in situ* generation of alkyl radicals. Two independent contributions from Tlahuext-Aca *et al.*⁶³ and Xia *et al.*⁶⁴ reported the use of these reagents in the oxoalkylation of styrene *via* radical trapping followed by Kornblum oxidation with DMSO. Later the same year Ouyang *et al.* described the use of alkyl *N*-hydroxyphthalimide esters in the alkyl amination of styrenes (Scheme 23).⁶⁵



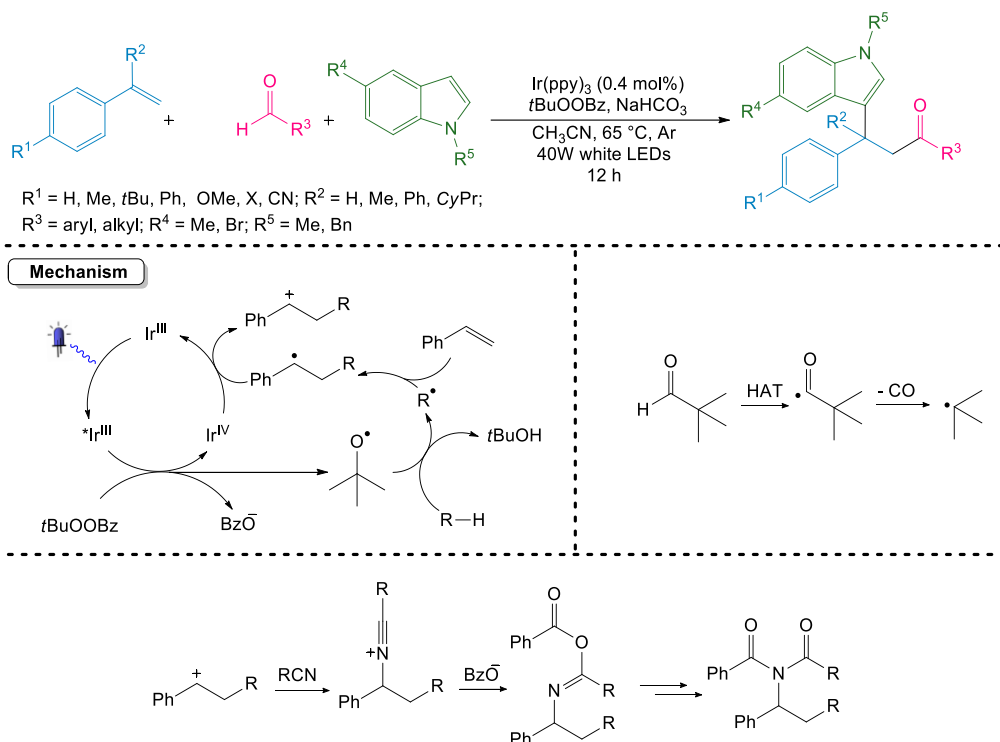
Scheme 23: Oxo and aminoalkylation involving *N*-hydroxyphthalimide esters as radical source.

In 2019, Fang *et al.* gave their contribution to the series of Kornblum oxoalkylations by employing α -bromo-esters and other alkylbromides as the source of alkyl radicals (Scheme 24).⁶⁶



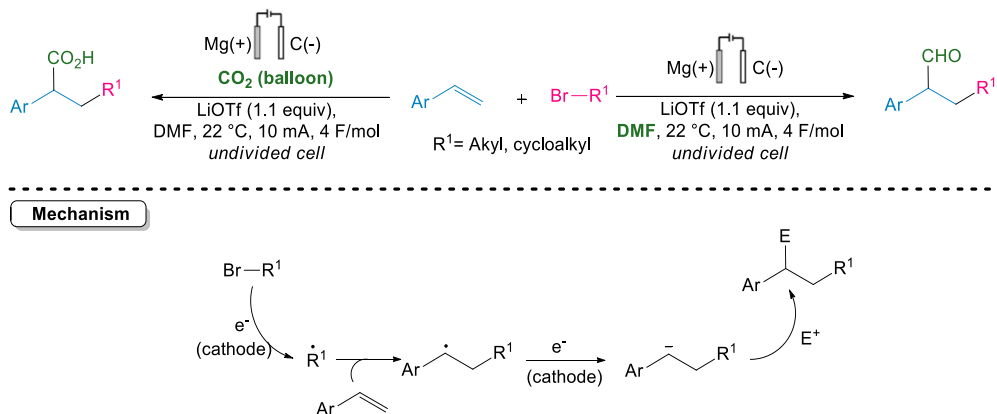
Scheme 24: Oxoalkylation with alkylbromides.

Finally, we report a recent work from Lux *et al.* where aldehydes have been successfully adopted for the generation of acyl radicals by the cooperative action of peroxides and iridium photocatalyst under visible light. As depicted in Scheme 25, *t*BuOOBz was used to quench the photocatalyst excited state $\text{Ir}^{\text{III}*}$ to its oxidized form. Concomitant formation of a *tert*-butoxyl radical leads to the activation of the aldehyde *via* HAT to deliver the acyl radical. Interestingly when tertiary pivaldehyde was used, the decarbonylated *tert*-butylated product was recovered in accordance with the formation of a stabilized *tert*-butyl radical by loss of CO. In the absence of other nucleophiles, *N*-acyl benzamide derivatives were obtained by trapping of the alkyl nitrile solvent and addition of peroxide byproducts.⁶⁷



Scheme 25: Three component dicarbofunctionalization of styrenes.

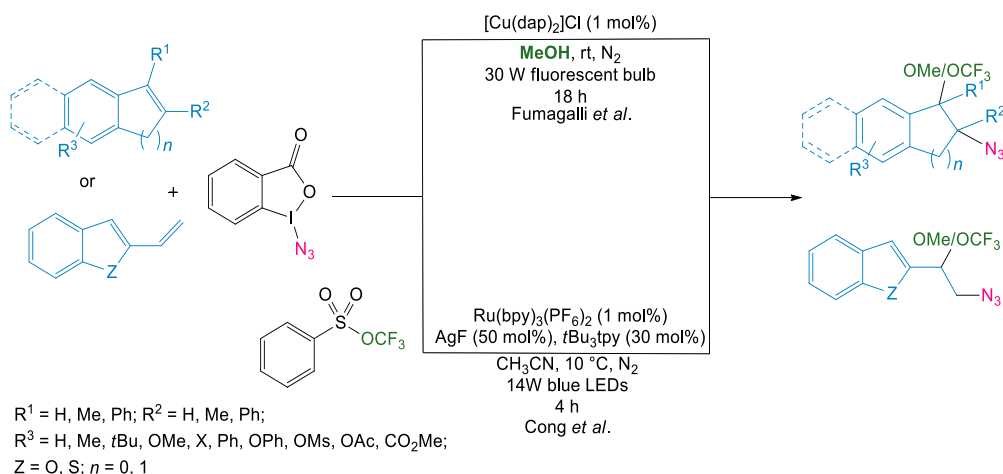
Recently, Zhang and Lin reported the carbonylation of alkenes by incorporation of DMF or CO₂ leading to the formation of formyl and carboxyl derivatives.⁶⁸ Upon thorough mechanistic investigation the authors came to the conclusion that the most plausible mechanism would involve an ECEC radical/polar crossover starting from reduction of the alkyl halide (E) followed by attack onto the vinyl arene (C). The newly formed benzyl radical undergoes further reduction to anion (E) finally trapped by the electrophile (C). Control experiments with Grignard reagents and with chiral alkyl bromides led to the exclusion of respectively an EEC polar mechanism involving nucleophilic attack of the carbanion to the double bond and, an ECEC radical anion pathway where the vinyl radical anion would react with the alkyl bromide *via* S_N². In the first case the reaction failed to provide the desired product, in the latter, a racemic mixture was obtained in contrast with the predicted inversion of configuration of the chiral center (Scheme 26).



Scheme 26: Electrocatalytic alkyl carbonylation.

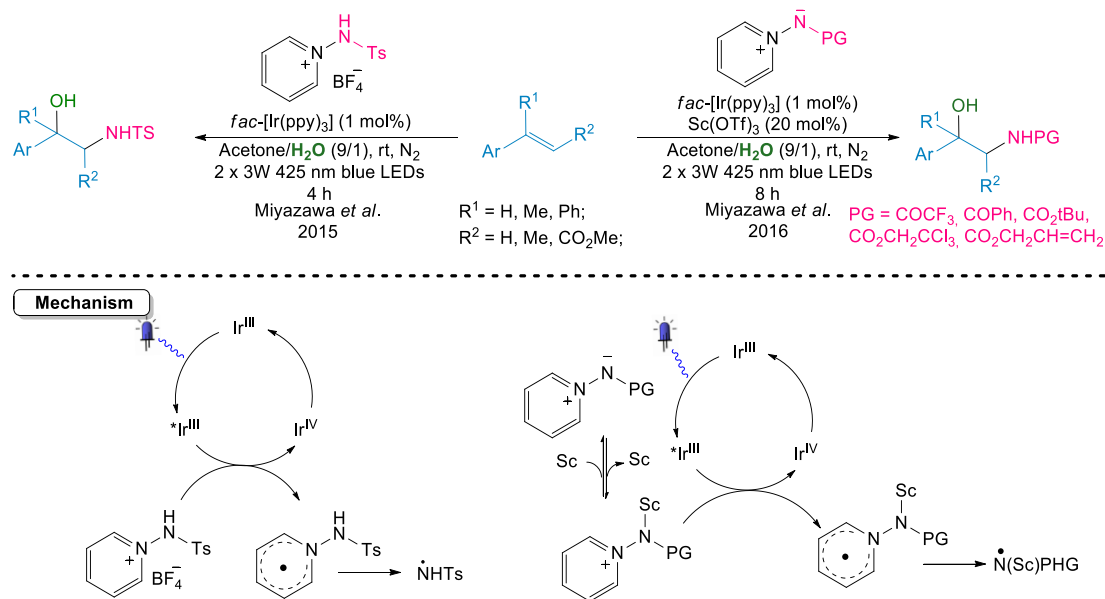
2.1.1.1.3. N-centered radicals:

In 2015, Fumagalli *et al.* reported the generation of azidyl radicals *via* photocatalyzed reduction of Zhdankin's reagent and its capture in a three-component coupling with styrene and *O*-nucleophiles. After unsuccessful attempts using common photoredox catalysts as Ir(ppy)₃ and Ru(bpy)₃Cl₂, the authors found [Cu(dap)₂]Cl to be the ideal catalyst.⁶⁹ Later, Cong *et al.* employed the same strategy for the azidotrifluoromethoxylation of styrenes with trifluoromethyl arylsulfonate by combining photoredox and silver catalysis (Scheme 27).⁷⁰



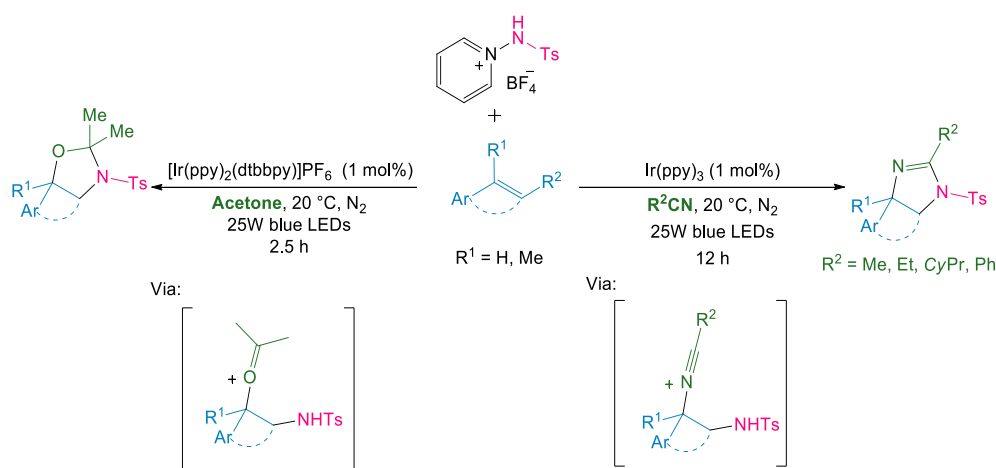
Scheme 27: Oxoazidation of vinylarenes with Zhdarkin's reagent.

In 2015, Miyazawa *et al.* reported the use of 1-aminopyridinium salts as *N*-centered radical source.⁷¹ Inspired by the characteristic reactivity of the electron-deficient Umemoto's and Togni's reagents as CF_3 radical precursors, the authors envisioned *N*-protected 1-aminopyridinium salts to be valid candidates for the photocatalyzed aminohydroxylation of double bonds employing water as nucleophile. Mechanistically, upon SET from the excited photocatalyst species, the aminopyridinium ring gains one electron forming a stable delocalized radical which fragments into pyridine and a reactive amidyl radical able to add to olefins. After screening a few different protecting groups, *N*-*p*-toluenesulfonyl 1-aminopyridinium salt was found most effective. When styrenes were treated with this salt in an acetone/ H_2O solvent mixture and in photocatalytic conditions, the corresponding aminohydroxylated products could be obtained in moderate to good yields. In a report from 2016, the same group reported the design of a cooperative photoredox/Lewis acid catalytic system allowing the use of more easily cleavable protecting groups as trifluoroacetyl and Boc. In detail, $\text{Sc}(\text{OTf})_3$ acts as an activator of the aminopyridinium ylide easing the single electron reduction from the catalyst. Fragmentation of the radical intermediate generates a Lewis-acid/amidyl-radical adduct which attacks the double bond (Scheme 28).⁷²



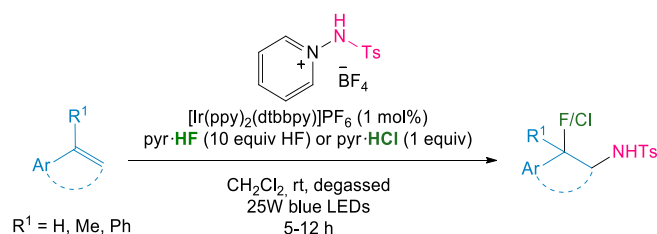
Scheme 28: 1-aminopyridinium salts as *N*-centered radical source.

Chen *et al.* employed 1-aminopyridinium salts reporting a new route to substituted imidazolines and oxazolidines. As discussed above, the first step consists of the formation of amidyl radicals followed by addition to styrene and subsequent oxidation to benzyl cation intermediate. Clever choice of the solvent (i.e. acetonitrile or acetone) furnished both a nucleophile able to attack the benzyl carbon and an electrophilic site susceptible of intramolecular nucleophilic attack by the NTs residue (Scheme 29).⁷³



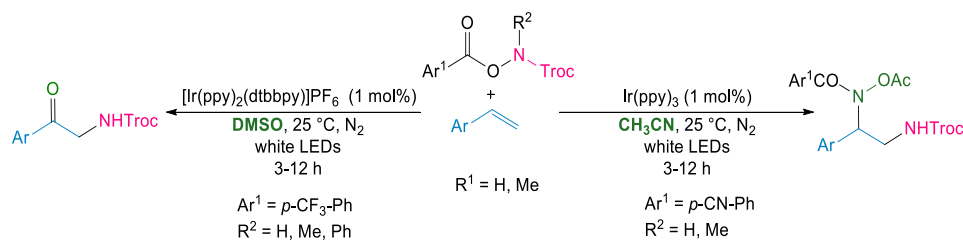
Scheme 29: Synthesis of substituted imidazolines and oxazolines.

Finally, Mo *et al.* reported the amino fluorination/chlorination of styrene employing HF or HCl as a source of nucleophile to trap the vinyl cation intermediate (Scheme 30).⁷⁴



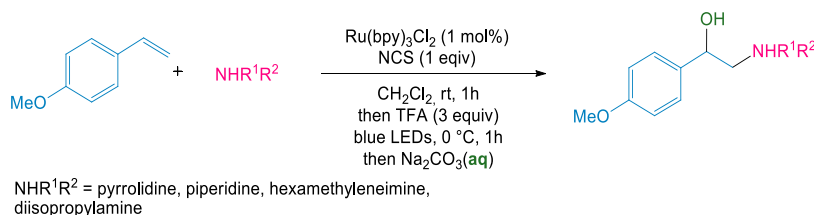
Scheme 30: Haloamination of styrenes.

As reported by Qin *et al.*, benzyloxycarbamates can be used as *N*-centered radicals as well.⁷⁵ Specifically, they found 2,2,2-trichloroethyl (Troc) aryloxycarbamate to be effective in the functionalization of styrenes through the formation of NHTroc radical. Such radicals could effectively react with styrene to give first a benzyl radical and then a benzyl cation intermediate. The choice of the solvent would direct the reaction toward Kornblum oxidation (DMSO) or Ritter type pseudo-four-component reaction (acetonitrile). The latter involved the addition of nitrile to the benzyl radical and subsequent nucleophilic attack by the benzoate residue of the carbamate. The newly formed intermediate undergoes rearrangement by acyl transfer to give the diamide product (Scheme 31).



Scheme 31: 2,2,2-trichloroethyl (Troc) aryloxycarbamate as radical source.

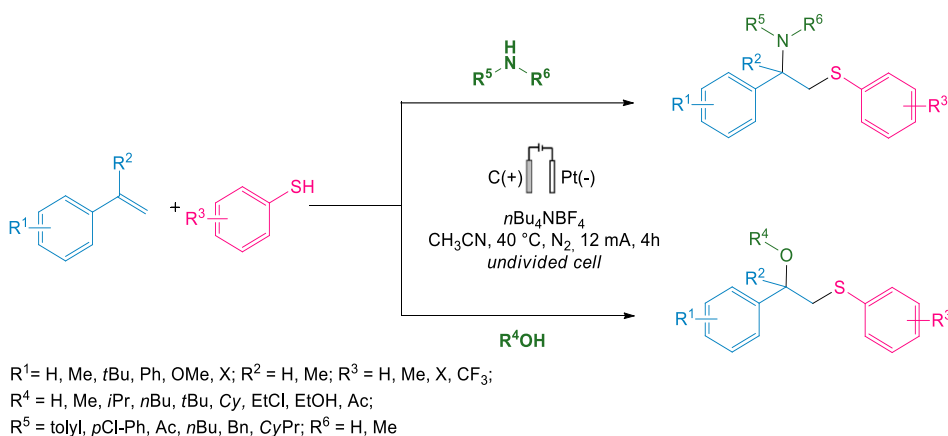
Recently Goaverts, Angelini *et al.* reported the photoinduced amino hydroxylation of styrenes *via* intermediate monochlorination in the presence of NCS ruthenium photocatalyst and a secondary amine (Scheme 32).⁷⁶



Scheme 32: Photoredox catalyzed hydroamination.

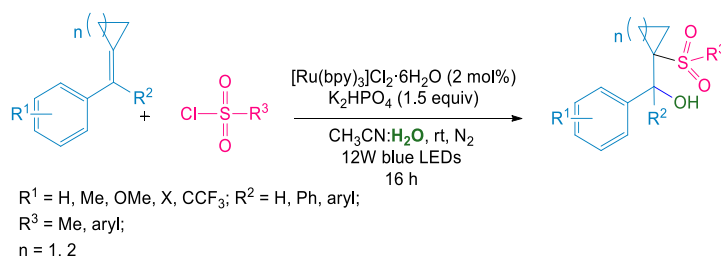
2.1.1.1.4 S-centered radicals:

In 2018 Yuan *et al.* reported the oxy and amino sulfonylation of styrene employing thiophenols and thiols as source of S-centered radical.⁷⁷ The same year Wang *et al.* reported the use of thiols for the oxysulfuration of styrenes with water or alcohols at room temperature.⁷⁸ Although it might appear like an obvious choice, it should be noted that overoxidation to unreactive sulfoxides and sulfones can easily occur. Nonetheless, electrochemical oxidation allows for far greater control compared to the conventional method, and the authors successfully obtained selective formation of thiyl radicals which could readily react with styrene. Subsequent oxidation to vinyl cation allows further functionalization through the nucleophilic attack. In this work, both O- and N-nucleophiles could be efficiently formed *via* cathodic reduction. A possible alternative mechanism sees the formation of disulfides *via* thiyl radical homocoupling. These could be oxidized to the corresponding arylbis(arylthio)sulfonium ion amenable of nucleophilic attack by the double bond and the nucleophile *via* intermediate formation of thiranium ring (Scheme 33).



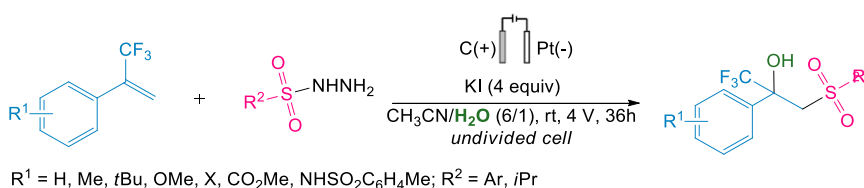
Scheme 33: Electrocatalytic sulphonylation.

Recently, a contribution from Liu *et al.* has expanded the scope of heteroatom-centered radicals to sulfur by using sulfonyl chlorides as precursors.⁷⁹ Upon excitation, the ruthenium photocatalyst reduces the sulphonyl chloride *via* SET with the formation of a sulphonyl radical which in turn attacks the double bond. Mild reaction conditions, characteristic of photoredox catalysis, allowed for the use of relatively delicate substrates containing a cyclopropyl scaffold. The reaction conducted in acetonitrile/water solvent mixture gave β -hydroxysulfones in moderate to good yields (Scheme 34).



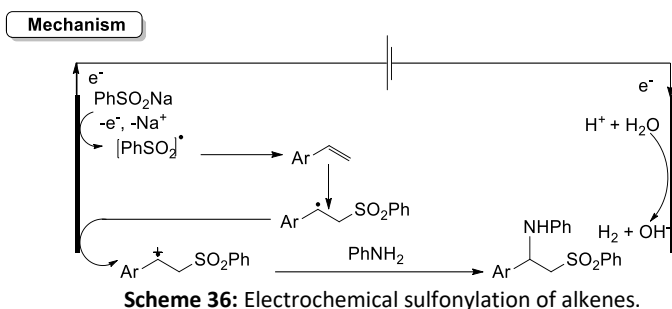
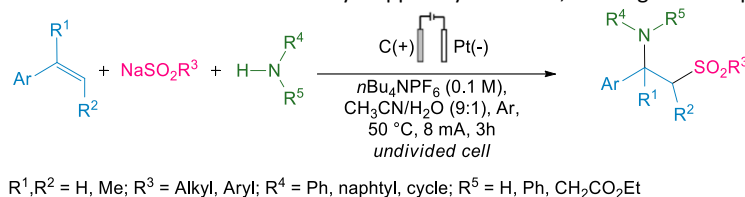
Scheme 34: Preparation of β -hydroxysulfones.

In 2021 Ye *et al.* reported an alternative route toward β -hydroxysulfones employing sulfonyl hydrazide as S-centered radical source in electrocatalytic conditions.⁸⁰ The activation of sulfonyl hydrazides can occur by direct oxidation at the anode, nonetheless, significant increment in yield upon addition of KI suggested an additional mechanism involving a series of HAT from the hydrazide to anodically formed iodine radicals, resulting in the elimination of nitrogen and formation of the sulfonyl radical. The usual radical attack/mechanism sequence leads then to the formation of a benzyl cation trapped by a hydroxide anion formed at the cathode. Control experiments could not exclude the installation of the OH group by the capture of the benzyl radical by molecular oxygen and consequent HAT/reduction sequence (Scheme 35). The substitution pattern on the phenyl ring had a strong influence as *meta* and *ortho*-substituted styrenes gave lower yields or even unsuccessful reaction. The scope of sulfonyl hydrazides included phenyl, heteroaryl and alkyl substituents, affording the product in good to excellent yields.



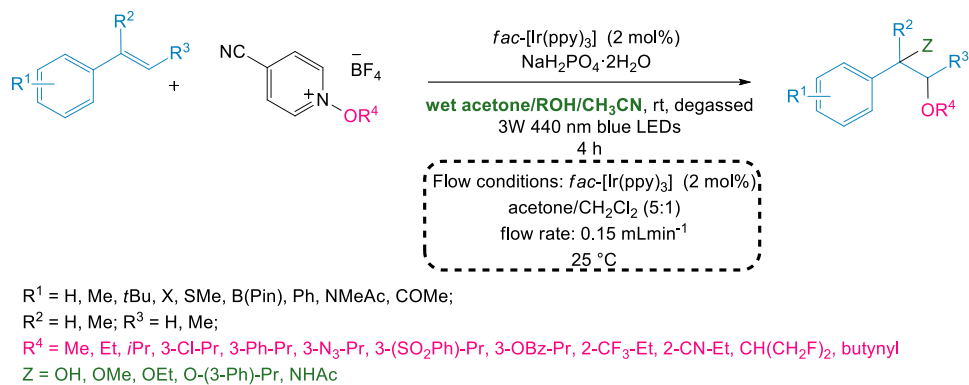
Scheme 35: Electrocatalytic preparation of β -hydroxysulfones.

Following the same strategy, the sulfonylation of alkenes was electrochemically obtained through the use of alkyl/aryl sulfinates and primary or secondary amines.⁸¹ Electron-donating groups led to better results and increased yields. Mechanistically, the anodic oxidation of sodium sulfinates generates a sulfonyl radical that then attacks the double bond of a styrene. Subsequently, another anodic oxidation generates a cationic intermediate that is finally trapped by an amine, forming the final product (Scheme 36).



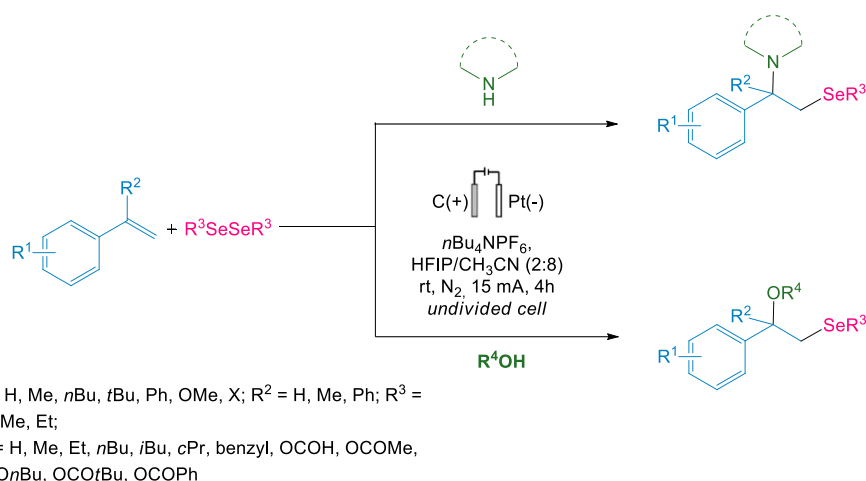
2.1.1.1.5. Other radical sources:

Similar to 1-aminopyridinium salts, *N*-alkoxy-pyridinium salts also have the ability to engage in oxidative quenching of a photocatalyst *via* SET and undergo fragmentation to form alkoxy radicals. In 2018, Barthelemy *et al.* reported the use of these *O*-centered radicals for styrene difunctionalization. They found 4-cyano-substituted *N*-alkoxy-pyridinium salts to be optimal oxygen radical source.⁸² Once again, the use of the solvent itself as nucleophile proved to be an efficient diversity-oriented strategy allowing for the formation of hydrate, alkoxyated and aminate products in good yields (Scheme 37).



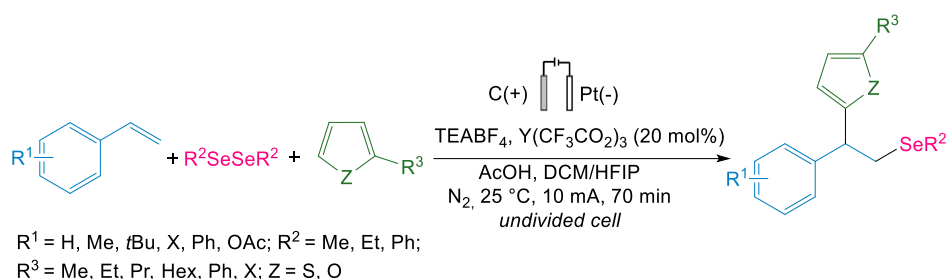
Scheme 37: *N*-alkoxy-pyridinium salts as radical source.

Sun *et al.* contributed to the expansion of the scope of radical sources reporting the use of diselenides in the difunctionalization of styrenes with amines or alcohols.⁸³ The authors suggested an intriguing mechanism for the activation of these substrates starting with reductive heterolytic cleavage of the Se-Se bond at the cathode to seleno radical and selenium anion. The latter can undergo anodic SET oxidation to radical. Radical addition to the double bond and oxidation to the benzyl cation follows. Finally, a nucleophile can trap the cationic intermediate and gives the substituted product. Nevertheless, diselenides could also add to the double bond through anodic activation followed by the formation of a three-membered cyclic selenium intermediate susceptible to nucleophilic attack (Scheme 38).



Scheme 38: Electrocatalytic selenodifunctionalization with *N*- and *O*-nucleophiles.

In 2021, the same group extended the scope of nucleophiles to thiophenes and furans achieving moderate to good yields with both phenyl and alkyl diselenides (Scheme 39).⁸⁴

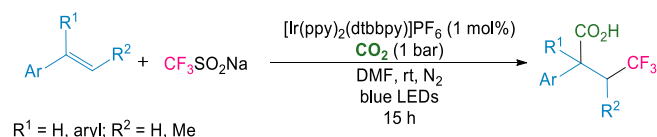


Scheme 39: Electrocatalytic selenodifunctionalization with heterocycles.

2.1.1.2. Reductive quenching

So far, we have described the cases where a benzyl radical is formed upon radical addition and is subsequently oxidized to a benzyl cation which then acts as an electrophile. Nonetheless, the radical intermediate could ride the opposite branch of the catalytic cycle undergoing reduction to a benzyl anion. This is possible when the photocatalyst excited state engages the reductive quenching cycle.

In 2017, Yatham *et al.* reported the trapping of CO_2 in the dicarbofunctionalization of styrenes applying the aforementioned mechanism.⁸⁵ Langlois' reagent was chosen as a radical source allowing the generation of trifluoromethyl radicals by reductive quenching of photocatalyst excited state. The reduced photocatalyst was then able to reduce the intermediate vinyl radical to anion. The three-component reaction finally undergoes a nucleophilic attack to a CO_2 molecule followed by protonation to give the trifluoromethylated carboxylic acids. The choice of photocatalyst drastically affected the reaction yield and only $[\text{Ir}(\text{ppy})_2(\text{dtbbpy})]\text{PF}_6$ ($E_{\text{red}}[\text{Ir}^{\text{III}}/\text{Ir}^{\text{I}}] = -1.51 \text{ V vs. SCE in MeCN}$) could efficiently reduce the 1,1-diphenyl 3,3,3-trifluoro-propane radical ($E_{\text{red}} = -1.34 \text{ V vs. SCE in MeCN}$) intermediate. The reaction showed good tolerance of several functional groups delivering the desired product in good yield. Moreover, other radical sources as sulfonates, benzyltrifluoroborates and oxalates were found amenable to reductive activation by the photocatalyst (Scheme 40).

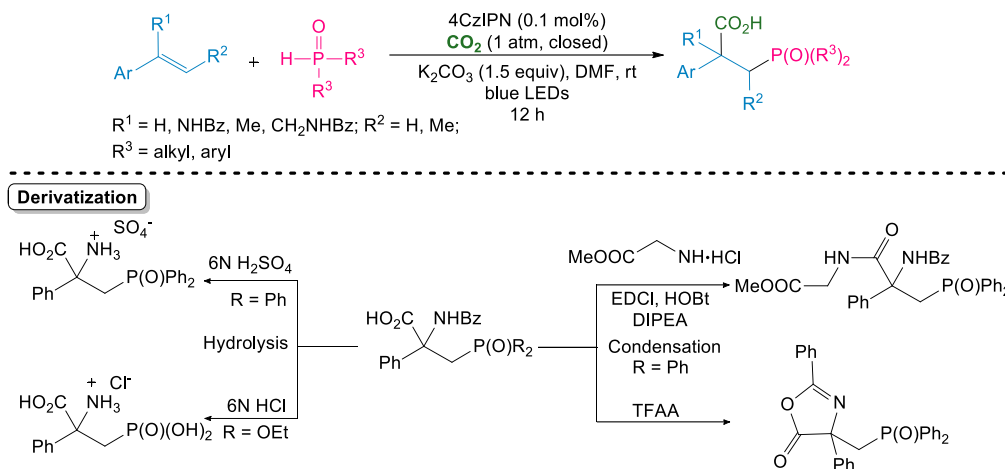


Scheme 40: Synthesis of trifluoromethylated carboxylic acids.

In the same year, Qin *et al.* reported the synthesis of α -trifluoromethylated ketones from vinyl azides. Upon attack by the trifluoromethyl radical an iminyl radical is formed with concomitant loss of N_2 . The intermediate undergoes reduction to imine followed by hydrolysis.⁸⁶

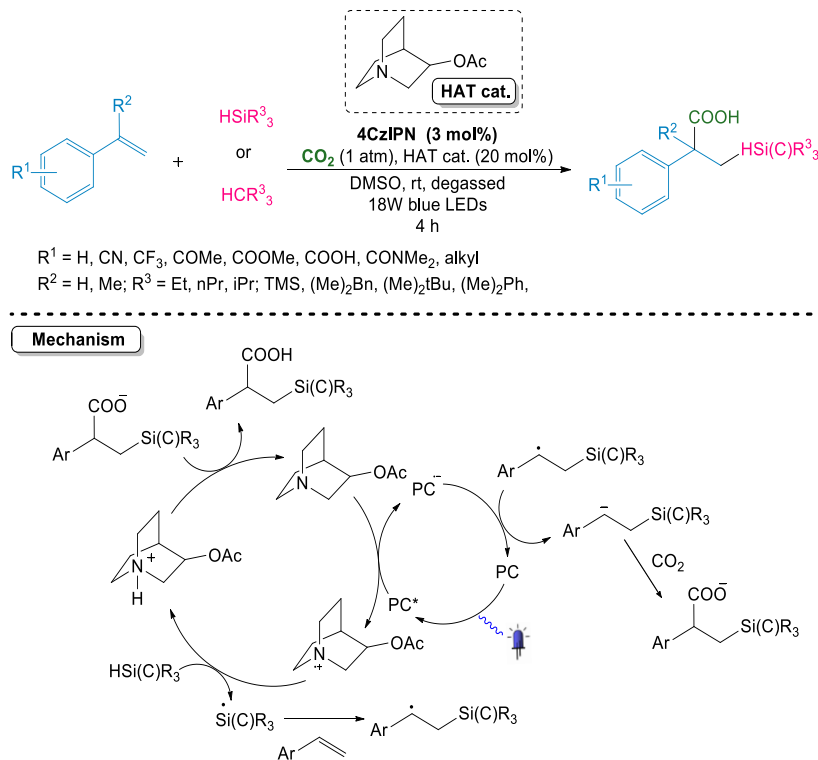
In 2019, Fu *et al.* exploited the photocatalyst reductive quenching for the phosphocarboxylation of *N*-(1-phenylvinyl) benzamide employing phosphine oxides as radical sources and CO_2 as a terminal electrophile.⁸⁷ Remarkably, the organic dye 4CzIPN outperformed common Ir photocatalysts and with outstanding performance (0.1 mol%). Moreover, the use of an inorganic base was crucial to avoid the formation of monosubstituted side products. The authors demonstrated the applicability of this protocol highlighting the facile derivatization of the obtained β -phosphono α -amino acids. As shown in Scheme 41, both the hydrolysis to primary amine as well as condensation reactions

delivered the products in high yields. Notably, the reaction also performed well in absence of the benzamide group, allowing the synthesis of a library of β -phosphono carboxylic acids. Alkyl acrylates were also found amenable to this reaction.



Scheme 41: Synthesis of β -phosphono carboxylic acids.

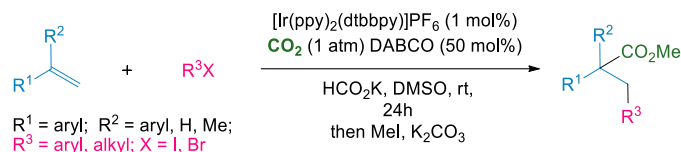
Alternatively, the reductive quenching can be conducted by a HAT reagent which, in turn, activates the radical precursor. An example of HAT/photocatalysis application to styrene difunctionalization has been reported by Hou *et al.* in 2018. Quinuclidin-3-yl acetate was chosen as a HAT reagent in order to match the reduction potential of the organic dye 4CzIPN which would engage its reduction in the photocatalytic cycle. The oxidized HAT reagent is then responsible for the generation of C-centered or Si-centered radical *via* H atom transfer from the corresponding precursor. Finally, the photocatalytic cycle is closed by the reduction of the benzyl radical intermediate to anion. Nucleophilic attack to CO_2 gives the corresponding carboxylic acid (Scheme 42).⁸⁸



Scheme 42: Photoredox catalyzed silanization/ CO_2 capture sequence.

Wang *et al.* applied the same strategy for the carboarylation of styrenes with CO_2 and aryl halides.⁸⁹ The authors selected $\text{DABCO}/[\text{Ir}(\text{ppy})_2(\text{dtbbpy})]\text{PF}_6$ as an optimal HAT/photocatalytic system. Upon reductive quenching of the photocatalyst, DABCO radical cation intermediate is formed and reacts with potassium formate to give CO_2 radical anion. This is then able to activate the halide and

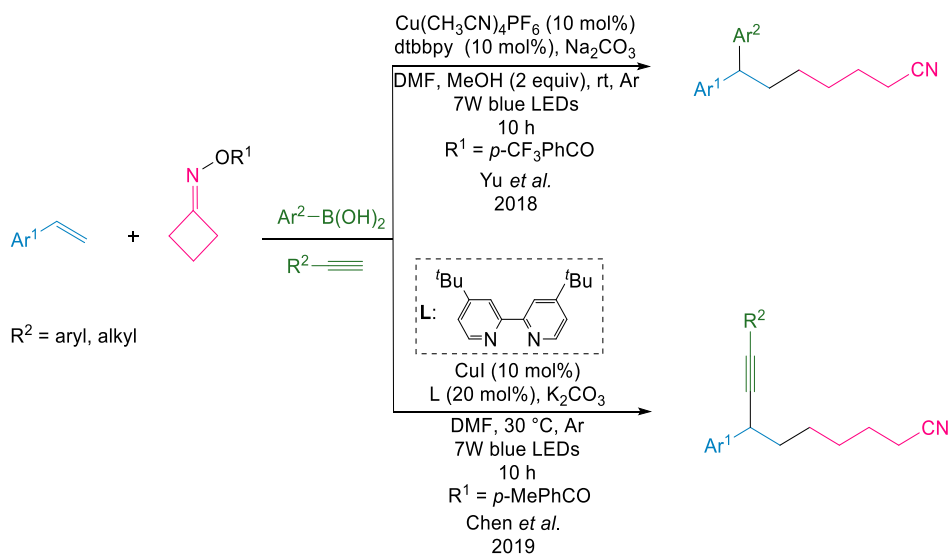
generate an alkyl or aryl radical. The newly formed C-centered radical adds to the C-C double bond providing the benzyl anion after reduction by the photocatalyst and reacts with CO₂. Finally, the carboxylate intermediate undergoes methylation in the presence of potassium formate (Scheme 43).



Scheme 43: Carboarylation of styrenes with CO₂ and aryl halides.

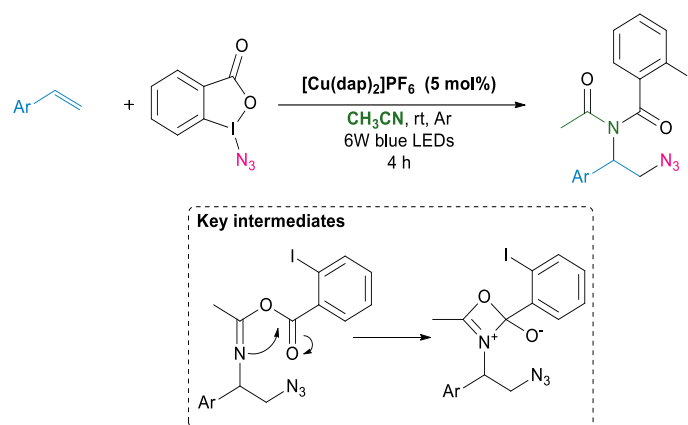
2.1.1.3. Organometallic complexes

Another method to harness the highly reactive open-shell intermediates involves the interaction with metal complexes which are able to trap the radical, allowing for further functionalization of the substrate *via* radical cross-coupling.⁹⁰ An elegant example has been reported by Yu *et al.* using copper catalyst both as a photocatalyst and for the activation of the substrate *via* oxidative addition. The authors designed carbo difunctionalization of styrenes employing cyclic oxime esters as radical sources and boronic acids as coupling reagents. As depicted in Scheme 44, the photocatalytic cycle starts with the formation of Cu(I) excited state *via* irradiation with visible light. Subsequent oxidation to Cu(II) through SET with the oxime ester results in its reduction and fragmentation to carboxylate (*p*-CF₃PhCO⁻) and a cyclic iminyl radical. The latter undergoes ring opening *via* β -scission to generate a cyanoalkyl radical that is promptly trapped by styrene. Simultaneously, the oxidized Cu(II) undergoes transmetalation with the boronic acid, followed by oxidative coordination of the benzyl radical intermediate (Cu(III)). Finally, reductive elimination delivers the desired product, closing the catalytic cycle. Given the experimental evidence, the authors could not rule out the activation of oxime ester by direct SET with Cu(I) ground state.⁹¹ Later, the same researchers extended the scope of this synthetic strategy employing alkynes as coupling partners.⁹²



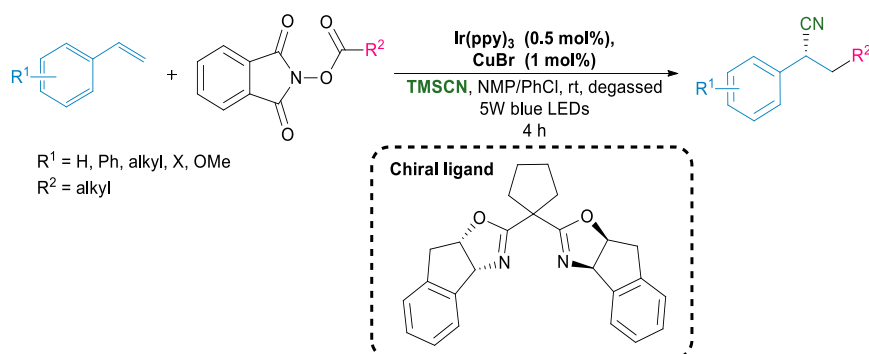
Scheme 44: Application of cyclic oxime esters as radical sources.

In the frame of copper photocatalysis, the work reported by Yu's group regarding the azidation/difunctionalization of styrenes through a three-component reaction with Zhdankin reagent is worth mentioning.⁹³ The reaction starts with the generation of azide radicals by reaction with the excited state of the photocatalyst which undergoes oxidative quenching. Addition to the double bond gives a benzyl radical intermediate which is trapped by a complex between the oxidized copper catalyst and the solvent, acetonitrile. The new copper complex gives a Ritter-type intermediate through reductive elimination. Capture by the iodobenzoate residue from Zhdankin reagent, followed by rearrangement, gives the final product. Interestingly electron-rich alkenes gave azidocarboxylated product by the oxidative formation of a benzyl cation and nucleophilic addition of iodobenzoate (Scheme 45).



Scheme 45: Photocatalyzed *N*-disubstitution of styrenes.

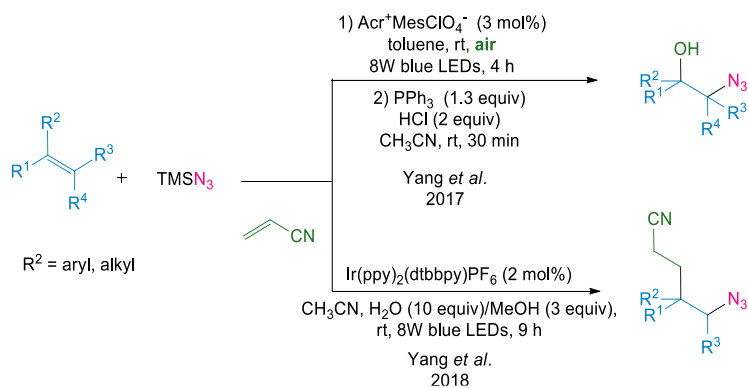
Finally, Sha, Deng *et al.* reported an elegant example of enantioselective carbodifunctionalization of styrenes by merging iridium photocatalysis and chiral copper complexes.⁹⁴ Mechanistically, alkyl radicals were obtained *via* photocatalyzed reduction of NHP esters and they readily added to the double bond. The photocatalyst is restored through oxidation of copper from Cu(I) to Cu(II) which in turn forms a complex with a chiral ligand. Addition of the benzyl radical results in further oxidation to Cu(III) species which can deliver the final product *via* reductive elimination. Chirality is induced in the formation of this C-C bond (Scheme 46).



Scheme 46: Photocatalyzed chiral azido alkylation of styrene.

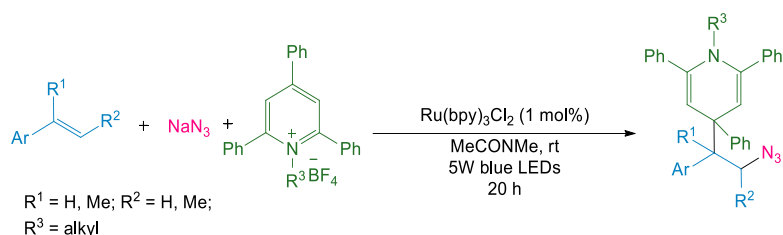
2.1.1.4. Other mechanisms

In all the aforementioned examples, vinyl radical intermediates experience straightforward quenching with the formation of ionic species. Nonetheless, under appropriate conditions, they can react further leading to the formation of new radical species. Perhaps, when a reagent acts as a radical scavenger, it traps the benzyl radical to form an open shell intermediate which finally gets reduced by the photocatalyst. An early example was reported by Lu's group in 2017 for the hydroxyazidation of alkenes.⁹⁵ TMSN₃ was the chosen azido radical source and molecular oxygen acted as the radical scavenger. Upon attack of the photocatalytically generated azido radical to styrene, the benzyl radical gets trapped by an O₂ molecule resulting in the formation of a peroxy radical, later reduced to an anion by the photocatalyst. The same product could also be formed by radical coupling with superoxide radical anion formed by photocatalyzed reduction of molecular oxygen. In 2018, the same group extended the scope employing acrylonitrile as radical scavenger obtaining highly derivatizable alkyl cyano azides as carboazidation products (Scheme 47).⁹⁶



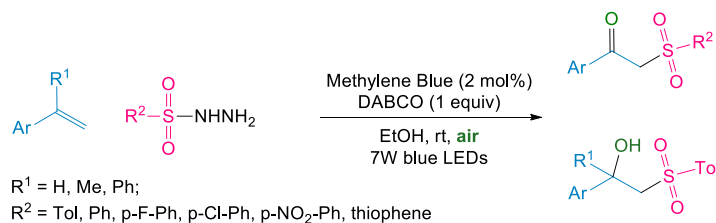
Scheme 47: Use of azide radicals toward oxo- and carbofunctionalization of styrenes.

Yang *et al.* contributed to the scope of carboazidation employing NaN_3 as radical source and pyridinium salts as radical acceptors for the synthesis of dihydropyridine derivative (Scheme 48).⁹⁷



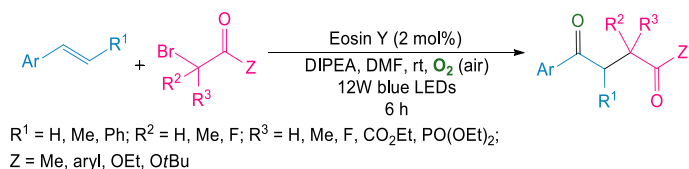
Scheme 48: Employment of NaN_3 as radical source.

In 2019, Wu *et al.* reported another example of MCR with molecular oxygen acting as a radical scavenger in the synthesis of β -keto/hydroxyl sulfones.⁹⁸ Upon the formation of peroxy radical by the reaction of vinyl radical with dioxygen radical, coupling occurs with a hydroperoxyl radical generated by photocatalytic reduction of oxygen to superoxide followed by protonation. This reaction sequence gives an unstable intermediate which decomposes to ketone through Russell fragmentation. The authors suggested radical homocoupling between vinyl and hydroperoxyl radicals as another plausible mechanism (Scheme 49).



Scheme 49: Synthesis of β -keto and β -hydroxyl sulfones.

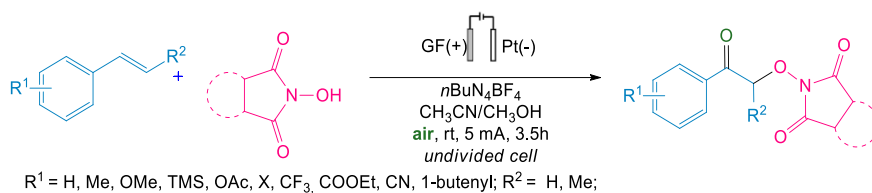
In 2020, Roy Chowdhury *et al.* reported the incorporation of dioxygen by vinyl radicals generated by the reaction of styrene with alkyl carbonyl radicals derived from α -bromoesters.⁹⁹ The peroxy radical reaction goes through a HAT-oxidation-deprotonation sequence where $i\text{Pr}_2\text{EtN}$ is also involved as HAT reagent to give the desired γ -ketoester or diketone (Scheme 50).



Scheme 50: Synthesis of γ -diketones and γ -ketoesters.

Dai *et al.* recently extended the scope to O -centered radicals by following the same reaction sequence in electrocatalytic conditions employing N -hydroxyphthalimides as a radical source.¹⁰⁰ Similar reaction manifold to the one described in photocatalysis is followed. Base-assisted SET oxidation of N -hydroxyphthalimide generates the O -centered radical. The base is formed *in situ* via cathodic reduction of water to hydroxide anion. Addition to styrene to form a stable carbon radical is followed by the capture of dioxygen from the air to give first a peroxy radical which decomposes to form a ketone through HAT and dehydration. Styrene dioxygenation efficiently occurred in the presence of both electron-donating and electron-withdrawing substituents on the phenyl ring. Notably, the presence of an aliphatic alkene, as in but-3-en-1-yl substituted styrene, did not affect the reaction and electrocatalytic oxidation

occurred selectively on the vinyl arene. Also, internal alkene smoothly reacted resulting in excellent regioselectivity (Scheme 51).



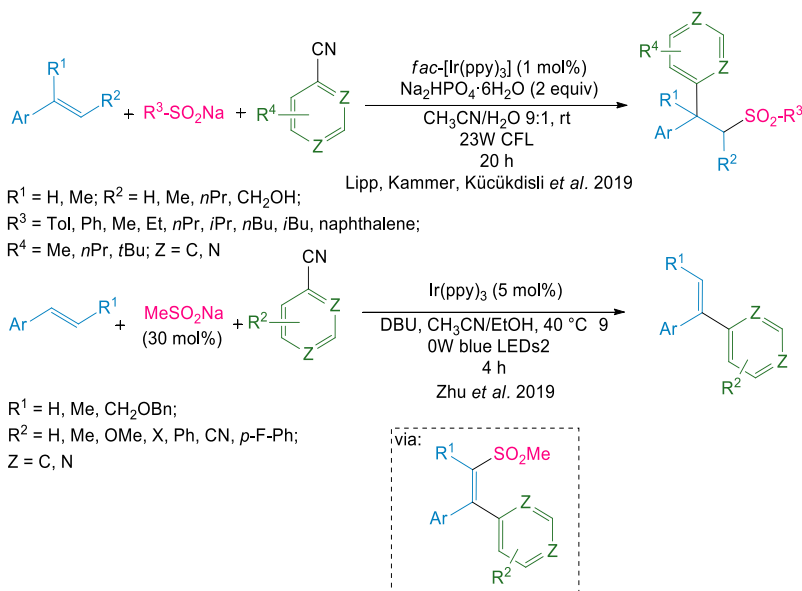
Scheme 51: Electrocatalytic oxidative functionalization with *O*-centered radicals.

Termination *via* radical coupling with *in situ* generated radicals has also been suggested by Ye *et al.* in their work on thiocarboxylation of styrenes where an iron/sulfur complex catalyst was responsible for the generation of a CO_2 radical anion and a thiol radical, which would sequentially attack the double bond (Scheme 52).¹⁰¹



Scheme 52: Photoredox catalyzed thiocarboxylation of styrenes.

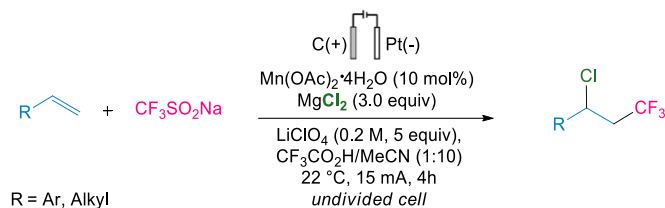
Nonetheless, to be able to undergo radical coupling with the vinyl radical the common radical polar crossover must be avoided. Persistent radical anions generated by the reduction of cyano pyridines have been proven effective to overcome the oxidation of vinyl radicals and delivering the radical coupling product. Two recent papers from Lipp, Kammer and Küçükdisli *et al.*¹⁰² and Zhu *et al.*¹⁰³ employed sulfonate as a radical source and cyano pyridine as a coupling partner. In both cases, the sulfone salts and the cyano pyridine are respectively oxidized and reduced by the photocatalyst to the respective radicals. First, the electrophilic sulfonyl radical reacts with the double bond followed by the C-centered radical anion. Interestingly in the conditions reported by Zhu *et al.* the difunctionalized product undergoes S-C bond cleavage and deprotonation to give the corresponding vinyl pyridine (Scheme 53).



Scheme 53: Photoredox carbofunctionalization with cyano pyridines.

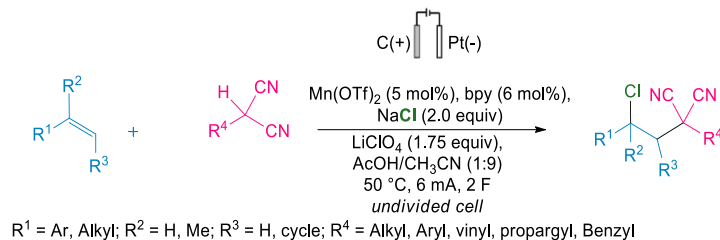
In 2018, Ye *et al.* reported the electrocatalytic trifluoromethyl chlorination of alkenes employing Langlois reagent as a radical source and MgCl .¹⁰⁴ The reaction was performed in galvanostatic conditions at room temperature in the presence of $\text{Mn}(\text{OAc})_2$ catalyst, LiClO_4 and trifluoroacetic acid in acetonitrile. In solution $\text{Mn}(\text{II})\text{-Cl}$ species is formed and undergoes anodic oxidation to $\text{Mn}(\text{III})\text{-Cl}$. Simultaneously the CF_3 radical is generated by anodic oxidation of Langlois reagent. This is possible thanks to redox potential matching of the two semi reactions: $\text{CF}_3\text{SO}_2^-/\text{CF}_3\text{SO}_2^-$ ($E_{p/2} = 800 \text{ mV}$) and $[\text{Mn}(\text{III})\text{-Cl}]/[\text{Mn}(\text{II})\text{-Cl}]$ ($E = 780 \text{ mV}$). Although competition of these two reactive species for the substrate could be possible, the rate of the two reactions is different enough to allow for a sequential mechanism that sees first the free radical addition to the double bond by the CF_3 radical, followed by reaction of the radical intermediate with the persistent radical, $\text{Mn}(\text{III})\text{-Cl}$, through metal-mediated chlorine atom transfer, more favorable than transient radical cross-coupling with a second CF_3 . Strong acid was required to avoid cathodic H^+ reduction to be a limiting factor. The reaction performed well with both activated and unactivated

alkenes delivering the products in moderate to good yields. Electron-rich styrenes underwent competing reactions and could not afford the disubstituted product. Natural products such as steroids and cinchonidine reacted smoothly confirming the benign nature of these mild conditions (Scheme 54).



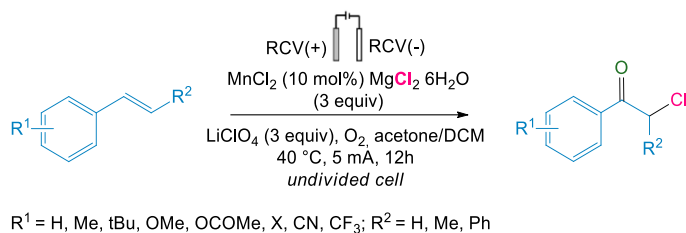
Scheme 54: Electrocatalytic trifluoromethyl chlorination of alkenes.

The same group in the following paper expanded the scope of alkyl radical sources to malononitriles.¹⁰⁵ The reaction conditions have been slightly modified to better fit the reactivity of malononitriles. In particular, the nature of Cl source was critical as MgCl_2 afforded solely the dichlorinated product. The choice, therefore, landed over the less soluble NaCl in order to control the concentration of Mn(III)-Cl and slow down the chlorination in favor of the attack by the malononitrile radical. As for the catalytic system, Mn(OTf)_2 as precatalyst in combination with 2,2'-bipyridine (bpy) as the ligand gave the best results. Notably, also a higher temperature was required. The reaction delivered the difunctionalized products in good to excellent yields with a variety of substituents. Functionalities as aldehyde and benzyl chloride were not affected by the reaction conditions and neither oxidation nor nucleophilic substitution occurred. As predictable the steric hindrance of malononitriles prevented successful reaction with polysubstituted alkenes. The authors also reported one example of bromoalkylation by replacing NaCl with NaBr and conducting the electrolysis at room temperature, and the product could be obtained in 40% yield (Scheme 55).



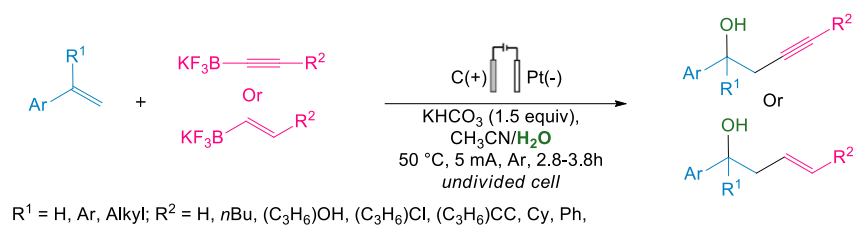
Scheme 55: Electrocatalytic alkyl chlorination.

As reported by Tian *et al.* in absence of other radical sources manganese can catalyze the direct addition of chlorine radicals to the double bond under electrolysis.¹⁰⁶ The reaction occurs upon anodic formation of the persistent Mn(III)-Cl radical metal complex. As the authors run the electrolysis in the presence of oxygen, the latter was reduced to superoxide radical and underwent homocoupling with the benzyl radical and decomposition to benzyl alcohol. Further oxidation generated chloroacetophenones as final products (Scheme 56).



Scheme 56: Electrocatalytic chlorine addition to styrenes.

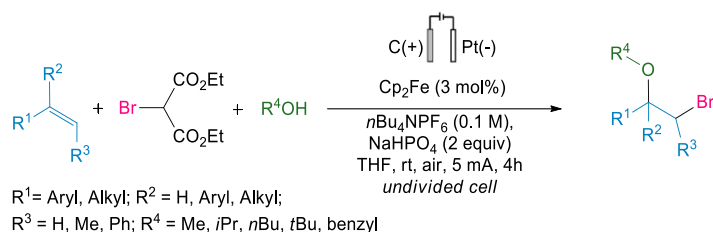
In 2018, Xiong *et al.* exploited the direct electrochemical SET oxidation of the double bond to a radical cation in the oxidative difunctionalization of styrenes with alkenyl and alkynyl trifluoroborate salts.¹⁰⁷ The electrophilic radical is believed to react with the trifluoroborate through a concerted mechanism with simultaneous formation of a C-C bond and cleavage of the C-B bond, resulting in a functionalized benzyl radical. This hypothesis was supported by DFT calculations. Further anodic oxidation gives a benzyl cation intermediate amenable to nucleophilic attack by water. Operatively, the reaction was conducted in galvanostatic conditions with graphite rod/Pt electrodes in an acetonitrile/water solvent mixture with the addition of KHCO_3 . The amount of water was crucial as it not only acted as reagent but was also required to reach adequate solubility of the salts. The best results were obtained with a 5:1 MeCN/H₂O ratio. Substitution of water with methanol smoothly delivered the methoxylated product. To underline the specificity of electrocatalysis in enabling the reaction, the authors subjected the reagents to previously reported non-electrochemical conditions for aryl alkenes SET oxidation. Both photocatalysis and chemical oxidants could not sustain the multi-component reaction and delivered solely oxidated monofunctionalized products (Scheme 57).



Scheme 57: Electrocatalytic oxidative addition of alkenes and alkynes.

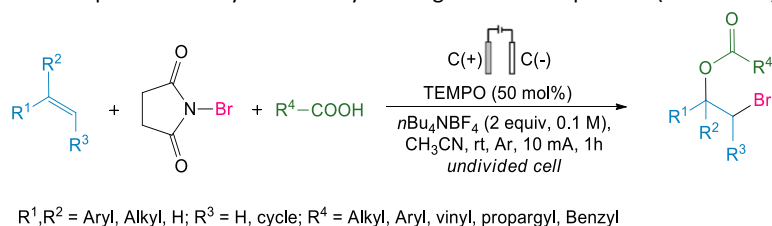
Later the same group reported the applicability of this strategy in the fluoroalkynylation of arylalkenes with trifluoroborates and $\text{Et}_4\text{NF}\cdot 3\text{HF}$ leading to fluoroalkynylation.¹⁰⁸ The reaction mechanism follows the same steps already described and the nucleophile, F^- , is generated through cathodic reduction of HF with concomitant H_2 evolution.

Recently Zhang *et al.* described another example of styrene activation by anodic oxidation in the presence of diethyl 2-bromomalonate and alcohol's alkoxyhalogenation reaction.¹⁰⁹ Interestingly, in contrast to previous reports, the alkyl bromide did not undergo oxidation to C-centered radical and attacked the double bond. Instead, styrene is believed to undergo anodic oxidation *via* the mediation of iron catalyst to radical cation. Meanwhile, bromide anions are generated *via* $\text{S}_{\text{N}}2$ between bromo malonate and methanol, or cathodic reduction of the malonate. Molecular bromine is also formed *via* anodic oxidation of bromide anions. Reaction of the radical cation intermediate with bromine the bromide itself gives the substituted benzyl radical subsequently oxidized to cation and trapped by the alcohol (Scheme 58).

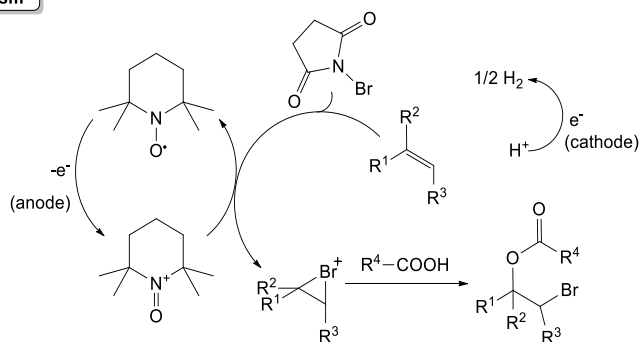


Scheme 58: Electrocatalytic oxidative bromination of styrene.

Wan *et al.* in 2019 devised an alternative approach toward oxibromination of styrenes by employing *N*-bromosuccinimide as a bromine source and carboxylic acids as nucleophiles.¹¹⁰ Electrolysis in galvanostatic conditions employing carbon rod as anode and carbon plate as cathode with $n\text{Bu}_4\text{NBF}_4$ as electrolyte, delivered the desired disubstituted product. The addition of an oxidant such as TEMPO, adjuvated the process resulting in a higher yield. Notably, the reaction was almost entirely suppressed when the current was not applied. Moderate to high yields could be obtained with variously substituted styrenes. Substitution on 1 and 2 positions did not significantly hamper the reaction and also aliphatic alkenes reacted in good yields. Both aryl and alkyl carboxylic acids smoothly reacted and also Boc protected amino acids could deliver the product in moderate yields. Mechanistically, a possible pathway sees as first step the bromine addition to the alkene, adjuvated by TEMPO⁺ formed at the anode, leading to the formation of a cyclic bromonium intermediate. Nucleophilic attack by the carboxylic acid gives the final product (Scheme 59).



Mechanism

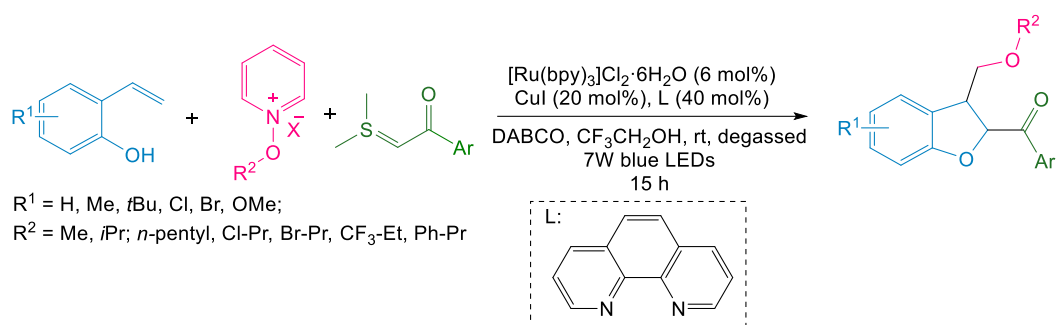


Scheme 59: Electrocatalytic oxibromination of alkenes with *N*-bromosuccinimide.

In 2021 Xiong *et al.* designed a four-component reaction following a similar pathway involving double bond activation through the

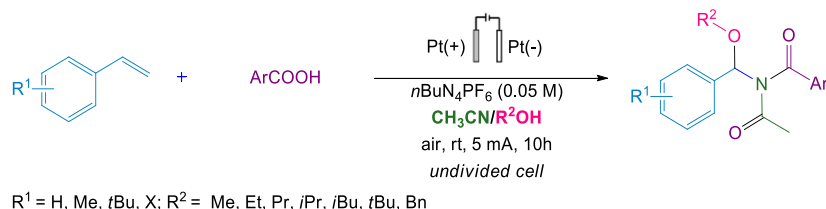
formation of a iodonium cyclic intermediate.¹¹¹ *Ortho*-amino styrene was the substrate of choice and ammonium iodide was selected as iodide source *via* anodic oxidation. An *in situ* formed carbamate by reaction between CO₂ and an amine act as a nucleophile. The reaction of the double bond with iodine gave the iodonium intermediate and cyclization to 3-iodoindoline followed. Finally, nucleophilic substitution with the carbamates occurs.

Recent work from Yuan *et al.* reported the generation of radical species on both reductive and oxidative sides of the photocatalytic cycle.¹¹² In particular, sulfur ylides and *N*-alkoxy pyridinium salts were found able to simultaneously undergo oxidation and reduction respectively when treated in photocatalytic conditions employing ruthenium catalyst. Copper-assisted attack of alkoxy radical onto 2-vinyl phenol followed by coupling with the alkylthio persistent radical, gives the key intermediate which evolves into the final dihydrobenzofuran *via* intramolecular S_N² (Scheme 60).



Scheme 60: Photoredox synthesis of dihydrobenzofurans from 2-vinyl phenol.

We find it worth ending this section with a recent work from Zhang *et al.* describing an example of a radical four-component reaction involving Mumm rearrangement *via* 1,3-(O→N) acyl transfer.¹¹³ The reaction involves direct anodic oxidation of styrene double bond followed by nucleophilic attack by an alkoxy anion formed through cathodic reduction. The benzyl anion is then oxidized to a cation amenable of addition by acetonitrile leading to an iminium intermediate. Meanwhile, the carboxylic acid is also reduced to carboxylate which combines with the iminium ion to form an unstable intermediate that readily undergoes Mumm rearrangement (Scheme 61).



Scheme 61: Electrochemical four-component functionalization of styrene.

2.1.2. Activated and unactivated alkenes

Together with styrenes, alkenes are also prolific substrates for radical addition reactions. The reactivity patterns developed closely follow the examples described in the first section for styrene functionalization.

In 2012, Courant and Masson presented a redox/neutral mechanistic approach for the α -alkylation of imines, where diethylbromomalonate was used as radical source, able to attack enamides, precursors of the desired acyliminium intermediate.¹¹⁴ Alcohols, together with triethylsilane as reducing agent and TMSCN, were employed as nucleophiles to further decorate the cationic intermediate (Scheme 62).



Scheme 62: Three-component synthesis of *N*-carbamoyl α -alkylated imines.

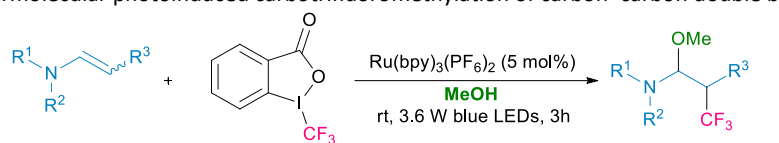
In 2017, Pettersson *et al.* developed a three component approach for the synthesis of β -functionalized δ -ketones, using carboxylic acids as acyl radical precursor, silylenolethers and electron-poor alkenes (Scheme 63).¹¹⁵



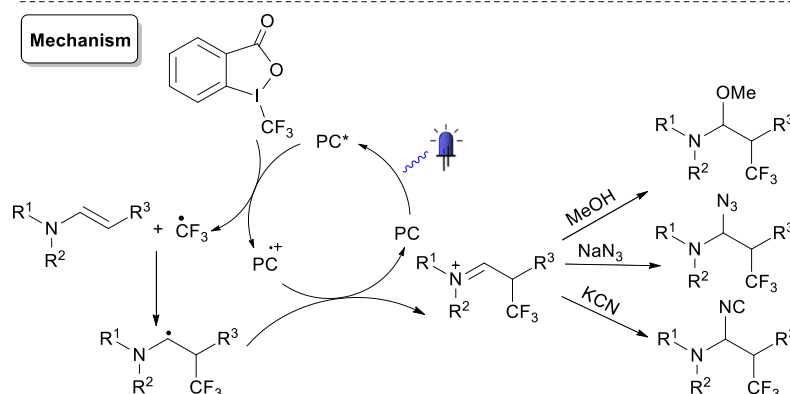
$R^1 = \text{X, Me, OMe}$; $R^2 = \text{alkyl, heterocycle}$

Scheme 63: 1,2-Acylalkylation of alkenes to form β -functionalized δ -diketones.

The highly decorated molecular scaffold obtained proved the versatility of this photoredox catalyzed approach, which was further enriched with the installation of a trifluoromethyl group and a nucleophilic substituent to form β -trifluoromethyl amines from enecarbamates in an efficient manner.¹¹⁶ Togni's reagent was employed as a trifluoromethyl radical source, obtained upon single-electron reduction, mediated by the photocatalyst. To form β -perfluoroalkylated amino derivatives, a hypervalent iodine reagent bearing a C_2F_5 substituent was used instead. Through this approach, C-, N-, and O-based nucleophiles could also be used to achieve this multicomponent intermolecular photoinduced carbotrifluoromethylation of carbon-carbon double bonds (Scheme 64).

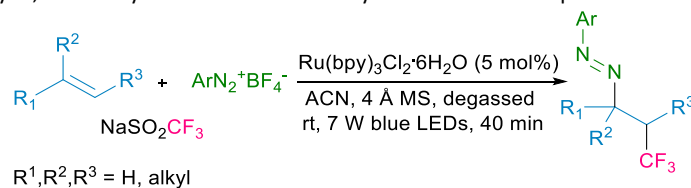


$R^1 = \text{Cbz, Bn, Boc etc.}$; $R^2 = \text{H, alkyl}$, $R^3 = \text{alkyl}$



Scheme 64: Three-component oxy-, amino-, and carbotrifluoromethylation of enecarbamates.

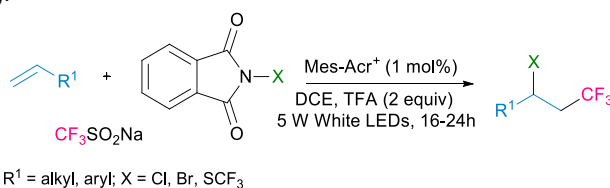
The trifluoromethylation of unactivated alkenes was also achieved using Langlois' reagent.¹¹⁷ Aryldiazonium salts were employed to form diazocompounds, useful precursors for the construction of heterocyclic scaffolds. A range of aliphatic alkenes, together with few styrenes, could be employed, and many substituents on the aryldiazonium counterpart were tolerated as well (Scheme 65).



$R^1, R^2, R^3 = \text{H, alkyl}$

Scheme 65: Azotrifluoromethylation of alkenes.

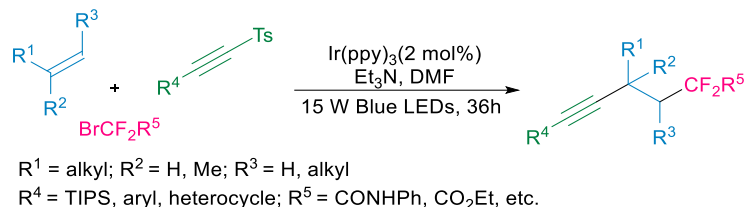
Given the importance of the trifluoromethyl group in drug discovery, many more transformations have been developed to achieve the difunctionalization of unactivated alkenes. As an example, Fang *et al.* were able to obtain the chloro-, bromo- and trifluoromethylthio- trifluoromethylation of structurally variegated alkenes in good yields, employing Mes-Acr⁺ as photocatalyst and N-halophthalimide or N-trifluoromethyl saccharin as halogen transfer reagents. Langlois' reagent was instead used to install the trifluoromethyl group (Scheme 66).¹¹⁸



$R^1 = \text{alkyl, aryl}$; $\text{X} = \text{Cl, Br, SCF}_3$

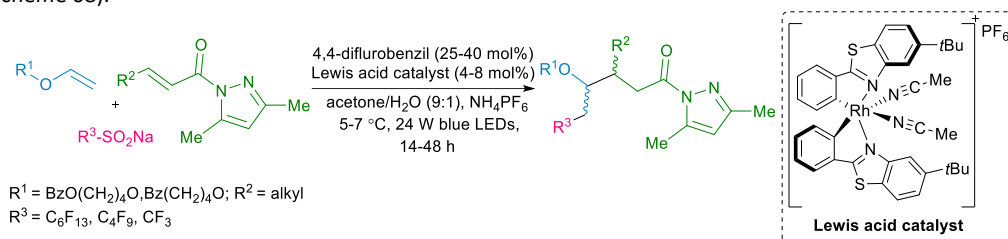
Scheme 66: Chloro-, bromo- and trifluoromethylthio-trifluoromethylation of unactivated alkenes.

β -Difluoro alkylated alkynes were also prepared using an elegant three-component strategy involving the first addition of a difluoroalkyl group on an unactivated alkene, then followed by a further attack on alkynyl sulfones.¹¹⁹ The optimal conditions were applied to both terminal and internal alkenes, while the electronic properties of the alkynes showed great influence on the reaction outcome, with electron-rich alkynes being more reactive. Various perfluoroalkylated reagents could be employed as well. The authors were therefore skillfully able to tune the reactivity towards the desired product, avoiding the possible side reactions that could occur in the presence of alkenes and alkynes in the same reaction mixture (Scheme 67).



Scheme 67: Alkynyldifluoroalkylation of unactivated alkenes.

In 2018, Ma *et al.* were able to achieve the asymmetric synthesis of fluoroalkyl containing compounds in a multicomponent fashion.¹²⁰ Upon radical formation, a fluorinated radical first attacks electron rich alkenes. This step is then followed by a chiral-at-rhodium Lewis acid stereo controlled addition on acceptor substituted olefins. Good diastereoselectivities were observed with natural chiral scaffold derivatives (Scheme 68).



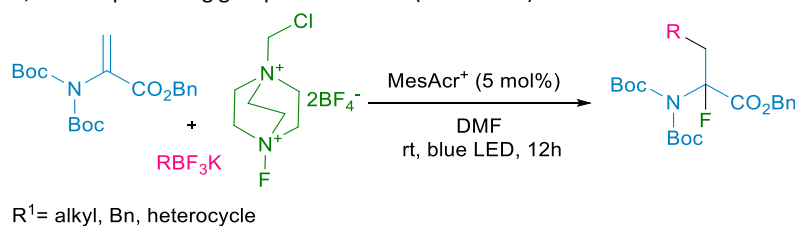
Scheme 68: Asymmetric synthesis of fluoroalkyl containing scaffolds.

In 2019, Li *et al.* incorporated fluoroalkyl reagents through radical addition catalyzed by visible light on non-activated alkenes.¹²¹ A HAT step is the key passage that enables the oxidation of a benzylic position in the presence of DMSO, acting as both solvent and oxidant. The construction of 1,6-fluoroalkyl ketones was achieved with mild reaction conditions and a variety of fluoroalkylating reagents, including bromodifluoroacetamide derivatives, perfluorohexyl and perfluorooctyl bromides (Scheme 69).



Scheme 69: Synthesis of fluoroalkyl ketones using DMSO as oxidant.

Another interesting approach to form α -fluoro- α -amino acid derivatives was presented in the same year by Sim *et al.*¹²² The preparation of unnatural amino acids has tremendous importance, and the implementation of mild radical approaches for the site-specific chemical mutagenesis of proteins is gaining increasing interest. In this context, trifluoroborates were employed as a radical source, enabling the installation of alkyl, α -alkoxymethyl, α -aminomethyl, β -aminoethyl and β -carbonylalkyl functionalities. On the other hand, Selectfluor was used as a fluorine source. With the aim to render these unnatural amino acids utilizable as building blocks for more complex peptides, various protecting groups were tested (Scheme 70).



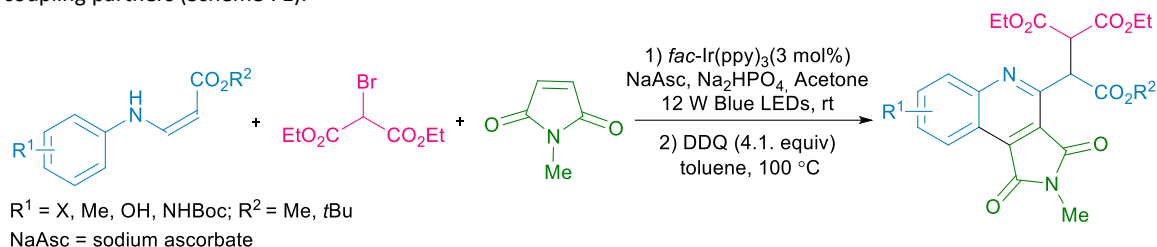
Scheme 70: Synthesis of α -F α -aminoacid derivatives.

To enrich the landscape of trifluoromethylated scaffolds, Wang *et al.* skillfully prepared a range of β -trifluoromethyl hydrazines, that show great utility as amine precursors or in the synthesis of heterocyclic scaffolds.¹²³

Guo *et al.* also applied trifluoromethylation strategy to functionalize unactivated alkenes and form, upon addition to vinyl sulfones,

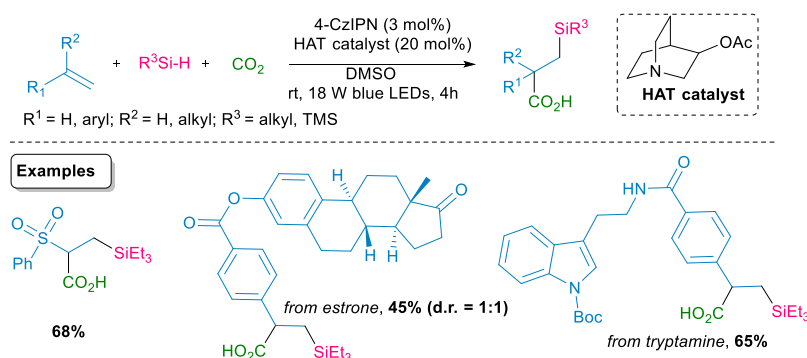
styrene-based activated olefines.¹²⁴ Through this strategy, the trifluoromethylation scope was therefore broadened to the formation of unsaturated bonds.

Alkene functionalization has also been applied to the synthesis of heterocyclic molecules, such as quinolines bearing different functionalities, through the careful tuning of the electronic properties of the reactants involved. For this purpose, a combination of electron-poor alkyl halides and alkenes (*N*-methyl maleimide, fumaronitrile as examples) and electron-rich β -aminoacrylates was studied.¹²⁵ This cascade reaction therefore led to the formation of three consecutive bonds, with the chemoselective incorporation of the coupling partners (Scheme 71).



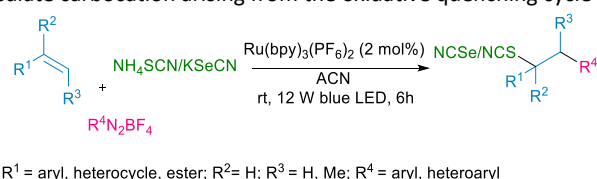
Scheme 71: Three component synthesis of quinolines.

With the aim to include different functionalities, Hou *et al.* used CO_2 as C1 synthon, Si-H and $C(sp^3)$ -H bonds as feedstock for the difunctionalization of electron-poor alkenes.⁸⁸ Atmospheric pressure of CO_2 was sufficient to obtain its incorporation into the organic skeleton, while the mediation of a HAT catalyst was necessary to avoid the hydrosilylation product derived from the protonation of the radical intermediate. The catalytic system was therefore employed to install not only alkylsilyl groups, but also α -*N*-, *O*- and *S*-alkyl groups. The implementation of the method using photo-flow technology enabled to perform a gram-scale synthesis of the desired product within 30 min of irradiation (Scheme 72).



Scheme 72: Difunctionalization of alkenes with CO_2 and silanes or $C(sp^3)$ -H alkanes.

The arylthiocyanation/ arylselenocyanation of acrylates was also accomplished by UI Hoque *et al.*¹²⁶ Aryldiazonium salts were employed as aryl radical source, while ammonium thiocyanate and potassium selenocyanate proved to be efficient nucleophiles for the functionalization of the intermediate carbocation arising from the oxidative quenching cycle of the photocatalyst (Scheme 73).



Scheme 73: Arylthiocyanation/ arylselenocyanation of acrylates.

Enamides, in combination with carboxylic acid derived redox active esters (RAEs) and indoles, were utilized to access chiral amine derivatives.¹²⁷ Interestingly, a chiral lithium phosphate catalyst was fundamental to promote the aggregation of enamides and RAEs through hydrogen bond interactions by acting as a pocket to form chiral iminium intermediates. This was then involved in a Friedel-Crafts reaction with indoles. An energy transfer mechanism facilitated by the photocatalyst, was devised by the authors to explain the observed reactivity (Scheme 74).



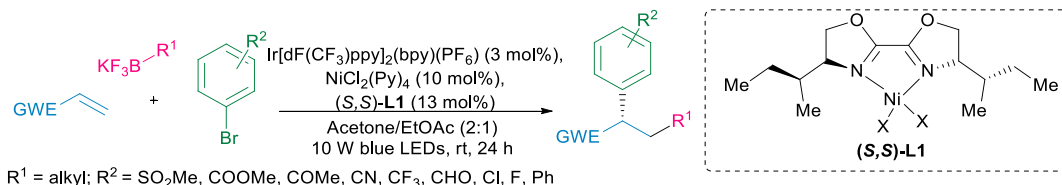
Scheme 74: Asymmetric dicarbofunctionalization of enamides.

In 2020, vinyl boronates were also difunctionalized in a chemoselective manner through a dual photoredox/ Ni catalyzed approach.¹²⁸ Sun, Duan *et al.* employed alkyl bromides as a radical source that, upon reduction mediated by the photocatalyst, are able to add on the vinyl boronate, giving rise to a stabilized radical intermediate that recombines with a Ni(II) species derived from the oxidative addition of an aryl bromide. The final reductive elimination step gives rise to the desired product. In addition to chemoselectivity, the reaction featured high functional group tolerance. Three different electrophilic reagents were therefore successfully combined in the same molecular scaffold (Scheme 75).



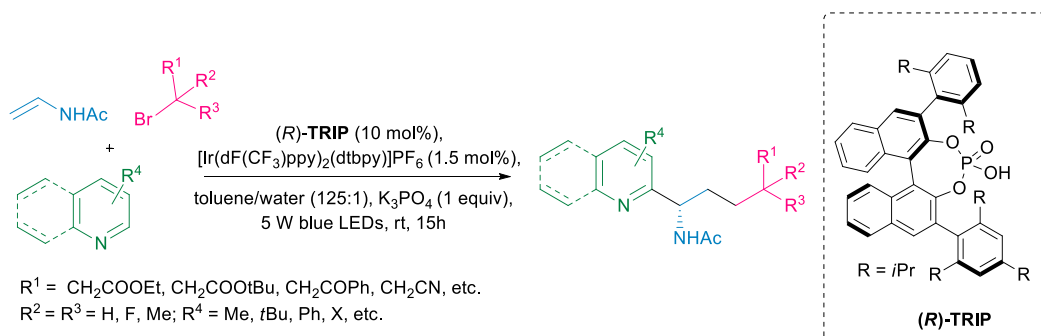
Scheme 75: Difunctionalization of vinyl boronates.

In the same year, a dual photoredox/ Ni catalysis approach was applied to the enantioselective difunctionalization of various electron-withdrawing alkenes (e.g. acrylates, vinyl amides, vinyl ketones, vinyl phosphonates).¹²⁹ Secondary and tertiary alkyltrifluoroborates were used as a radical source, together with aryl bromides. A chiral bioxazoline ligand was chosen for this enantioselective transformation. Interestingly, the utility of the method was demonstrated through the synthesis of a lead compound of piragliptin, reducing the number of synthetic steps from eight to three (Scheme 76).



Scheme 76: Enantioselective carboarylation of alkenes.

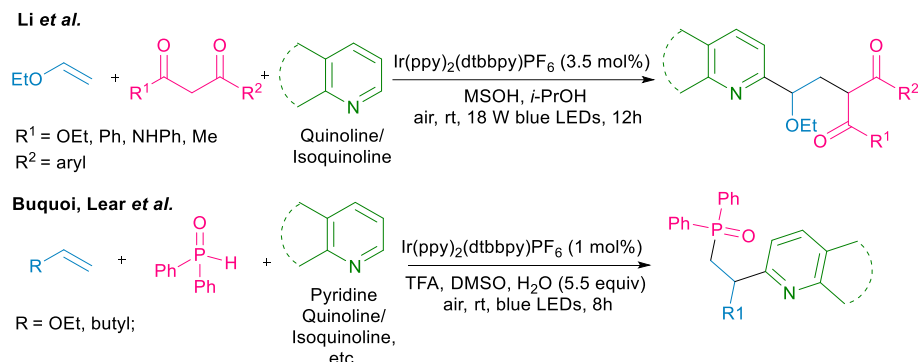
With the aim to expand the applicability of the Minisci reaction to more than two components, Zheng and Studer presented a multicomponent enantioselective radical addition on *N*-heterocycles, employing a chiral phosphoric acid to achieve enantioselectivity.¹³⁰ γ -Amino acids and heterocyclic diamines were synthesized, as a result of the use of enamides as radical acceptor and α -bromo carbonyl or *O*-acyl hydroxylamines as radical precursors. Whether enantioselectivity is controlled by radical addition on the heterocyclic core or by the final deprotonation step remains unclear. Nevertheless, the reaction proved to be highly regioselective for the C2 position of heteroarenes, and gave high levels of enantioselectivity (Scheme 77).



Scheme 77: Asymmetric synthesis of heterocyclic γ -amino acids.

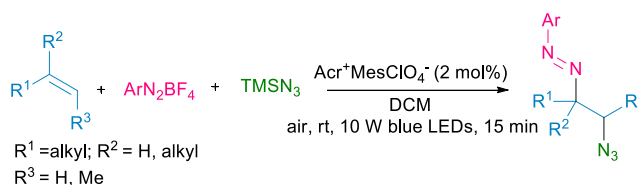
Li *et al.*¹³¹ and Buquoi, Lear *et al.*¹³² also reported the combination of a radical precursor and electron-rich or unactivated alkenes multicomponent alkylation of *N*-heterocycles. 1,3-Dicarbonyl compounds and phosphine oxides were respectively employed as

radical source. In the first case, both quinolines and isoquinolines were subjected to the transformation, while in the second work, pyridines were reactive as well, expanding the scope. The presence of air as the oxidant was necessary for the regeneration of the photocatalyst. To ensure the polarity match between the radical intermediates, fine tuning of the electronic properties of the reagents was required (Scheme 78).



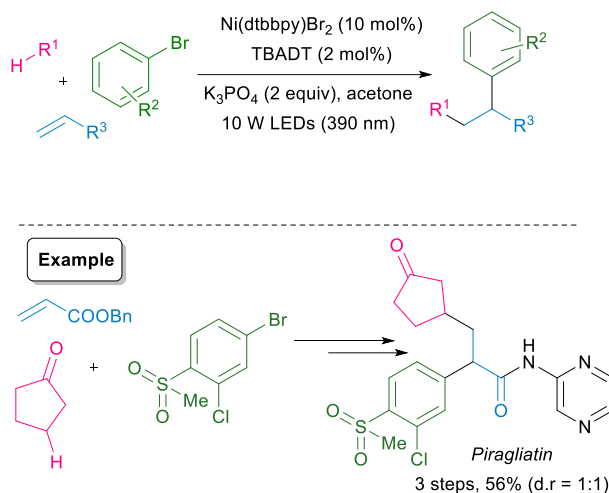
Scheme 78: Multicomponent alkylation of heterocyclic scaffolds in a Minisci fashion.

This year, Shen *et al.* presented the formation of unsymmetric azo compounds with the aid of photoredox catalysis to form an azido radical from TMSN_3 , which could attack unactivated alkenes in a Giese type fashion.¹³³ In this case, in contrast to the common employment of aryl diazonium salts as radical source, these species behaved as radical acceptors, enabling the generation of i.a. diazocompounds -common structures in pigments-, food additives, and drug molecules (Scheme 79).



Scheme 79: Synthesis of unsymmetric azo-compounds.

In addition to the reported examples, it is remarkable to mention a recent methodology developed by Xu *et al.*,¹³⁴ that combined tetrabutylammonium decatungstate (TBADT) as a direct hydrogen atom abstractor together with Ni-catalysis to achieve the difunctionalization of alkenes with alkanes (cyclic, acyclic, heteroatom containing) and aryl halides. The power of this strategy relies on the ability to obtain C-H functionalization without the need of pre-activated starting materials, and enables the late stage functionalization of relevant scaffolds (camphene, sclareolide, tropinone). Interestingly, through the developed method, the authors accomplished the synthesis of piragliatin in 3 steps instead of the previously necessary 12 steps (Scheme 80).



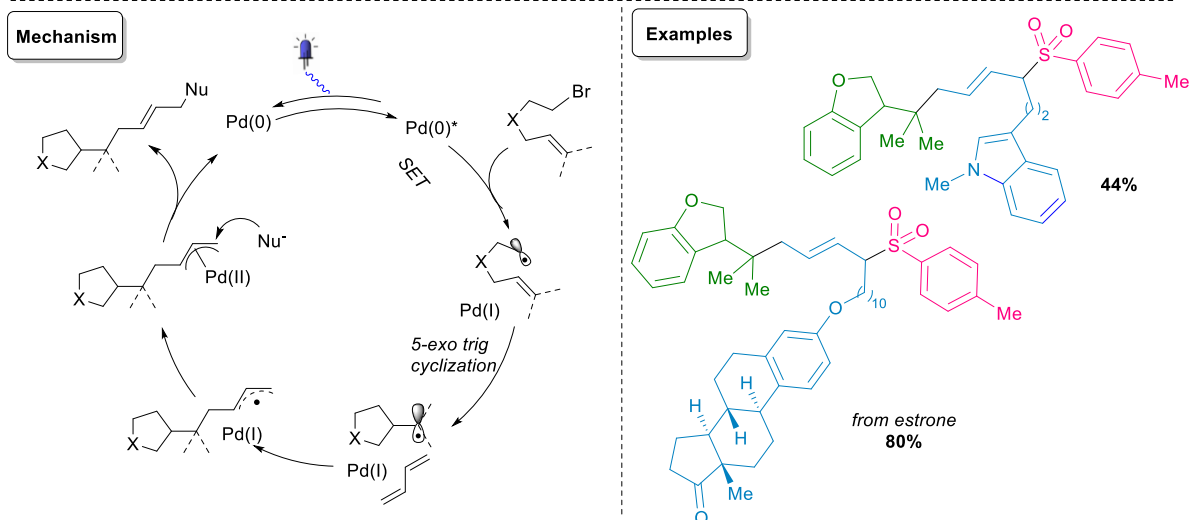
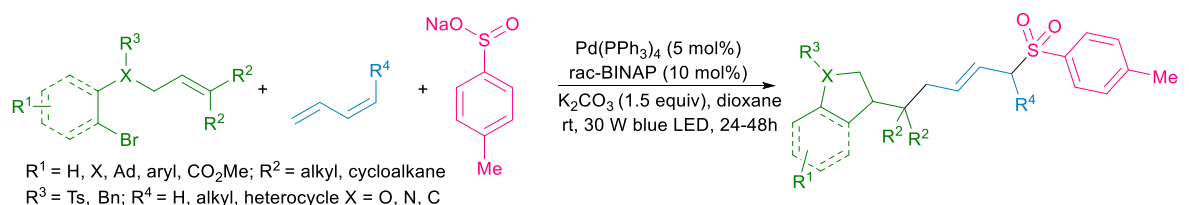
Scheme 80: Alkene functionalization through direct HAT/ Ni-catalyzed synthesis.

A free radical cascade cyclization was also presented in 2020 by Huang *et al.*¹³⁵ Alkyl and aryl sulfonates were employed as radical source to initiate the cascade reaction upon addition on dienes. By means of intermediate radical interception by a Ni catalyst, aryl halides were added to the molecular skeleton as well. The strategy was usefully applied to the synthesis of diversified unsaturated carbon cycles bearing a wide variety of functionalities, enabling the exploration of chemical space towards privileged scaffolds in medicinal chemistry and natural product synthesis (Scheme 81).



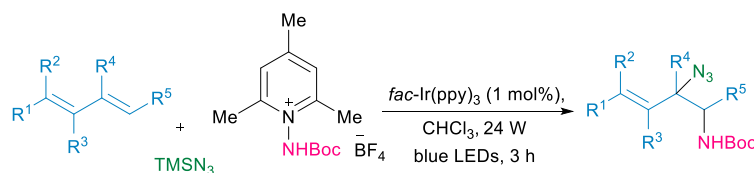
Scheme 81: Radical addition/cyclization/cross-coupling of 1,3-dienes.

In a report by Bellotti *et al.*, both a photochemical transformation and a cross-coupling step were catalyzed by a palladium-phosphine complex.¹³⁶ The authors developed a three-component dicarbonylation/allylic substitution reaction in a radical-to-polar fashion. With the aim to construct highly congested scaffolds, they employed olefin-tethered alkyl/aryl bromides, 1,3-dienes and nucleophiles as reaction partners. The mechanism of the reaction involved Pd(0) excitation by visible light, followed by reduction of the alkyl/aryl bromide to form an alkyl/aryl radical. Upon ring closure (5-*exo trig* cyclization), the radical intermediate intercepts the 1,3-diene to form a stabilized allyl radical, that is trapped by a Pd(I) complex to form a Pd(II)-allyl intermediate. Various nucleophiles were then employed to undergo allylic substitution and generate the final product. The robustness of the method was confirmed by its group tolerance and by the possibility to perform the reaction in the presence of water and at various concentrations. The reaction was also performed in flow, and higher efficiency was observed (Scheme 82).



Scheme 82: Dicarbonylation/allylic substitution reaction of 1,3-dienes.

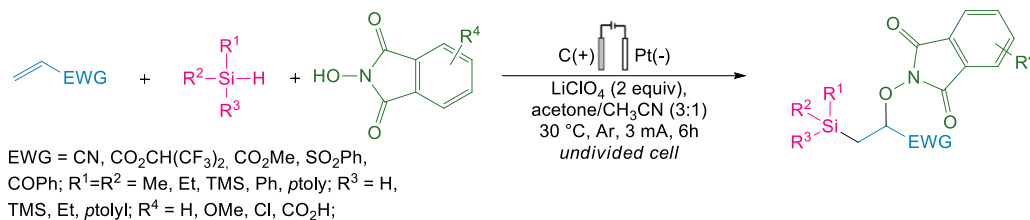
1,3-Dienes were also employed in a three-component amido-azidation reaction, where *N*-amidopyridinium salts were used as radical source and TMSN_3 as a nucleophile.¹³⁷ The authors noted that 1-alkyl and 1-aryl 1,3-dienes behaved differently under the optimized reaction conditions. While the aryl substitution only afforded the 1,2-amidoazidation product, the same regioselectivity was not observed for the alkyl counterpart. In this case, different selectivity ratios between 1,2- and 1,4-regioisomers were observed. The authors skillfully addressed the lack of selectivity by introducing a PPh_3 mediated reduction step. A facile 1,3-azide shift (Winstein rearrangement) of allyl azides takes place, thus forming an excess of the 1,2-regioisomer. To prove the utility of this scaffold, heterocyclic molecules were synthesized from 1,2-amidoazides (Scheme 83).



$\text{R}^1 = \text{aryl}, \text{heterocycle}; \text{R}^2 = \text{H}, \text{Ph}, \text{Me}; \text{R}^3 = \text{H}, \text{Me}$
 $\text{R}^4 = \text{H}, \text{alkyl}; \text{R}^5 = \text{H}, \text{Me}$

Scheme 83: Aminoazidation of 1,3-dienes.

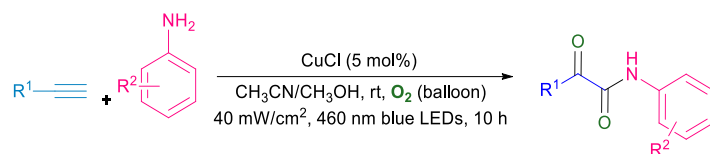
Finally, concomitant *O*- and *Si*- functionalization of activated alkenes has been recently reported by Ke *et al.* in electrocatalytic conditions employing hydrosilanes and *N*-hydroxyphthalimide (Scheme 84).¹³⁸



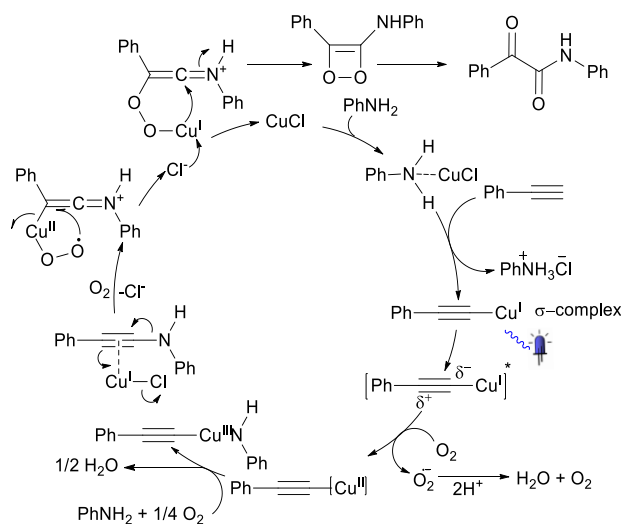
Scheme 84: Electrocatalytic radical silyloxygation of activated alkenes.

2.2. Alkynes

The presence of an additional C-C bond and concomitant change in hybridization results in different degrees of possible functionalization of alkynes compared to alkenes. This provides access to the synthesis of highly functionalized or complex cyclic structures. The activation of terminal alkynes by copper catalysts has largely proven to be a robust strategy. The umpolung of alkyne reactivity allowed the design of extremely successful reactivity pathways granting copper(I)-alkyne complexes long-lasting notoriety. Among others, we can name the reaction with azides which opened the way to click chemistry, and transmetallation reactions, mechanisms exploited in several palladium-catalyzed processes.¹³⁹⁻¹⁴¹ In the field of alkynes reactivity in photocatalysis,^{23,142,143} copper catalysis experienced a new wave of rising interest as the discovery of novel reactivity features demonstrated its ability to catalyze reactions previously believed to be exclusive of noble metals. The report of a visible light palladium-free copper-photocatalyzed Sonogashira reaction serves as a brilliant example.¹⁴⁴ Several studies on copper photocatalyzed multicomponent difunctionalization of alkynes have been reported and often oxygen acts as the ultimate quencher leading to the synthesis of carbonyl compounds. An early example from Sagadevan *et al.* involved the use of CuCl catalyst in the preparation of ketoamides from terminal alkynes and anilines.¹⁴⁵ Blue light irradiation has a crucial role in the progressing of the reaction through excitation of the alkenyl-Cu(I) sigma-complex. As result, ligand-to-metal charge transfer (LMCT) occurs, and a partial positive charge localizes on the acetylene ligand as well as a partial negative charge on the metal center. Further oxidation to Cu(II) intermediate and nucleophilic addition by aniline leads to C-N bond formation through reductive elimination. Trapping of molecular oxygen by a Cu π -complex forms a peroxy intermediate which through isomerization and consecutive formation of two C-O bonds restores CuCl. A peculiar dioxete intermediate is also formed in this step. Final cleavage of the O-O bond results in formation of the desired carbonyl compound. Several keto-anilides could be obtained in good to excellent yields employing a variety of electron-poor anilines and alkynes bearing both aryl and alkyl groups. The same strategy has been applied to the preparation of keto-esters¹⁴⁶ and diketo-sulfoximines (Scheme 85).¹⁴⁷



Mechanism



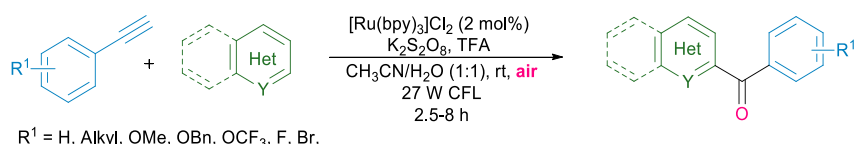
Scheme 85: Copper photocatalyzed oxoamination of styrenes.

The generation of highly reactive intermediates by oxidation of the triple bond has been widely explored and allowed for the unconventional use of alkyne synthons.

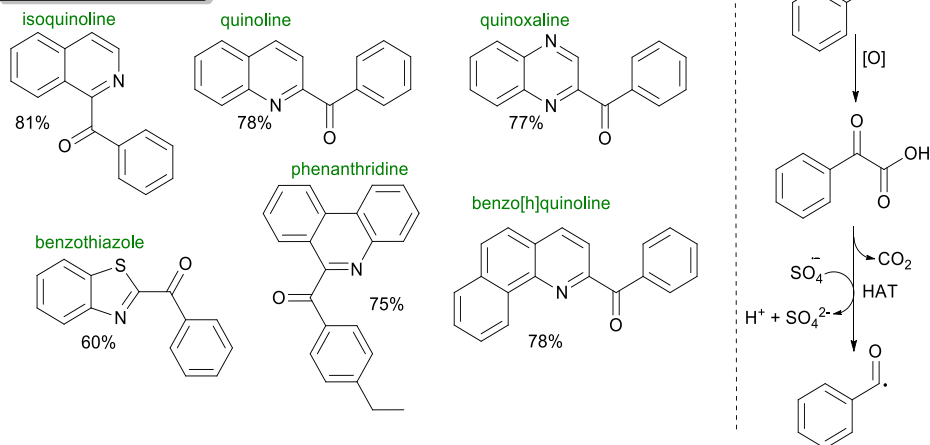
In an interesting paper from Ragupathi *et al.*, the authors reported the rearrangement of a ketoamide intermediate to amide with the evolution of CO.¹⁴⁸ The authors employed 2-aminopyridine as a substrate which, upon formation of the ketoamide through the aforementioned mechanism, is speculated to coordinate Cu(I) and promote the formation of a bidentate chelated Cu(II) superoxo/-peroxo complex. The latter reacts with the ketoamide generating an *N*-centered radical anion. Finally, CO elimination and radical recombination deliver the amide. In 2017, Sagadevan *et al.* obtained aryl ketones by applying the same conditions to the reaction between alkynes and phenols.¹⁴⁹

In situ formation of photoactive copper acetylide has been employed for the synthesis of 3-arylcoumarins through oxidative cascade cyclization with *N*-tosylhydrazones.¹⁵⁰

Fragmentation of oxidized alkyne derivatives was also reported by Sultan *et al.* in their work regarding photocatalyzed acylation of heteroarenes, where oxidation/decarboxylation/HAT sequence is believed to be responsible for the formation of an acyl radical subsequently trapped by *N*-heteroarenes (Scheme 86).¹⁵¹ Dioxete intermediate is also believed to be formed in the acetamidation of terminal alkynes by arylamines as reported by Katta *et al.*¹⁵²

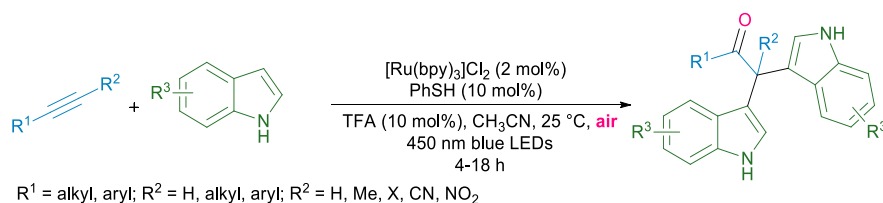


Scope of heteroarenes:

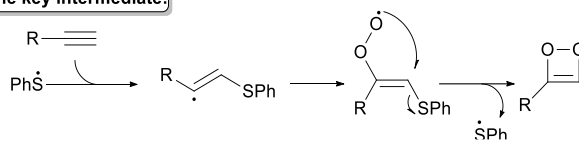


Scheme 86: Photocatalyzed oxidative synthesis of diaryl ketones.

Chatora *et al.* reported the oxocarbofunctionalization of alkynes mediated by catalytic amounts of thiophenol radical.¹⁵³ In this case, the S-centered radical generated through SET-oxidation/deprotonation sequence attacks the triple bond forming a vinyl radical, which is promptly trapped by molecular oxygen. As shown in Scheme 87, cyclization and concomitant elimination of the thiophenol radical, give the highly reactive dioxete intermediate which undergoes nucleophilic attack by two molecules of indole. The reaction conditions delivered the product in good yield with both alkyl alkynes and variously substituted phenylacetylenes. Internal alkynes were also found amenable to this reaction. The indole scope showed good results with both halogens and electron-withdrawing substituents such as NO₂. Employment of two different indoles has been attempted and the asymmetrical product could be obtained with yields as high as 41%.

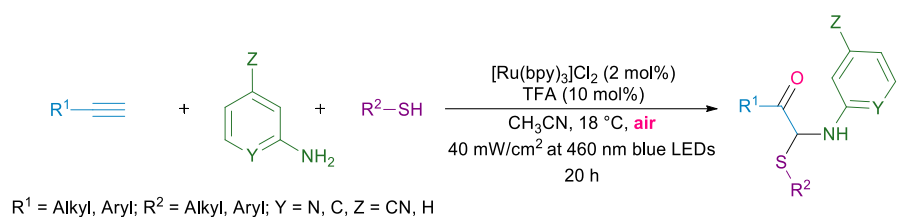


Synthesis of the key intermediate:

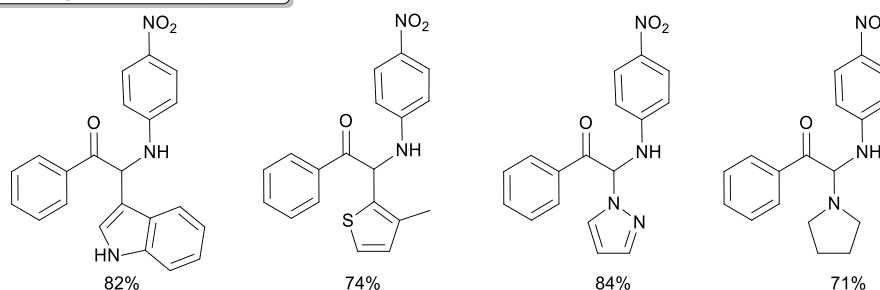


Scheme 87: Aminoazidation of 1,3-dienes

In a follow-up work, the researchers managed to trap an *N*-nucleophile as well as the thiol obtaining a wide scope of α,α -aminothioketones. The reaction performed well with alkyl and aryl substitution on both alkynes and thiols. The researchers successfully explored further exploitation of the optimized synthetic pathway through late-stage substitution of the thiophenol residue with carbon and *C*- and *N*-nucleophiles (Scheme 88).¹⁵⁴



Late-Stage modification products

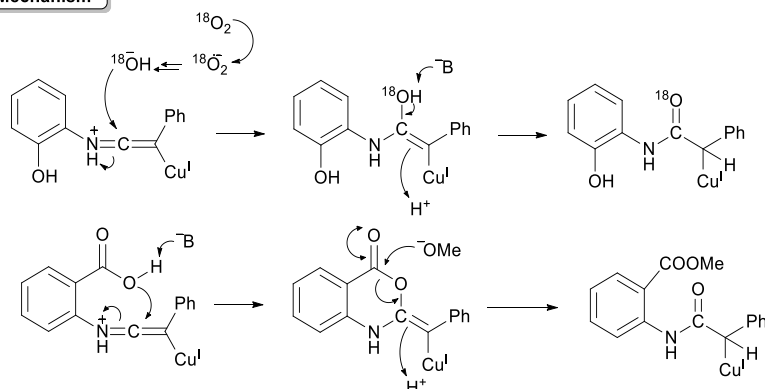


Scheme 88: Photoredox oxidative synthesis of α,α -aminothioketones.

Pampana *et al.* reported the synthesis of acetamides *via* a visible-light-promoted copper-catalyzed process between terminal alkynes and anilines.¹⁵⁵ Anilines bearing a carboxylic group on the *ortho* position yielded the corresponding methyl esters by further reaction with the solvent. Oxygen incorporation is believed to occur through nucleophilic attack onto the enamine intermediate by a hydroxyl anion generated *via* SET reduction of molecular oxygen to superoxide followed by decomposition in a basic environment. Interestingly, isotope labeling experiments with $^{18}\text{O}_2$ showed barely any isotope incorporation in the case of carboxylated substrates (2% against 92% for non carboxylated). This was explained by the authors suggesting the formation of a lactone intermediate followed by acyl substitution by the methoxide anion. Both alkyl and aryl alkynes were found amenable to the reaction conditions providing the desired amides in good yields (Scheme 89).



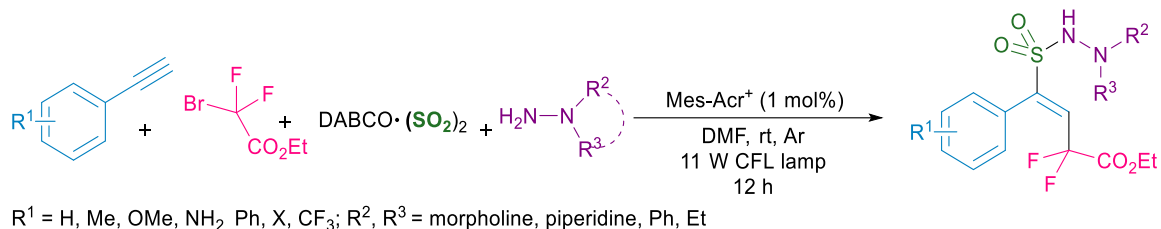
Mechanism



Scheme 89: Copper-catalyzed photoredox synthesis of arylamides.

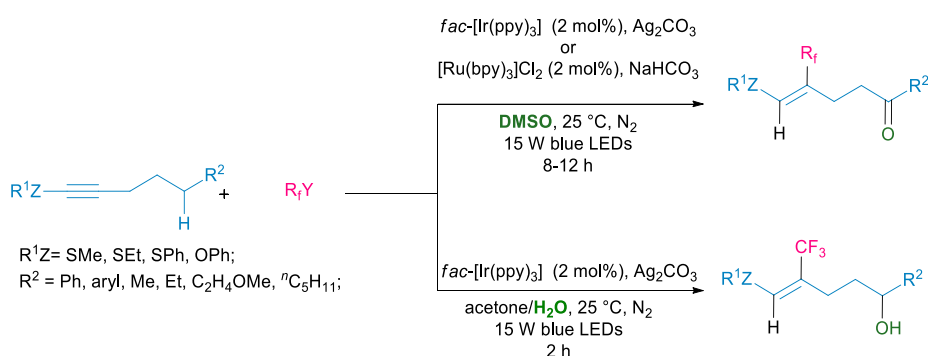
Malpani *et al.* employed Umemoto's reagent as radical source and water as nucleophile for the oxidative trifluoromethylation of alkynes.¹⁵⁶ The reaction follows the oxidative quenching cycle already extensively covered in section 2.1.1.1.. Recently, Lee *et al.* adopted the same activation strategy for the installation of fluorine atoms by the addition of hydrofluoric acid to the reaction mixture.¹⁵⁷ As expected, the vinyl cation intermediate successfully underwent nucleophilic attack by F^- anions delivering the desired fluoro-trifluoromethylated products in moderate to good yields. In 2017, Xiang *et al.* designed a four-component reaction through

difluoroalkylation/aminosulfonylation of alkynes.¹⁵⁸ The choice of the radical source landed on ethyl 2-bromo-2,2-difluoroacetate which generates a C-centered radical upon reduction by the photocatalyst *via* SET. Reaction with the triple bonds gives a vinyl radical subsequently trapped by SO₂. The sulfonyl radical finally combines with the N-centered radical obtained by photocatalytic oxidation of hydrazine, affording the desired product exclusively as (E)-isomers. Notably, attempts to extend the scope to alkyl-substituted terminal alkynes and other nucleophiles were unsuccessful (Scheme 90).

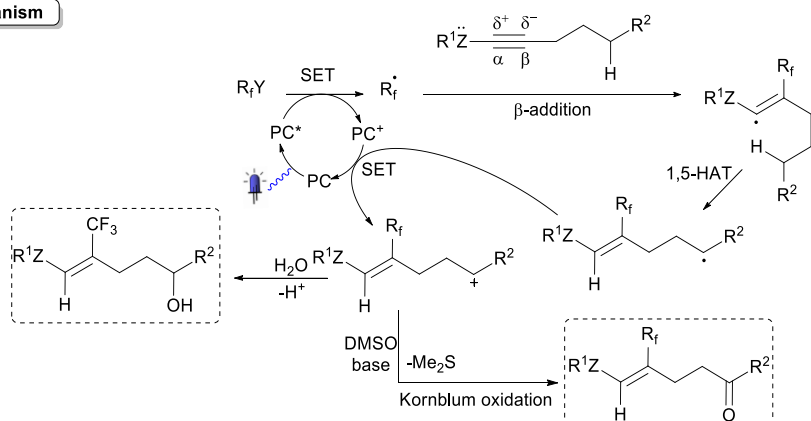


Scheme 90: Four component difluoroalkylation/aminosulfonylation of alkynes.

As a final example of fluoro-alkylation the recent report from Shang *et al.* is worth mentioning where remote oxyfluoroalkylation occurred employing *S*- and *O*-substituted alkynes.¹⁵⁹ The presence of a heteroatom enhances the nucleophilicity of the β -carbon which selectively reacts with the electrophilic radical. The vinyl radical formed on the α -carbon undergoes 1,5-HAT localizing the radical onto a distal carbon. Oxidation to carbocation follows and the reaction is completed by a nucleophilic attack either by water or DMSO to give the product as alcohol or ketone (Kornblum oxidation) (Scheme 91).

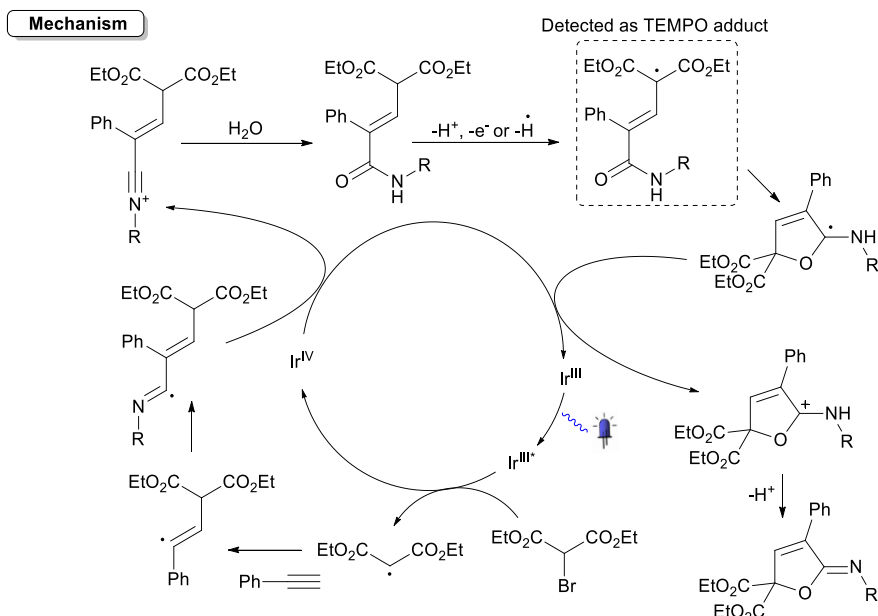
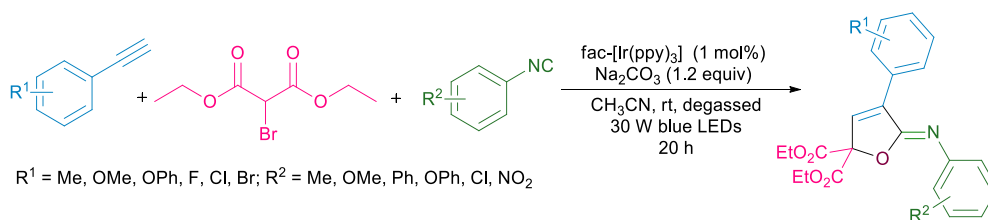


Mechanism



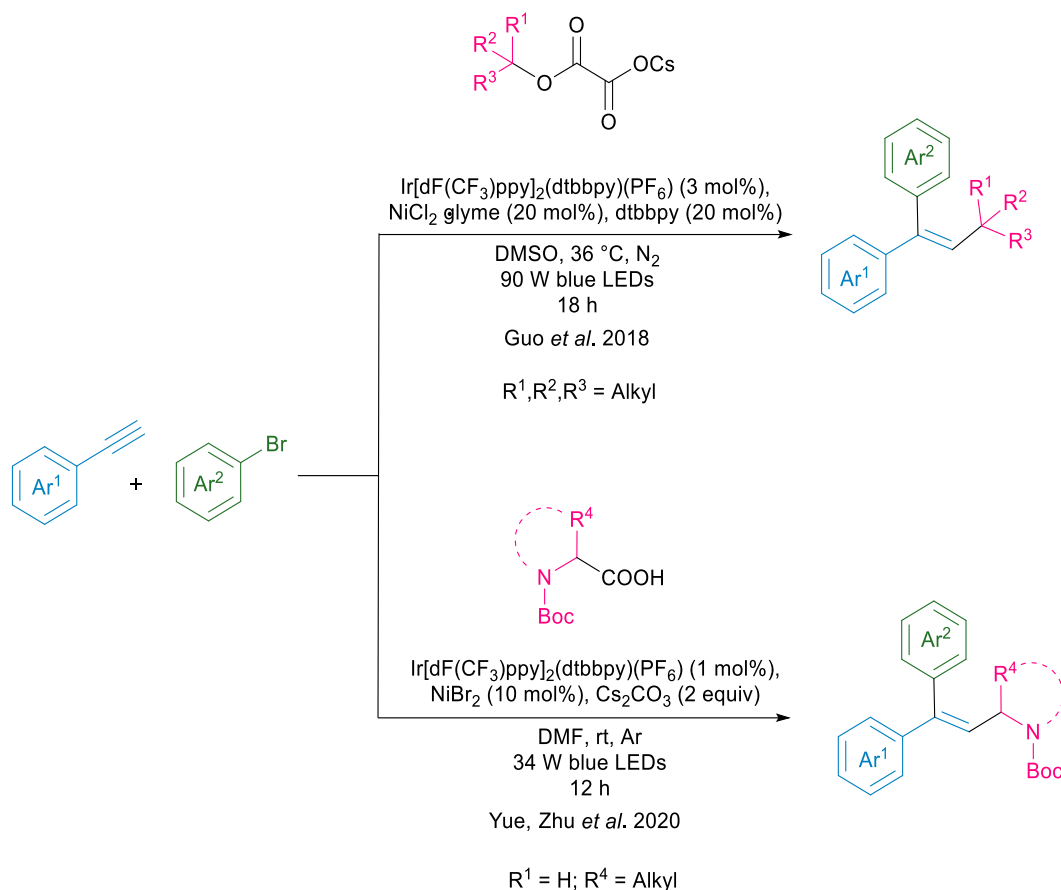
Scheme 91: Remote oxyfluoroalkylation of *S*- and *O*-substituted alkynes.

Moving on to other C-centered radical sources, in a recent report from Pelliccia *et al.* diethyl bromomalonate was employed to kick start the preparation of iminofurans *via* a photocatalytic multicomponent domino reaction with isonitriles and phenylacetylenes.¹⁶⁰ The reaction starts with the formation of an alkyl radical by photocatalytic reduction of the bromomalonate and C-Br bond cleavage. Attack onto the triple bond gives a vinyl radical which undergoes somophilic isocyanide insertion and photocatalytic oxidation to generate a nitrilium ion. Nucleophilic attack by water gives an enamide intermediate, which was confirmed by isotope labeling running the reaction with ¹⁸O-labeled water. The enamine forms an alkyl radical either by an oxidation deprotonation sequence or *via* HAT. This radical species detected as TEMPO adduct, cyclizes and the product is formed upon oxidation by the catalyst and deprotonation. A library of iminofurans could be obtained in moderate yields (Scheme 92).



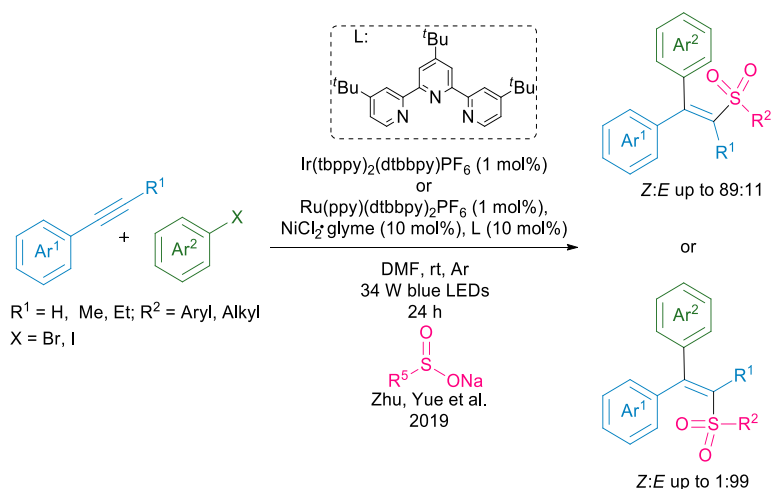
Scheme 92: Three component photoredox synthesis of iminofurans.

In 2018, Guo *et al.* reported the alkylation of alkynes through the combination of photoredox and nickel catalysis.¹⁶¹ The authors design the metallophotoredox process in order to exploit two different activation strategies: generation of highly reactive radicals and oxidative addition/ reductive elimination sequence. To this goal, tertiary alkyl oxalates were chosen as radical source and bromoarenes as coupling partners. Oxalate half ester chemistry, introduced by Overman and MacMillan¹⁶² allows for mild generation of a tertiary radical *via* decarboxylation of stable and easily prepared salts. The reaction is initiated by photoredox activation of the oxalate. The tertiary alkyl radical readily adds to the terminal alkyne delivering a vinyl radical intermediate. Nickel catalyst is able to trap the radical with the formation of a (*E*)-alkenyl-Ni(I) complex and then undergoes oxidative addition with the arylbromide to afford a (*E*)-alkenyl-Ni(III) complex. Reductive elimination delivers the (*E*)-substituted alkene and restores the Ni(I) catalyst. Finally, photoinduced isomerization leads to the formation of the (*Z*)-isomer as a predominant product. To support this sequential reaction order, the nickel-bromoarene complex was prepared and let react in the same photocatalytic conditions resulting in no product formation. The optimized protocol allowed the preparation of a diverse library of diaryl alkenes with high variability of tertiary alkyl groups on the β -position. The reaction showed good tolerance for functional groups on the phenylacetylene ring. The products could be obtained in good to excellent yields and with *Z*:*E* ratios as high as 98:2. More recently the scope has been expanded to alkylamines employing α -aminoacids as the radical source. Also, in this case the formation of the *E*-isomer as a major product is supposed to occur *via* triplet-triplet energy transfer with the photocatalyst (Scheme 93).¹⁶³



Scheme 93: Photoredox arylation of terminal alkynes.

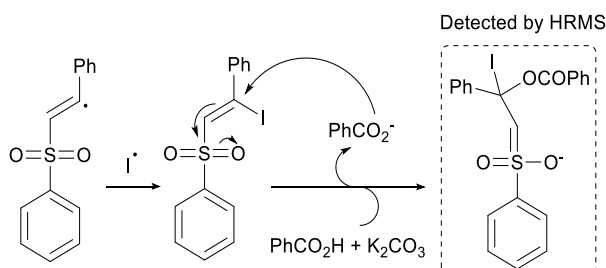
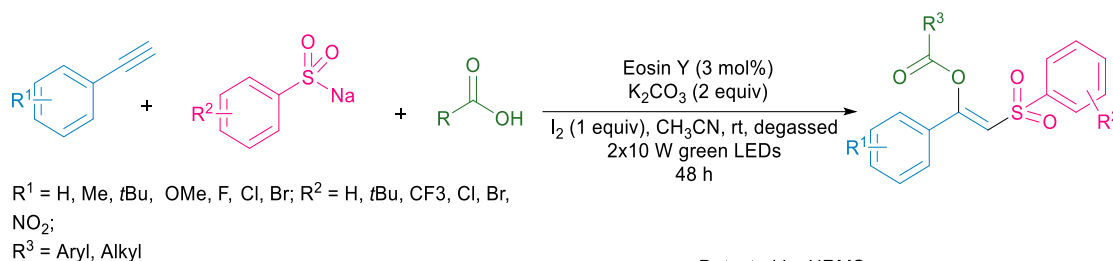
The same group in a previous report regarding the sulfonylarylation of alkynes under similar metallophotoredox conditions deeply investigated the *E/Z*-isomerization step.¹⁶⁴ The authors discovered that the tendency to undergo isomerization was closely related to the energy of the triplet state of the photocatalyst and the excited state of the two isomers. Specifically, when the photocatalyst triplet state energy was lower than that of the excited state of the anti-addition product (iridium catalysts) isomerization was negligible and the (*E*)-isomer was isolated as the major or only product. Otherwise, when the energy of the photocatalyst triple state was higher than the excited state of the anti-product but lower than that of the syn-product (rhodium catalysts) the isomerization could occur delivering the (*Z*)-isomer as major product (Scheme 94).



Scheme 94: Photocatalyst dependent stereoselective synthesis of (*E*) and (*Z*) diarylalkenyl sulfones.

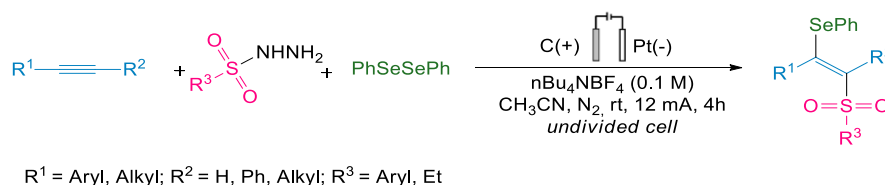
Recently Sahoo *et al.* reported another example of terminal alkyne difunctionalization employing sulfinate salts as radical precursors and

carboxylic acids as nucleophiles.¹⁶⁵ When the reaction was carried out with Eosin Y as photocatalyst and under green light, in the presence of a base, no product could be obtained. Nonetheless, the addition of a stoichiometric amount of iodine successfully delivers the product suggesting the formation of a key β -iodo sulfone intermediated able to undergo nucleophilic attack by the acid. Such intermediate could be detected by HRMS and likely evolves in the final product by elimination of I⁻. Radical iodine could be formed by the reaction of the sulfinate with I₂ to give a sulfonyliodide intermediate subsequently photocatalytically reduced to give both iodine and sulfonyl radicals. Both alkyl and aryl carboxylic acids could be employed and delivered the desired product in moderate to good yields (Scheme 95).



Scheme 95: Photoredox S- and O-difunctionalization of alkynes with sulfinate salts and carboxylic acids.

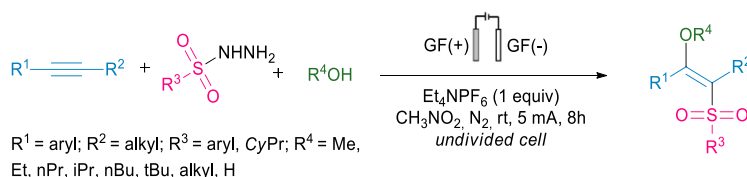
Electrolytic oxidative activation of sulphonyl hydrazines provides an efficient route to sulfonyl radicals. Several works involving radical sulphonation towards alkyne difunctionalization have been reported recently. Kong *et al.* applied it to the selenosulfonylation of alkynes with diphenyl diselenides.¹⁶⁶ Upon formation of a sulfonyl vinyl radical, the phenylselenol group is added through direct reaction with diselenide or by radical homocoupling with a phenylselenium radical generated by oxidation/heterolytic cleavage of the diselenide. Phenylacetylenes bearing both electron-donating and electron-withdrawing substituents, including *p*-NO₂, gave the products in good yields. Alkyl alkynes could also undergo selenosulfonylation though with slightly lower yields. The sulfonyl hydrazine scope revealed good substituent tolerance on the phenyl group (Scheme 96).



Scheme 96: Electrocatalytic selenosulfonylation of alkynes.

This approach also proved to be effective in the iodiosulfonylation of alkynes by employing sodium iodide as a radical source through anodic oxidation.¹⁶⁷

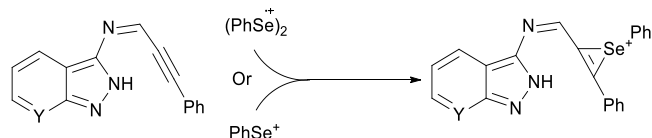
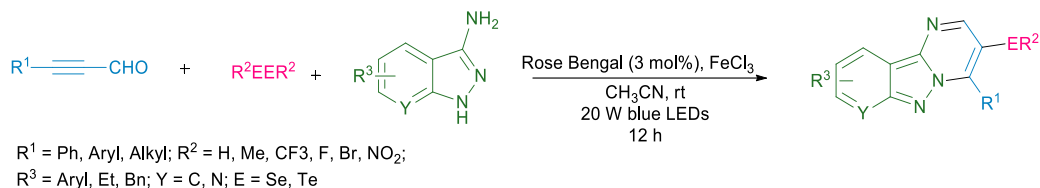
Alternatively, the sulfonyl vinyl radical can get oxidized to the cation which undergoes the addition of a nucleophile. This approach was recently described by Du *et al.* employing alcohols to generate *O*-centered nucleophiles through cathodic reduction.¹⁶⁸ The alkyne and sulphonyl hydrazine scope were comparable to what was already mentioned above. Good to excellent yields could be obtained with ethanol and methanol whereas other alcohols generally performed inferior (Scheme 97).



Scheme 97: Electrocatalytic alkoxysulfonylation of alkynes.

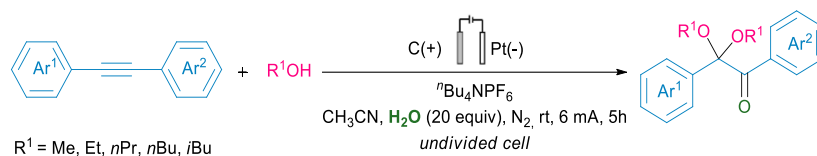
In a recent work, Zhou *et al.* reported the use of diselenides and digermanides in the preparation of pyrimido[1,2-*b*]-indazoles.¹⁶⁹ Organoselenium compounds are attracting great interest in the pharmaceutical field and novel approaches for the installation of selenium atoms are being investigated. Conventional methods involve electrophilic difunctionalization of unsaturated bonds and require the use of

oxidants together with the activation by either acid or Lewis bases. The authors envisioned photoredox catalysis as a valid alternative. Specifically, the model reaction involved phenylal, 3-aminoindazole and diphenyl diselenide. Initial condensation between the aldehyde and the amine gives an imine intermediate, which could react either with a selenide radical cation species or with a phenylselenium cation *via* electrophilic cyclization. Intramolecular cyclization delivers the final product (Scheme 98).



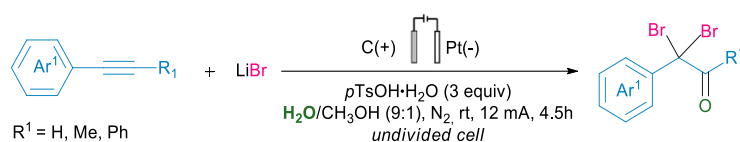
Scheme 98: Photoredox synthesis of chalcogen-containing pyrimido[1,2-*b*]-indazoles.

In 2020, Yang, Lu *et al.* reported the electrocatalytic oxidative *ipso*-difunctionalization of diphenyl alkynes with alcohols.¹⁷⁰ Electrolysis at a constant current of an acetonitrile solution of the alkyne, the alcohol, and 20 equivalents of water resulted in the formation of the corresponding benzoin bis-ethers in moderate to good yields (Scheme 99).



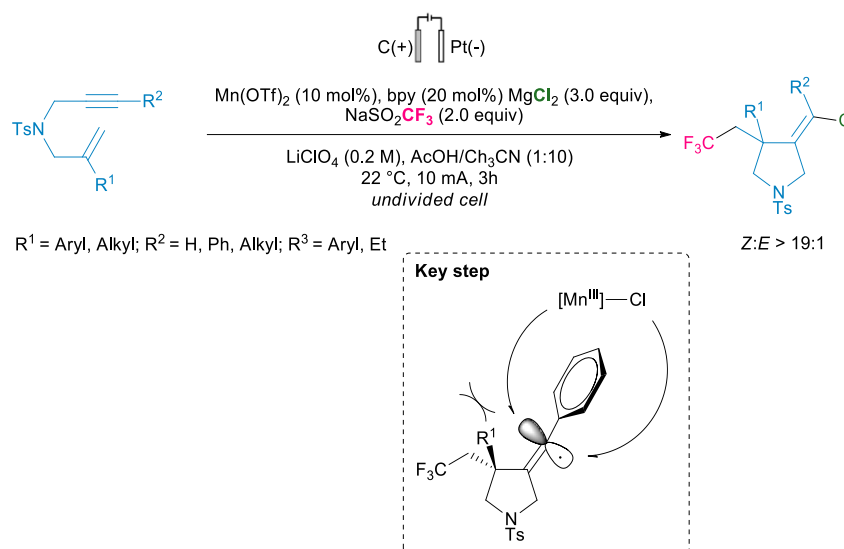
Scheme 99: Electrocatalytic oxidative *ipso*-dialkoxylation of internal alkynes.

Recently, the same group reported the preparation of α,α -dibromo aryl ketones employing LiBr as halogen source.¹⁷¹ The reaction is believed to occur *via* the formation of vinyl radical intermediate which is readily oxidized to the cation. Trapping of a molecule of water and subsequent attack by a bromide radical gives the dibromo ketone. Terminal and internal alkynes performed well under the reaction conditions. Application of an electrochemical continuous flow cell allowed easy scale-up while maintaining an acceptable yield of 62% (Scheme 100).



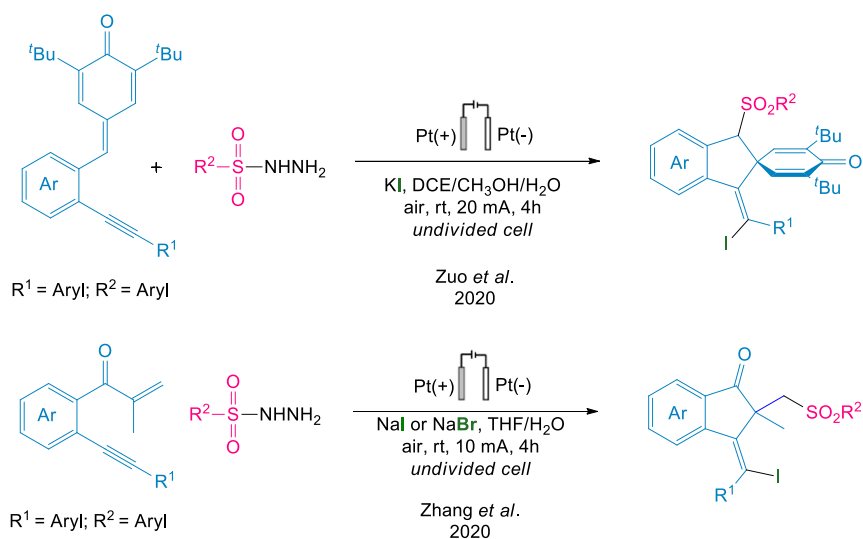
Scheme 100: Electrocatalytic oxidative *ipso*-dibromination of alkynes.

Finally, we would like to mention three reports involving enynes. In the first one from 2018, Ye *et al.* explored the chlorotrifluoromethylation of 1,6-enynes toward the preparation of pyrrolidines.¹⁷² The reaction is initiated by anodic oxidation of Langlois reagent to a trifluoromethyl radical. The addition to the double bond is rapidly followed by cyclization to *sp*-hybridized α -aryl alkenyl radicals. As already described in 2.1.1.4., the reaction then involves the formation of a persistent Mn(III)-Cl radical complex through coordination of the chloride anion by MnII and anodic oxidation. The asymmetric substitution pattern on the pyrrolidine ring affects the access to the singly occupied molecular orbital, resulting in preferential attack from the less hindered side giving a *Z/E* ratio of up to 19:1 (Scheme 101).



Scheme 101: Electrocatalytic annulation-chlorotrifluoromethylation of 1,6-enynes.

The other two contributions come from Jiang's group who reported the electrochemical annulation-iodosulfonylation of both 1,5-¹⁷³ and 1,6-enynes¹⁷⁴ employing sulphonyl hydrazine as the radical source and iodide salts. In both cases, platinum electrodes were used and the reaction proceeded smoothly even without the addition of supporting electrolytes. Interestingly in the reaction with 1,6-enynes, brominate analogues could be obtained when sodium bromide was employed (Scheme 102).



Scheme 102: Electrocatalytic annulation-iodosulfonylation of 1,5- and 1,6-enynes.

2.3. Carbonyl compounds

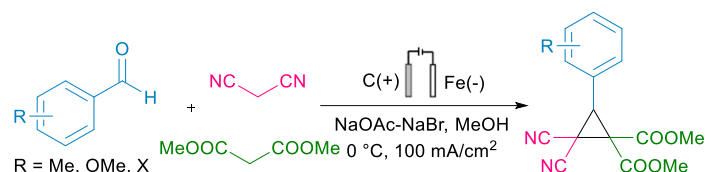
2.3.1. Functionalization of the Carbonyl group

Carbonyl compounds have always been employed as privileged scaffolds to access the formation of various functional groups. Radical mediated mechanisms catalyzed by light or electrochemistry have also begun to become popularly employed, due to the mild and convenient reaction conditions. In particular, if considering multicomponent approaches, the alkyl/arylation of *in situ* generated imines has been largely explored. Nevertheless, the functionalization of the carbonyl group has also been differently accomplished, leading to the formation of heterocyclic scaffolds in an expedient manner. The advancement of the topic will therefore be highlighted in this section, that has been divided in two main parts: generation of heterocyclic scaffolds and functionalization of *in situ* formed imines.

2.3.1.1 Synthesis of heterocyclic scaffolds

An early report of electrocatalytic functionalization of aldehydes and malononitrile, in the presence of malonates to form substituted-2,2-dicyanocyclopropane-1,1-dicarboxylates, was presented in 2006 by Elinson *et al.* The authors reported the formation of halogens (I_2 or Br_2) at the anode from the corresponding salts, while at the cathode H_2 evolution was observed. In solution, a first step is

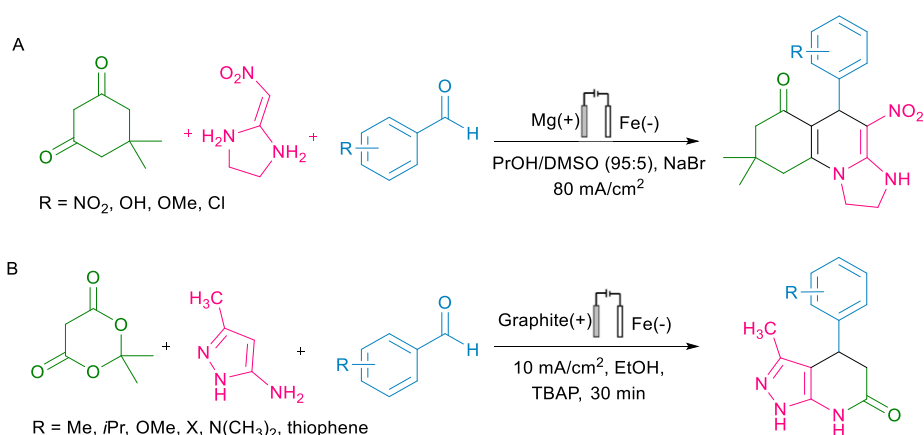
represented by the Knoevenagel condensation of the aromatic aldehyde and malononitrile, in the presence of a base. The *in situ* formed halogen then adds on the malonate, and subsequent addition to the alkylidenmalononitrile leads, upon rearrangement, to the formation of the final product (Scheme 103).¹⁷⁵



Scheme 103: Electrocatalytic multicomponent formation of substituted-2,2-dicyanocyclopropane-1,1-dicarboxylates.

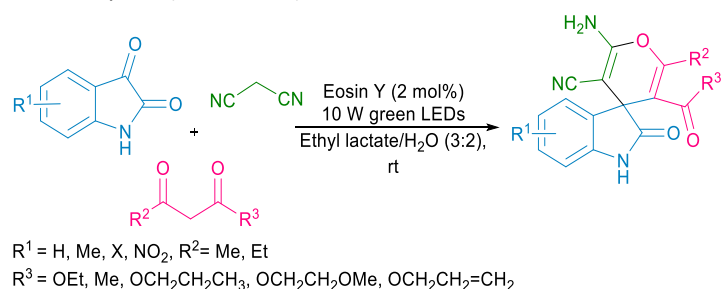
Following a similar reaction pathway, the functionalization of *in situ* generated alkylidene malononitrile was achieved with the use of a wide variety of hetero(cyclic) and acyclic structures, leading to the formation of different molecular scaffolds.^{176–187}

The use of dimedone (Scheme 104, A) and Meldrum's acid (Scheme 104, B), instead of malononitrile, also led to the formation of interesting molecular architectures, such as octahydro-imidazo[1,2- a]quinolin-6-ones or 3-methyl-4-aryl-2,4,5,7-tetrahydropyrazolo[3,4-b] pyridin-6-ones, respectively.^{188,189}



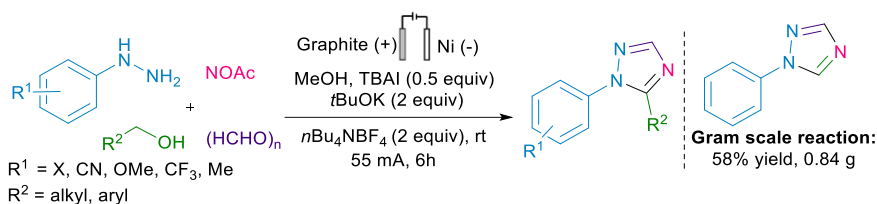
Scheme 104: Electrocatalytic formation of octahydro-imidazo[1,2- a]quinolin-6-ones or 3-methyl-4-aryl-2,4,5,7-tetrahydropyrazolo[3,4-b] pyridin-6-ones.

A photoredox catalyzed methodology employing malononitrile and 1,3-dicarbonyl compounds was also presented by Chen *et al.* in 2020. In this case, a light-induced Knoevenagel condensation between malononitrile and isatines happens, while the 1,3-dicarbonyl compounds serve as a radical source in a HAT mechanism mediated by eosin Y, that leads to the formation of the final spiro[4*H*-pyran-oxindoles]. Given the relevance of this molecular scaffold, many isatins and 1,3-dicarbonyl compounds were tested, leading to product formation in good to excellent yields (Scheme 105).¹⁹⁰



Scheme 105: One-pot synthesis of spiro[4*H*-pyran-oxindole] structures under photoredox catalyzed conditions.

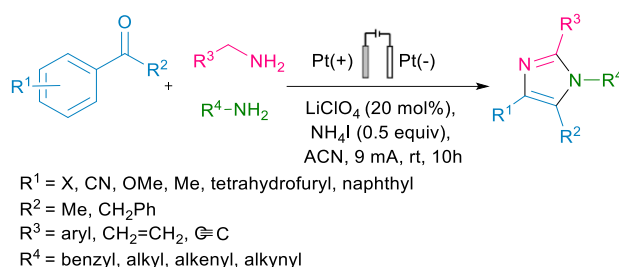
The electrocatalytic synthesis of 1,5-disubstituted and 1-aryl 1,2,4-triazoles was also accomplished by Yang and Yuan.¹⁹¹ The authors employed aryl hydrazines, paraformaldehyde, NH_4OAc and alcohols as starting materials in a multicomponent approach in an undivided cell and without the need of strong exogeneous oxidants or transition metal catalysts. Key steps of this transformation are the anodic oxidation of TBAI (*n*- Bu_4NI) to iodine radical or molecular iodine, and the concomitant reduction of NH_4^+ at the cathode, thus generating the required NH_3 . Overall, the reaction was found to be tolerant to many alcohols, together with variously substituted hydrazines. Electron-poor hydrazines in particular showed better results. The gram-scale reaction also afforded a 58% isolated yield of the desired product, prolonging the reaction time from 6 to 10 h (Scheme 106).



Scheme 106: Multicomponent electrochemical synthesis of 1,5-disubstituted and 1-aryl 1,2,4-triazoles.

The scope of the transformation was further expanded by Zhao, He *et al.*¹⁹² Indeed, they were able to avoid the use of a strong base, that was instead necessary under the previously described reaction conditions. As an example, aliphatic, alkenyl and alkynyl aldehydes could be successfully functionalized, together with heterocycle containing aldehydes and hydrazones.

Imidazoles could also be synthesized *via* an electrochemical procedure by Zeng, Li *et al.*¹⁹³ To achieve the formation of this heterocyclic scaffold, aryl ketones and amines were employed in a multicomponent fashion. Despite not being amenable to aliphatic ketones, many functionalities were tolerated, including heterocyclic structures, alkenyl and alkynyl bearing amines, and the methyl ester of glycine as well (Scheme 107).



Scheme 107: Electrochemical cascade annulation of ketones and amines for the synthesis of imidazoles.

2.3.2. α -Functionalization of *in situ* formed imines

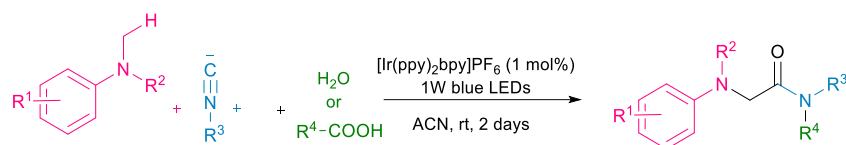
2.3.2.1. Imines as radical acceptor

The functionalization of *in situ* formed imines *via* a multicomponent reaction manifold is an extremely well-known strategy for the construction of amines, ubiquitous functional groups in drug molecules, agrochemicals and natural products. Mannich reaction¹⁹⁴ as well as Strecker amino acid synthesis¹⁹⁵ clearly showed the potential for carbonyl compounds to undergo difunctionalization reactions upon formation of a reactive intermediate (*i.e.* imine), followed by an attack from a nucleophile. With the implementation in the use of visible light photoredox catalysis, many straightforward processes for the functionalization of imines in a multicomponent fashion were exerted, facilitated by an array of radical precursors that suited well for this transformation. These strategies can be generalized in two main complementary approaches:

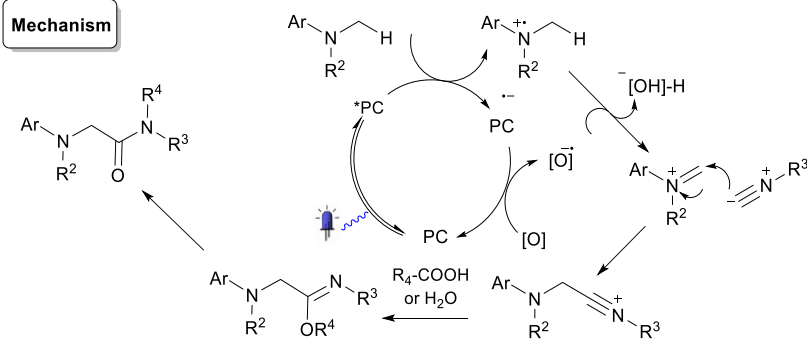
1. Functionalization of imines exploiting the intrinsic electrophilic nature of the species.
2. Generation of an α -amino nucleophilic radical from imines.

In 2013, the combination of TiO_2 and $(\text{NH}_4)_2\text{S}_2\text{O}_8$ as co-catalyst was found effective in promoting, upon UV irradiation, the formation of alkyl radicals from cyclic ethers and therefore enabling the alkylation of *in situ* generated imines.¹⁹⁶ Similar results were obtained one year later by Lahm *et al.* In their report, dimethoxymethane and 1,2-dimethoxyethane were instead used as a radical source to alkylate a range of different anilines and aldehydes, in this case including aliphatic aldehydes as well.¹⁹⁷

It was not until 2013 that Rueping and Vila presented a photoredox catalyzed three-component version of the renowned Ugi reaction, where the generation of imines was achieved through the single-electron oxidation of tertiary amines, followed by hydrogen atom abstraction operated by oxygen.¹⁹⁸ The optimized reaction conditions enabled the formation, upon nucleophilic attack of isocyanides on the electrophilic imines and water/carboxylic acid addition, of α -amino amides or imides, valuable synthons in many drug molecules and natural products. The reaction was tolerant to many functional groups and allowed the functionalization of the $\text{C}(\text{sp}^3)\text{-H}$ bond next to the nitrogen atom of the various tertiary amines employed (Scheme 108).

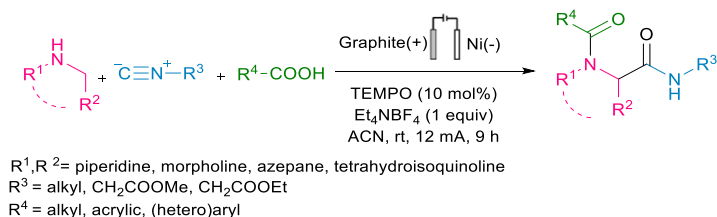


R¹ = H, Me, X R³ = CH₂Ts, butyl, cyclohexyl, CH₂COOMe, CH₂Ph
 R² = Me, Et R⁴ = aryl, benzyl, naphthyl, tetrahydrofuryl, CH₂CH₂C≡C



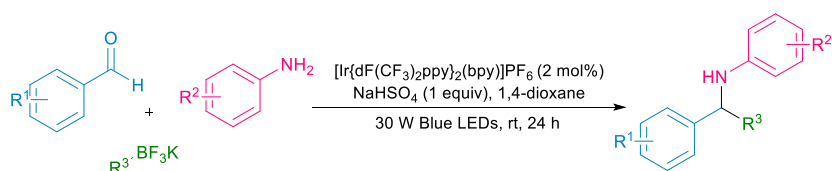
Scheme 108: Photoredox catalyzed Ugi reaction.

A different approach for a similar reactivity pattern was presented in 2019 by Pan *et al.*. They explored an electrocatalytic strategy to indirectly form an iminium ion through the addition of 10 mol% of TEMPO. Upon anodic oxidation, TEMPO forms a cationic species (TEMPO⁺) that then reacts with a secondary cyclic amine.¹⁹⁹ After hydride transfer, the desired iminium ion is formed. The reactivity pattern then resembles an Ugi-Joullié isocyanide-based multicomponent mechanism, and C(sp³)-H α-carbamoylated products were obtained with good to moderate yields. The reaction was performed in an undivided cell, using graphite as working electrode, Ni as counter electrode and tetraethylammonium tetrafluoroborate as electrolyte. The reaction was subjected to a constant current electrolysis for 9 h (Scheme 109).

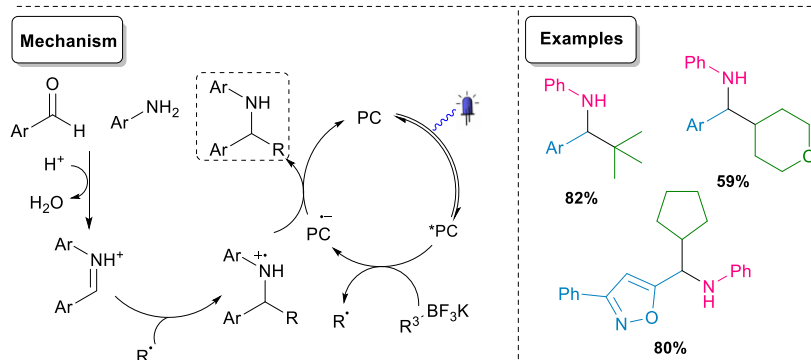


Scheme 109: Multicomponent C(sp³)-H α-carbamoylation of unprotected secondary amines.

In 2019, Yi, Badir *et al.* translated the traditional Petasis reaction into a milder version, without the requirement of directing groups or harsh conditions.²⁰⁰ Alkyl trifluoroborates were directly employed as source of alkyl radicals, and BF₃, liberated after the SET step, played a key role in both imine formation and in facilitating radical attack. Mechanistically, [Ir{dF(CF₃)ppy}₂(bpy)]PF₆ is responsible for the single electron oxidation of trifluoroborates, thus generating a radical that attacks the *in situ* formed protonated imine. The radical intermediate is then reduced to form the final product with concomitant photocatalyst turnover. The authors could not completely rule out the possibility of an oxidative quenching cycle, with imine reduction as first step. Sterically demanding tertiary alkyl radicals, together with secondary and primary alkyl radicals (the latter showing high oxidation potentials) were delightfully employed (Scheme 110). More importantly, the reaction conditions allowed the late-stage functionalization of decorated drug molecules (indomethacin, fenofibrate, sulfadimethoxine as examples) and the one-step synthesis of a glucagon receptor modulator was also accomplished.

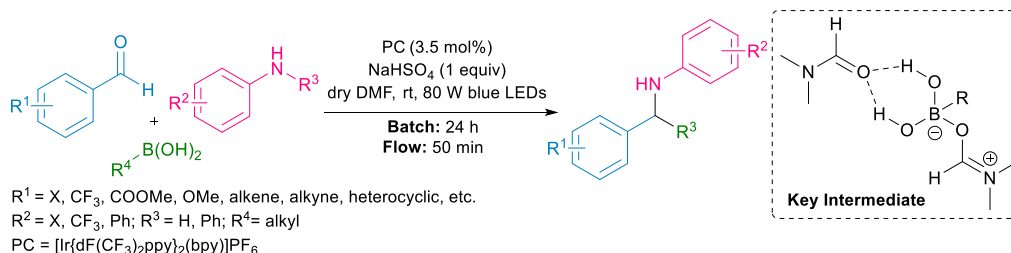


$R^1 = X, CF_3, COOMe, SO_2Me, OMe, OPh, \text{heterocyclic, etc.}$
 $R^2 = X, CF_3, OMe, Bn, \text{etc.}; R^3 = \text{alkyl}$



Scheme 110: Visible-light mediated Pétasis reaction using trifluoroborate salts.

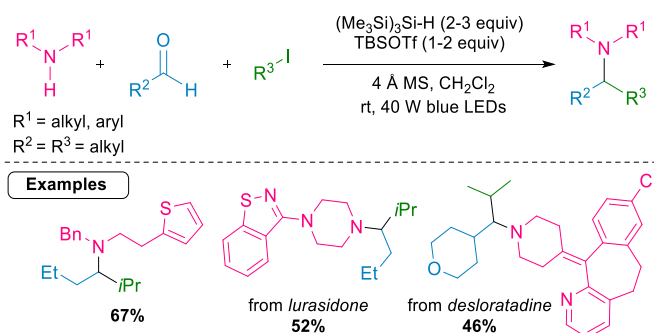
A similar approach by Oliva and Ranjan *et al.* recently appeared. This methodology allowed the use of free boronic acids, as in the traditional Pétasis reaction, without the need for preactivated starting materials to allow the formation of the key boronate complex. Indeed, in the light of recent procedures to achieve the solvent-assisted activation of boronic acids^{201,202} the authors used hydrogen-bonding assisted activation with DMF to form primary and secondary alkyl radicals from boronic acids. Various substitutions on both the aldehyde and aniline counterparts were tolerated. More interestingly, the method was implemented under photo flow conditions, and product formation was obtained within 50 min of irradiation (using a 150 W blue light) (Scheme 111).²⁰³



$R^1 = X, CF_3, COOMe, OMe, \text{alkene, alkyne, heterocyclic, etc.}$
 $R^2 = X, CF_3, Ph; R^3 = H, Ph; R^4 = \text{alkyl}$
 $PC = [Ir(dF(CF_3)_2ppy)_2(bpy)]PF_6$

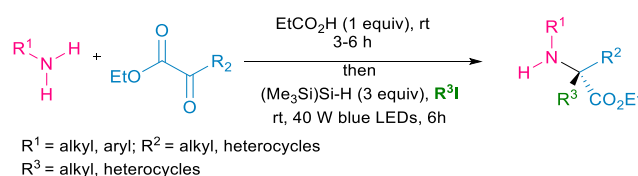
Scheme 111: Visible light mediated Pétasis reaction using boronic acid.

In 2020, a modular approach that avoids the need of preformed unstable iminium ions or the use of highly nucleophilic organometallic reagents for the preparation of tertiary amines was accomplished by Kumar *et al.*²⁰⁴ In an attempt to develop a mild and robust approach, they optimized the reaction conditions employing secondary alkyl amines and alkyl aldehydes, together with alkyl iodides as radical precursors and *tert*-butyldimethylsilyl trifluoromethanesulfonate (TBSOTf) as an acidic additive. UV absorption analyses showed that the combination of enamine, alkyl iodide and additive caused a red shift in the absorbance spectrum, which could lead to radical generation upon excitation *via* blue LEDs. The reaction mechanism comprises the profile delineated before, with radical addition on the iminium ion followed by a HAT step (Scheme 112). The novelty of this work relies on the mildness and robustness of the method, which was applied to an interesting variety of all three components, and extended to the use of alkyl bromides as well. In addition, methyl iodide also proved to be reactive, allowing to form an important class of branched alkylamines. In the case of primary alkyl iodides, to overcome the difficulties in the radical generation, 5-10% of a radical initiator (ethyl 2-iodo-2-methylpropionate) was added. Overall, the reaction only showed reduced efficiency with electron-poor amines, which rather underwent reduction, or electron-poor alkyl iodides, which were involved in a HAT step instead, due to the lower rate of attack to the electrophilic iminium ion. In addition, as a result of the increasing interest in the derivatization of desloratadine to find drug candidates with better pharmacokinetic properties, the further functionalization of desloratadine was also explored.



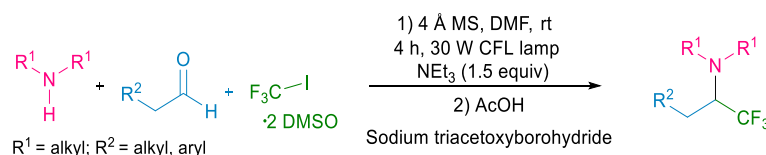
Scheme 112: Synthesis of tertiary amines.

As a result of the inactivity of ketones under these conditions, the same group then focused on the optimization of a reaction platform that could enable their use. Therefore, they recently presented a strategy for the construction of unnatural amino acids (all-alkyl α -tertiary amino esters).²⁰⁵ In this case, they thoroughly investigated the role of tris(trimethylsilyl)silane [(Me₃Si)₃Si-H] as a HAT reagent to induce a rapid termination of the reaction. Indeed, a HAT step is responsible for the successful stabilization of the *N*-alkyl aminium radical cation arising after radical addition on the all-alkyl ketiminium ion. To overcome the issues related to the slow ketimine formation and its lower electrophilicity, they stirred a solution of primary amine and α -ketoester for 3 to 6 h prior to the addition of [(Me₃Si)₃Si-H], radical source (alkyl iodides) and irradiation with blue light. The reaction was pleasingly applied to a broad scope, where only primary amines bearing electron-withdrawing groups were unreactive, and lower yields were obtained from the sterically hindered β -branched α -ketoesters or from reactive unstabilized radicals (for example, the radical forming from iodomethane), which underwent dehydrohalogenation instead. The method was also successfully applied to the preparation of ω -borono- α -amino acid arginase inhibitor analogues in a single step (Scheme 113).



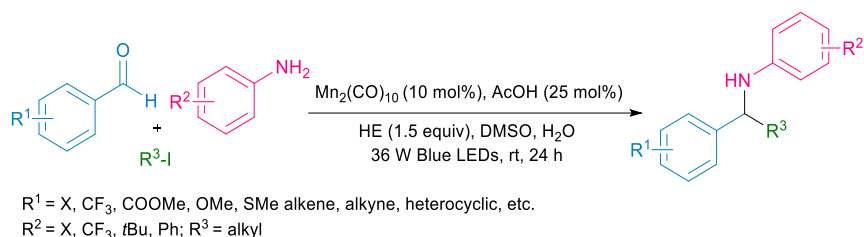
Scheme 113: Synthesis of all-alkyl α -tertiary amino acid derivatives.

Kolahdouzan *et al.* also reported the multicomponent synthesis of β -trifluoromethylated tertiary alkylamines. In this case, they exploited the polarity match between an electrophilic trifluoromethyl radical and an *in situ* formed enamine (through condensation of secondary alkylamines and aliphatic aldehydes).²⁰⁶ The absence of a photocatalyst was justified by the fact that enamines become potent reductants upon excitation with visible light, but an EDA complex between enamine and CF₃I can be formed as well. Homolytic cleavage of CF₃I is the first step for the generation of a trifluoromethyl radical that can attack the enamine. The authors then proposed that the arising α -amino radical intermediate can undergo different mechanisms, which lead to chain propagation and generation of either α -iodoamines (through a halogen atom transfer (XAT)), or an alkyl iminium ion. A reductive work-up is then responsible for product formation. Remarkably, the method was tolerant to the co-presence of tertiary amines, often involved in single-electron oxidation events, and was amenable for the derivatization of complex molecular scaffolds. In this regard, fenpropimorph and fenpropidin trifluoromethylated derivatives, with potentially enhanced metabolic resistance, were synthesized. Only branched aldehydes (with groups adjacent to the carbonyl moiety) were found to be unreactive because of a steric hindrance (Scheme 114).



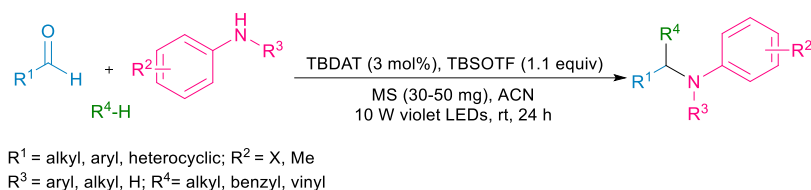
Scheme 114: Synthesis of trifluoromethyl bearing tertiary amines.

Alkyl iodides, despite their low reduction potential, can be subjected to halogen atom transfer. Wang *et al.* exploited this feature to obtain radical formation by the employment of Mn₂(CO)₁₀ which, upon irradiation with blue LEDs, homolytically cleaves to generate [Mn(CO)₅][•], responsible for iodine abstraction. Following the general three-component pathway described by Yi and Badir *et al.*,^{200,207} the method was efficaciously applied to a broad substrate scope, where only primary alkyl iodides failed to deliver the desired secondary amine because of a more favorable reduction of imine to amine and nucleophilic substitution to form tertiary amines. Overall, the method was amenable to orthogonal functionalization of halide bearing substrates, which could be further utilized in a subsequent Suzuki or Sonogashira coupling step (Scheme 115).²⁰⁸



Scheme 115: Visible light mediated Mn-catalyzed synthesis of secondary amines.

In a recent complementary strategy, Qi *et al.* focused on the use of unactivated alkanes as radical source for the alkylation of *in situ* formed imines.²⁰⁹ Violet irradiation of tetrabutylammonium decatungstate (TBADT; $[W_{10}O_{32}] (nBu_4N)_4$) is known to enable radical generation through HAT of strong aliphatic bonds. This photocatalyst was therefore used to form mainly tertiary, but also secondary amines. Both alkyl and aryl amines and aldehydes underwent the transformation smoothly (Scheme 116).



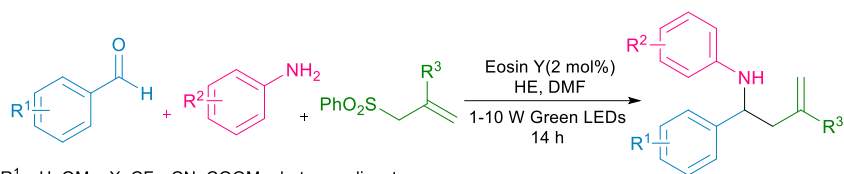
Scheme 116: HAT mediated synthesis of tertiary and secondary amines.

Similarly, Pillitteri *et al.* succeeded in the formation of secondary amines using the same catalytic system. Ethers, together with simple alkanes, were also included as radical precursors. Halogen containing aldehydes/anilines were employed, and -BPin substitution was tolerated as well, despite forming the desired product in lower yield.²¹⁰ In both reports, despite the possible competition between the starting materials for the generation of radicals and the risk of low selectivity of the photocatalyst, skillful optimization of the reaction conditions enabled to avoid the issues.

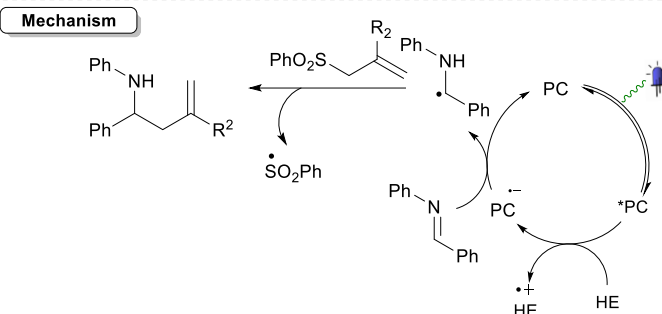
2.3.2.2. Generation of α -amino radicals from imines

The umpolung synthesis of amines from imines was interestingly leveraged by Fuentes de Arriba *et al.* in 2016, when an electron-rich α -amino radical was formed through single-electron reduction of an *in situ* formed imine to generate γ -amino acid derivatives.²¹¹ This key radical intermediate then engages in a Giese-type addition on electron-withdrawing allyl sulfones. The authors, therefore, managed to obtain the formation of a nucleophilic radical, despite the well-known electrophilic nature of imines and their propensity to react with nucleophiles.

To explain this interesting reactivity, the authors hypothesized and confirmed through radical and fluorescence quenching experiments that, upon excitation, Eosin Y first oxidizes a Hantzsch ester, generating a radical cation (HE^{*+}). The reduced photocatalyst is then able to transfer one electron to the *in situ* formed imine. The authors highlighted that, for this process to happen spontaneously, a proton transfer from a donor (in this case HE^{*+}) should concurrently occur (through a proton-coupled electron transfer process, PCET) to lower the redox potential of the imine. Once formed, the α -amino radical can then attack the allyl sulfone and generate the final product through the exclusion of a benzene sulfinyl radical. This radical intermediate is then finally reduced by the Hantzsch ester, its oxidized form or by the reduced photocatalyst. In the analysis of the substrate scope, it was observed that electron-donating groups on the aldehydes gave the best results (Scheme 117). Electron-poor aldehydes also reacted moderately, but in some case, overreduction products were observed. Heterocyclic aldehydes also gave promising results. The aniline counterpart was tolerant to many functionalities as well, while, when considering different substitutions on the alkenes, only the cyano group and diethylphosphonate were tolerated. The gram-scale reaction was also successfully accomplished.



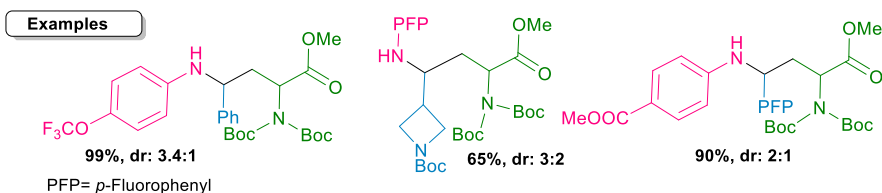
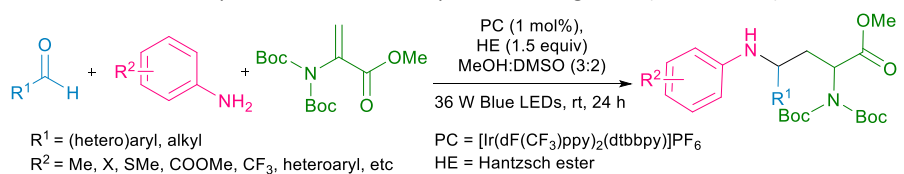
$R^1 = \text{H, OMe, X, CF}_3, \text{CN, COOMe, heterocyclic, etc.}$
 $R^2 = \text{NO}_2, \text{OMe, heterocyclic; } R^3 = \text{CO}_2\text{Et, COOtBu, CN, PO(OEt)}_2$
 HE = Hantzsch ester



Scheme 117: Umpolung synthesis of amines from imines.

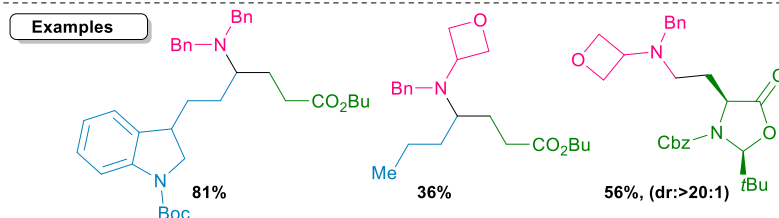
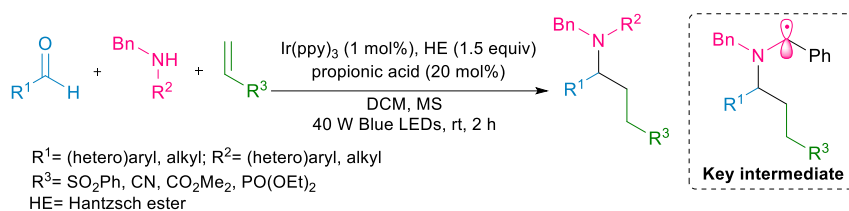
Aliphatic aldehydes were instead employed in the same year by Qi *et al.*, who only developed a three-component strategy for unstable imines with unachievable reduction potentials ($E_0^{1/2} < -3.0\text{V}$ vs. SCE in acetonitrile). Isobutyl, cyclopropyl, butyl and pentyl aldehyde, therefore, gave the desired γ -amino acid derivatives in moderate to good yields.²¹²

With a similar reaction manifold, in 2018 Rossolini *et al.* sought to develop the umpolung synthesis on 1,3-diamines through the alkylation of the unnatural amino acid dehydroalanine (DHA). In accordance with their previous strategy, they accomplished the desired reactivity by generating a nucleophilic α -amino radical by a PCET (Proton Coupled Electron Transfer) involving *in situ* formed imines. The functional group tolerability of this reaction manifold was found to be as good as the previously developed method, with increased reactivity of electron-rich (hetero)aromatic aldehydes, confirming the nucleophilic nature of the intermediate α -amino radical. Notably, a range of aliphatic aldehydes was employed too. The synthesis of 1,3-diamines is of great importance in different fields, including drug synthesis and ligands for catalysts. The utility of this reaction manifold was therefore extended to the synthesis of a γ -lactam fundamental intermediate, precursor of CB-1 receptor inverse agonists (Scheme 118).²¹³



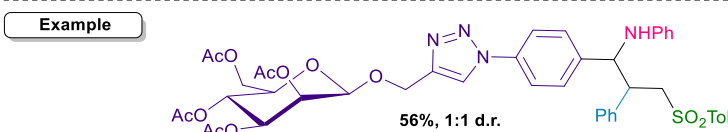
Scheme 118: Photocatalytic umpolung synthesis of 1,3-diamines.

The single-electron reduction of iminium ions in a multicomponent reaction was also applied to alkyl amines and aldehydes by Trowbridge *et al.*²¹⁴ They overcame the high redox potential of these iminium ions and their tendency of forming enamines, achieving the hydroamination of alkenes. The incorporation of alkyl amines in complex molecular scaffolds is indeed of great interest in drug discovery, but the limited availability of mild methods precluded the synthesis of functionally diverse scaffolds. At first, the authors explored the reactivity of benzylamines with a broad variety of alkyl aldehydes and electron-withdrawing alkenes. They reasoned that enamine formation cannot be avoided, but it can serve as an off-cycle precursor of iminium ions. The reaction then follows the same steps as delineated by Fuentes de Arriba *et al.*²¹¹ to close the photocatalytic cycle. They proved by deuterium labeling experiments that 1,5-HAT happens after radical addition on the electron-withdrawing alkene. Indeed, this step leads to the formation of a stabilized benzyl radical. The desired product is then obtained through HAT between a Hantzsch ester or its radical cation. In order to extend the scope to secondary alkyl amines (other than benzyl amines), they shifted to the use of alkenes that would form a less electrophilic radical intermediate upon α -amino radical addition, avoiding the need of the 1,5-HAT. The success of this strategy allowed to use drug-like alkylamines and to obtain product formation with high levels of diastereoselectivity in some cases (Scheme 119).



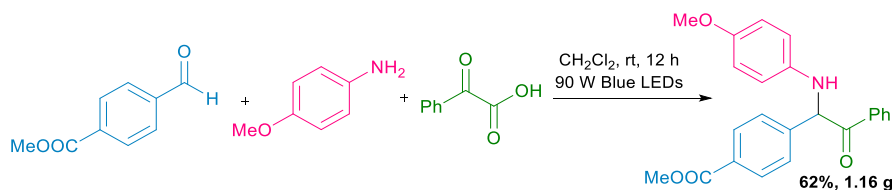
Scheme 119: Multicomponent reaction for the synthesis of tertiary amines.

The remarkable effort of Kammer *et al.* in the fine tuning of the reaction conditions and starting material choice for the development of a four component sulfonylation/aminoalkylation of styrenes is also worth mentioning.²¹⁵ This highly atom economical method allows the construction of complex scaffolds, employing the radicals generated from a first reduction step of an *in situ* formed imine and a subsequent oxidation of sodium sulfonates for a double styrene functionalization. The procedure was also applied to di and tri-saccharide derivatives, whose utility in dendritic cell targeting is being continuously investigated (Scheme 120).



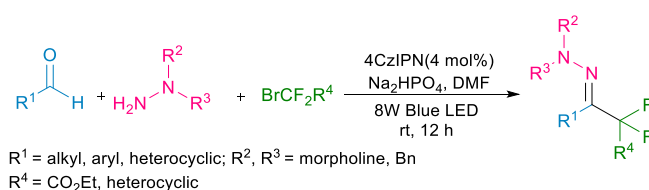
Scheme 120: Four-component reaction for the synthesis of complex secondary amines.

A conceptually different methodology employed the excitation of an EDA complex between an *in situ* formed imine and phenyl oxalate to generate a pair of radicals.²¹⁶ Upon CO_2 extrusion, a radical-radical coupling happens, forming an α -aminoketone in 62% yield (gram scale reaction: 1.16 g). Despite being mainly applied to preformed imines, the prospect to use this strategy in a multicomponent way is appealing (Scheme 121).



Scheme 121: Acylation of imines with ketoacids.

A different approach developed to exploit the reactivity of the iminyl group was devised by Li *et al.*²¹⁷ In their work, the *in situ* formation of a hydrazone through the condensation of aryl/alkyl aldehydes and (hetero)alkyl hydrazines was employed in combination with halodifluoromethylated reagents to access the synthesis of α, α -difluoroketone hydrazones, which could further serve for subsequent functionalization reactions, as demonstrated in this work. The gram-scale reaction also delivered the desired product in good yield (78%), allowing in addition the recovery of the photocatalyst (4CzIPN) (Scheme 122).



Scheme 122: Three-component coupling of aldehydes, hydrazines and bromodifluorinated reagents.

A photocatalyzed version of the traditional Wolff–Kishner reaction was also developed, through a three-component mechanism involving preformed tosyl hydrazones, thiols and CO₂ or benzaldehydes as final electrophiles to trap the carbanion derived from N₂ and tosyl group extrusion.²¹⁸ The benefit of this strategy, besides being a convenient multicomponent approach to form quaternary carbon centers, is the possibility to employ mild conditions and to avoid the use of strong bases to achieve the key carbanion generation. Indeed, under photoredox catalyzed conditions, the first SET step allows the formation of a thiyl radical that then attacks the tosylhydrazone, leading to the loss of a tosyl radical and aminyl radical formation. Upon a Wolff–Kishner N₂ extrusion, a carbanion is generated. Further reaction in the presence of CO₂ or aldehydes in a Barbier fashion, leads to the final product. More than 50 examples of this multicomponent approach were presented, therefore showing high functional group tolerance (Scheme 123).



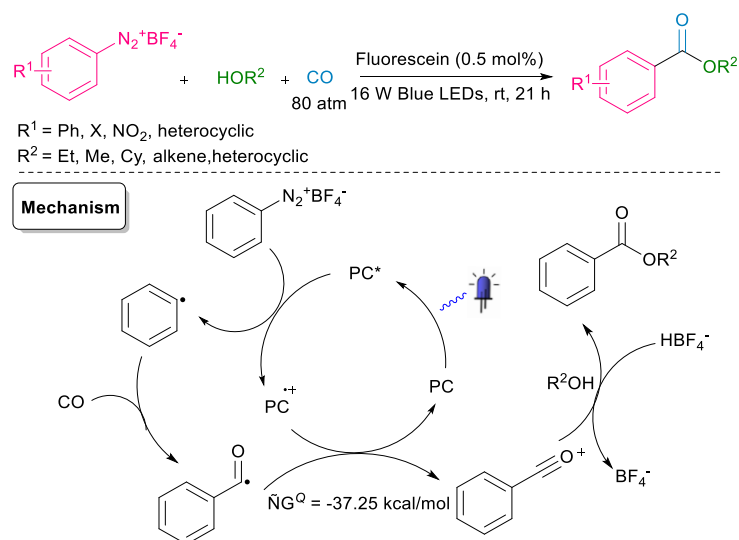
Scheme 123: Umpolung difunctionalization of carbonyls.

3. Carbonylation

The chemistry involving the incorporation of carbon monoxide (CO) as a C1 source into organic molecules is rich in examples, and the evergreen interest in the topic is demonstrated by the remarkable number of strategies developed to access CO incorporation.²¹⁹ The high dissociation energy of the CO bond has been overcome, among all, through photocatalytic methodologies. Indeed, CO tends to react with radical species to form acyl radical intermediates, which can be involved in further acylation reactions. Indeed, the propensity of CO to react with radicals to form an acyl radical is well established, a fundamental intermediate involved in further acylation reactions. As a result, high-intensity light-assisted metal-catalyzed carbonylation reactions, together with atom transfer carbonylation methods, have received noticeable interest.²²⁰ Recently, the development of both photoredox catalysis and the renowned interest in electrochemistry as enabling tools to access radical formation under mild conditions, have led to a shift in the attention from the use of high energy irradiation sources. Considering the existence of exhaustive reviews on photochemical carbonylation methodologies, this section will highlight the main strategies developed to access radical multicomponent carbonylation reactions using photoredox catalysis and electrochemistry.

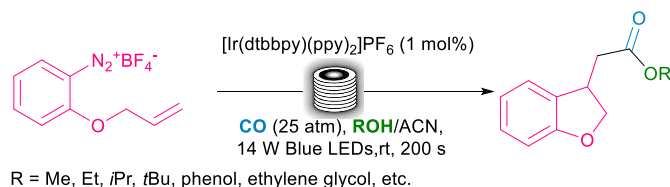
In general terms, the photocatalytic cycle starts with the excitation of a photocatalyst which, in its excited state, can undergo an oxidative (or reductive) quenching cycle, thus leading to the formation of radical species from the chosen radical source. The radical is then involved in an addition step on CO, therefore forming the crucial acyl radical, which is then involved in subsequent steps, generating the desired acylated product. To complete the photocatalytic cycle, the photocatalyst in its reduced (or oxidized) form is then involved in a further oxidation (or reduction) step.

The first photoredox catalyzed carbonylation reaction appeared in 2014, when Guo *et al.* reported a mild, metal-free, alkoxy-carbonylation of aryl diazonium salt tetrafluoroborates.²²¹ Upon excitation, an extremely low amount of fluorescein was found to be sufficient for the successful generation of aryl radicals through a reduction step. The radicals generated were trapped by CO, whose pressure was found to be fundamental to avoid the fast hydrogen abstraction from the solvent by aryl radicals. The benzoyl radical formed was then further oxidized by the photocatalyst to close the catalytic cycle. The benzylideneoxonium intermediate then reacted with an alcohol to deliver the final product through a nucleophilic attack. The reaction was found to be tolerant to a wide variety of functional groups and opened the gate to a myriad of applications (Scheme 124).



Scheme 124: Metal-free, room-temperature, radical alkoxy carbonylation.

A similar work was presented by Majek *et al.* soon after.²²² In this case, the proposed reaction pathway was substantiated by detailed mechanistic investigations and the utility of the transformation was highlighted by the synthesis of tertiary esters, otherwise difficult to obtain through traditional esterification methods due to the high steric hindrance of *tert*butyl alcohol. Notably, to expand the scope, the method proved to be tolerant and efficient with chemically diverse substituents on both the aryl diazonium salts and alcohols, leading to the formation of industrially relevant esters. Another interesting approach for the annulative carbonylation of alkenyl tethered arenediazonium salts was presented in 2018 by Micic *et al.*²²³ The use of continuous flow reactors allowed to reduce the pressure of CO needed (25 atm) and to obtain a facile scale-up. The reaction was found to be amenable with primary, secondary, tertiary alcohols, and internal alkenes were also tolerated. Both alcohols and arenediazonium allyl ethers bearing halogens underwent the reaction smoothly. The only limitation was related to the presence of electron-donating groups at the C5 position (Scheme 125).

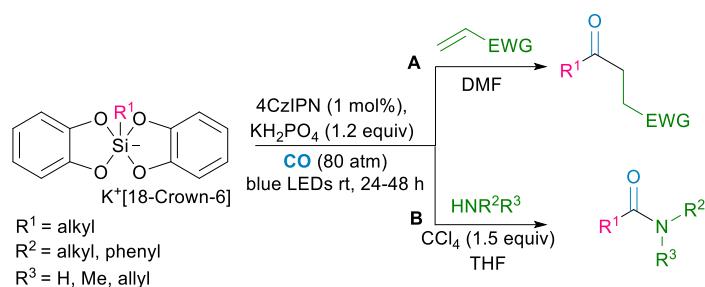


Scheme 125: Multicomponent synthesis of 2,3-dihydrobenzofurans.

Aryl diazonium salts were largely employed as radical precursors in many carbonylation strategies, allowing the formation of (hetero)aryl ketones,²²⁴ indol-3-yl aryl ketones,²²⁵ aryl carboxylic acids.²²⁶ Given the versatility of radical carbonylation reactions, many radical precursors were explored, enabling the construction of various carbonyl-containing scaffolds, not only esters, but also amides and ketones.

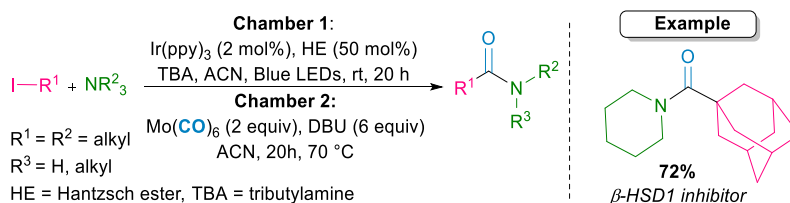
In 2015, carboxylic acids were employed in a decarboxylative carbonylative alkylation reaction in the presence of CO and thynylbenziodoxolones (EBX) reagent.²²⁷ Arylsulphonylchlorides were also viable substrates for the construction of indol-3-yl aryl ketones,²²⁸ and the use of Katritzky salts to form α,β -unsaturated ketones was also developed.²²⁹ Catechol silicates also proved to be viable substrates for radical carbonylations. Indeed, in 2019, Cartier *et al.* achieved a radical carbonylation of electron-withdrawing alkenes in a Giese type fashion and a radical carbonylative allylation as well, obtaining the formation of unsymmetrical ketones. Primary, secondary, and tertiary catechol silicates were found to be reactive.²³⁰ A variety of electron-withdrawing alkenes as radical acceptors and an organic photocatalyst (4CzIPN) were conveniently employed (Scheme 126, A).

Soon after, the same group reported the use of the same radical source in the attempt to build aliphatic amides through a radical carbonylation strategy.²³¹ In this regard, CCl_4 was added to the reaction mixture as a Cl-radical source to generate *in situ* acyl chloride intermediates which could further react with the amine to form the desired product. Besides being widely applicable to both the silicate and the amine counterpart, the reaction was found to be amenable to the intramolecular construction of the pyrrolidinone moiety (Scheme 126, B).



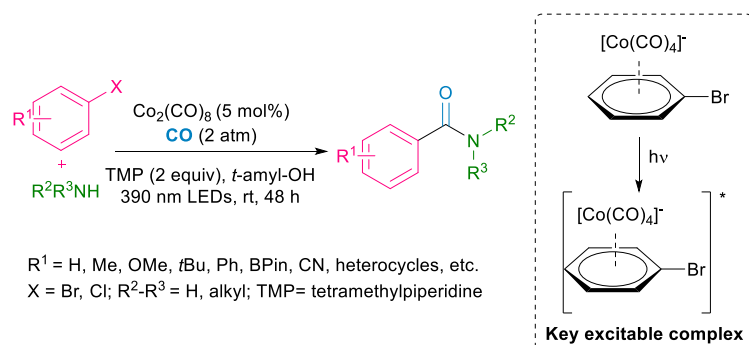
Scheme 126: A) Carbonylation of alkyl radicals from silicates through a Giese type addition; B) Synthesis of aliphatic amides through a photoredox catalyzed carbonylation process.

Complementary strategies for the construction of amide bonds have also been developed. In this regard, amines were employed as nucleophiles to attack the acylium ion intermediate, common in radical-mediated carbonylation reactions. In 2016, Chow *et al.* reported a *fac*-Ir(ppy)₃-mediated radical aminocarbonylation of unactivated alkyl iodides, employing a two-chamber strategy to access the generation of gaseous CO from CO surrogates.²³² Mo(CO)₆ was employed to explore the scope, but many other CO surrogates were tested and provided acceptable yields. The two-chamber system allowed the *ex situ* generation of CO (through heating chamber 1 at 70 °C). Chamber 1 was instead irradiated with blue LEDs to achieve the excitation of the photocatalyst. In its excited state, the photocatalyst reduces the alkyl halide to access the formation of an alkyl radical, further involved in the carbonylation process. The reaction was found to be amenable to a wide range of substrates and, notably, the synthesis of a selective 11b-HSD1 inhibitor could be achieved as well. Only primary alkyl halides underwent amination in the presence of non-sterically hindered amines, as a result of the unfavorable formation of unstabilized primary alkyl radicals. Benzyl and allyl iodides were also unreactive since the stability of the resulting radical prevents the carbonylation step (Scheme 127).



Scheme 127: Aminocarbonylation of unactivated alkyl iodides

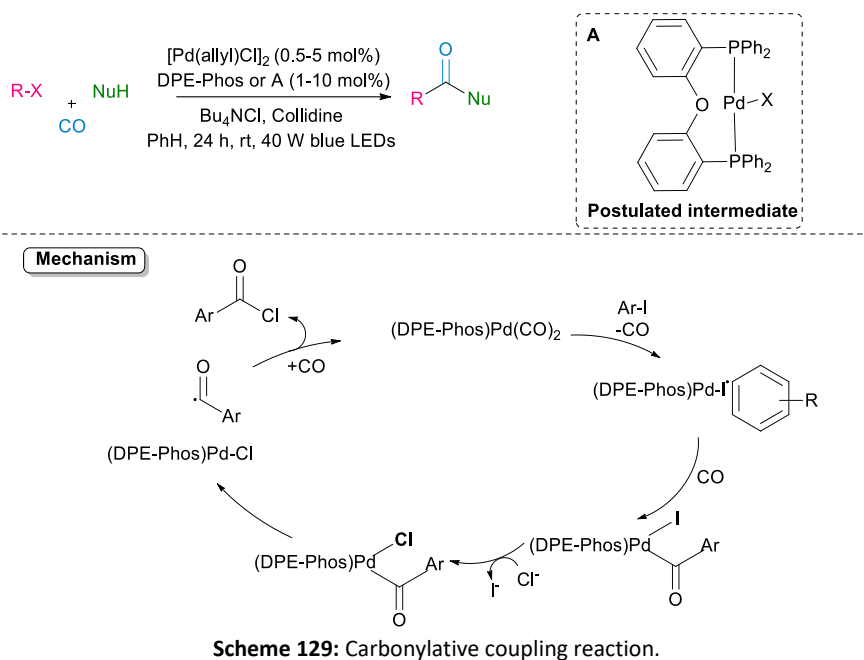
Another interesting strategy was presented in 2020 by Veatch *et al.*²³³ In this case, the aminocarbonylation of (hetero)aryl halides was accomplished through the mediation of cobalt catalysis (Co₂(CO)₈) and irradiation with visible light (390 nm). Despite the mechanism being still under investigation, the authors proposed that, upon the addition of an amine or tetramethylpiperidine, Co₂(CO)₈ disproportionates to form a cobaltate anion. The formation of a donor-acceptor complex between the cobaltate anion and the heteroaryl halide or triflate leads to a light-mediated charge transfer, followed by loss of the halide and radical generation. After recombination, an intermediate cobalt/(hetero)aryl species is formed, followed by migratory insertion of CO. Subsequent substitution of the amine nucleophiles brings to product formation and catalyst regeneration. The reaction was amenable to (hetero)aryl bromides, triflates and, despite the decreased reactivity level, to chlorides. A wide variety of primary and secondary amines was employed, and preliminary encouraging results using ammonium carbamate forecast the possibility to generate primary amides (Scheme 128).



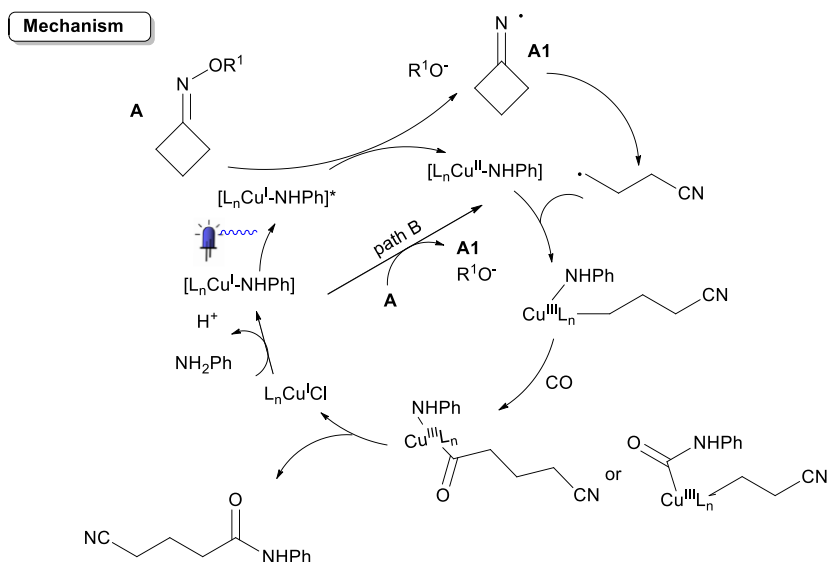
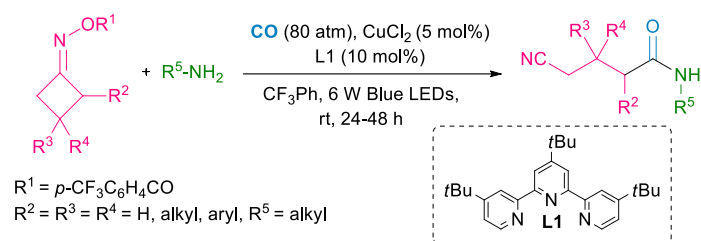
Scheme 128: Cobalt-catalyzed aminocarbonylation of (hetero)aryl halides.

In 2020, Torres, Liu *et al.* presented an efficient and broadly applicable carbonylation strategy that was applied to the synthesis of acyl chlorides, esters, amides and ketones.²³⁴ The authors elegantly employed blue light to favor both the oxidative addition and the

reductive elimination step of this palladium-catalyzed carbonylation reaction, overcoming the challenges arising from the different requirements of these two steps. They employed $[\text{Pd}(\text{allyl})\text{Cl}]_2$ and [(2-diphenylphosphino)phenyl]ether (DPEphos) as ligand, in combination with alkyl/aryl iodides or bromides, in the presence of challenging nucleophiles. Upon irradiation, they proposed the homolytic scission of the aryl/alkyl halide, thus forming a Pd(I) intermediate and a C-centered radical. In the presence of CO, an addition step occurs, leading to the formation of an acyl radical. The crucial acylpalladium chloride complex is formed upon oxidative addition of the acyl radical and halogen exchange between iodide and a chloride source (Bu_4NCl). At this stage, the authors proposed that visible light triggers the reductive elimination step through a homolytic cleavage of the Pd-acyl bond, followed by chlorine abstraction. Nucleophile addition to the reaction mixture allowed the synthesis of a broad scope of structures, including the construction of complex terpenoids, steroid acid chlorides and β -amino acids among all, proving the versatility of this light triggered carbonylation reaction (Scheme 129).

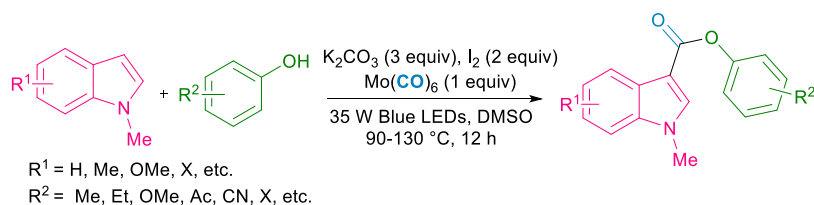


In 2019, Lu *et al.* developed a copper-catalyzed aminocarbonylation of cycloketone oxime esters to form cyanoalkylated amides.²³⁵ A CO atmosphere (80 atm) was required to perform the reaction. Several substituents on the oxime esters were tolerated, and the same was observed for both anilines and alkyl amines. The authors highlighted the utility of the method in the late-stage functionalization of the drug molecule mexiletine. Regarding the mechanism, they proposed that CuCl, together with a *N,N,N*-tridentate ligand and the chosen amine form the active complex, are able to reduce the oxime ester upon irradiation with visible light. Because of the redox properties of the complex, the authors could not exclude the unnecessary of light excitation. As a consequence, the resulting iminyl radical undergoes a β -C-C bond cleavage to form the intermediate cyanoalkyl radical that can attack the Cu(II) catalyst to afford a high valent Cu(III) complex. After CO insertion, a reductive elimination step delivers the desired product and regenerates the Cu(I) catalyst (Scheme 130).



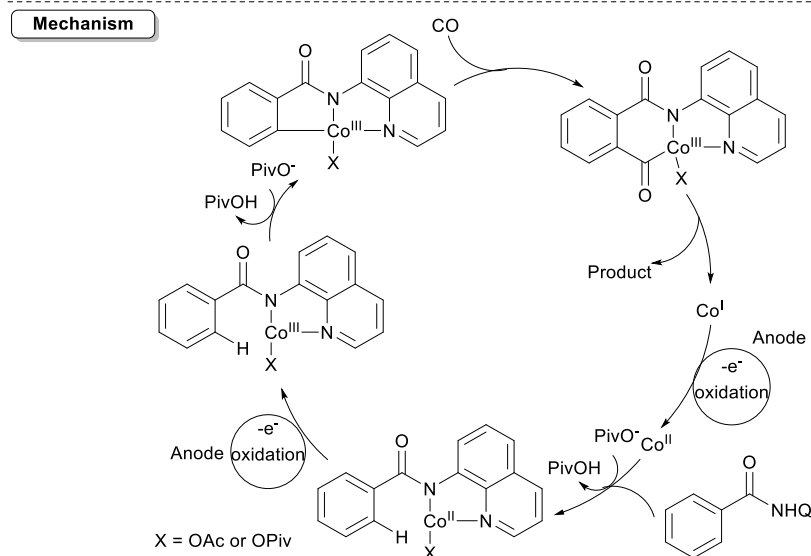
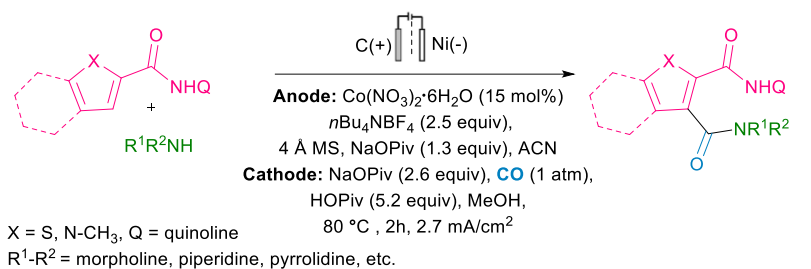
Scheme 130: Copper-catalyzed aminocarbonylation of cycloketone oxime esters.

This year, an interesting methodology for the construction of indole-3-carboxylates was developed by Qi *et al.*²³⁶ I_2 (2 equiv) was chosen as a photosensitizer to induce, upon blue-light irradiation, the formation of a phenol radical. Notably, $\text{Mo}(\text{CO})_6$ was used as CO source. The reaction required a temperature of 120 °C or 90 °C for more sensitive functional groups, like the cyano group, and was performed in the presence of differently substituted phenols as well as indoles. The *N*-indole substitution with electron-withdrawing groups was not tolerated. Several natural products were functionalized too, including estrone, eugenol, α -tocopherol (Scheme 131).



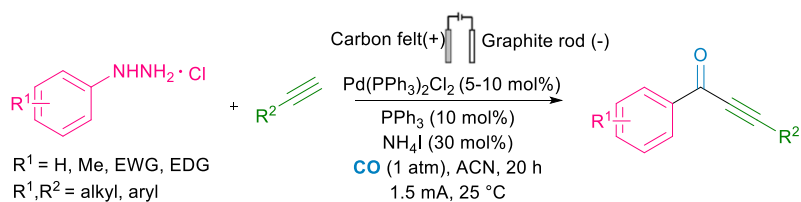
Scheme 131: Carbonylation of indoles with phenols using I_2 as photosensitizer.

Some recent strategies are also worth mentioning in which the multicomponent oxidative carbonylation reaction was achieved by electrocatalytic methods, avoiding the need for an additional oxidant like O_2 . In 2018, Zeng *et al.* presented an elegant strategy for the cobalt catalyzed oxidative C-H/C-N carbonylation of heterocyclic amides with alkyl amines.²³⁷ Thiophene and pyrrole-bearing amides were successfully carbonylated in the presence of various cyclic secondary amines and aliphatic primary amines. Unfortunately, benzamides and acrylamides revealed a stronger attitude to undergo intramolecular carbonylation to form succinamides and maleimides. Mechanistic studies revealed that, in the presence of the amide-containing starting materials, $\text{Co}(\text{acac})_2$ formed a complex able to be oxidized by a constant current of 15 mA to generate $\text{Co}(\text{III})$ species. Cyclic voltammetry analyses also showed a lowered oxidation peak at 1.08 V. With the help of a base (NaOPiv), $\text{C}(\text{sp}^2)\text{-H}$ activation of the *ortho* position became possible, followed by CO insertion and reductive elimination to deliver the final product. The $\text{Co}(\text{I})$ species then generated could be oxidized at the anode to obtain the turnover of the Co catalyst. The reaction was performed in a divided cell, generating H_2 at the cathode (Scheme 132).



Scheme 132: Cobalt-catalyzed electrochemical oxidative C-H/N-H carbonylation.

A further methodology for the electrochemical palladium-catalyzed synthesis of ynones through a Sonogashira carbonylation mechanism was presented this year.²³⁸ Wu and Zeng *et al.* demonstrated the possibility to achieve the carbonylation of alkynes and arylhydrazines in an undivided cell with constant current mode, without the need for external oxidants or oxygen. A carbon felt anode and a graphite rod cathode under 1.5 mA current were employed, leading to a range of valuable ynones. In particular, steric factors did not preclude the reaction, and electron-donating and withdrawing groups, including halogens, were tolerated on both the starting species. A 10 mmol scale reaction was also feasible, highlighting the potential of this methodology (Scheme 133).



Scheme 133: Palladium-catalyzed oxidative Sonogashira carbonylation of arylhydrazines and alkynes to ynones.

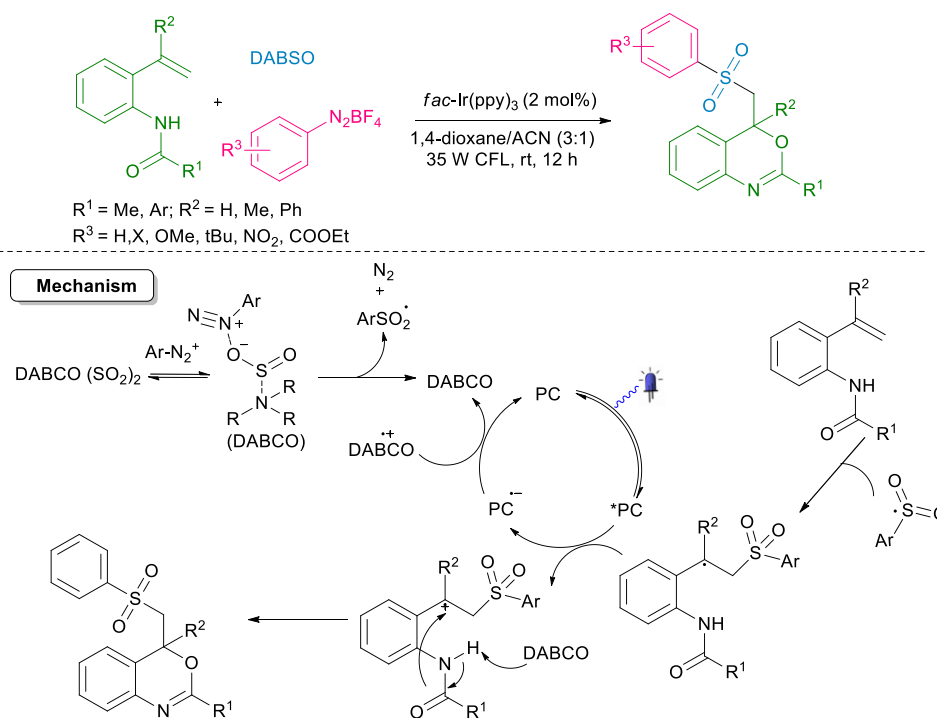
4. Sulfur Dioxide insertion

In the multicomponent reaction landscape, the insertion of SO_2 in the difunctionalization of unsaturated moieties (alkenes and alkynes) has been playing a central role, as an increasing number of reaction manifolds have appeared over the years. This evergreen interest in the installation of sulfonyl groups first relies on the biological activity that sulfonyl-containing compounds have demonstrated, keeping the interest in drug discovery, medicinal chemistry and agrochemical synthesis high.²³⁹⁻²⁴² In addition, the facility by which SO_2 is involved in radical reactions, acting as a radical trap, reinforced by the advent of photoredox catalysis and electrochemistry, has renewed the efforts in the construction of sulfonyl compounds employing mild and easily applicable conditions. Several SO_2 surrogates have been introduced and developed over the years to avoid the use of gaseous SO_2 , which requires specific handling techniques for its toxicity and corrosiveness. Among all, the most used in photoredox catalyzed reactions are DABSO (1,4-diazabicyclo[2.2.2]octane-bis(sulfur dioxide) adduct), sodium and potassium metabisulfite ($\text{Na}_2\text{S}_2\text{O}_5$, $\text{K}_2\text{S}_2\text{O}_5$) and the recently introduced SOgen.²⁴³ The first has observed wide employment as a convenient source of 2 equivalents of SO_2 , but its widespread utilization is hindered by the cost of the commercially available reagent and its poor solubility in many organic solvents. Its poor atom economy, due to the release of DABCO as waste, has also led to the employment of metabisulfites instead, but similar solubility

problems in organic solvents occur. An alternative to SO₂ surrogates, especially useful when performing electrochemical reactions, is represented by SO₂ stock solutions in organic solvents, some of which are commercially available. In light of the advance that sulfonylation reactions have faced over the years, many reviews describing recent progress in SO₂ fixation have appeared. We, therefore, decided to compile a selection of relevant reaction platforms to highlight the main strategies to achieve this transformation.^{244–249} Generally speaking, three mechanistic scenarios for the incorporation of SO₂ into organic molecules can be devised. On the one hand, upon photocatalyst-assisted radical generation, SO₂ acts like a radical trap, thus forming an intermediate sulfonyl radical that is then involved in addition reactions on unsaturated bonds. The arising radical intermediate can then undergo different pathways, including radical couplings and radical polar crossover reactions. On the other hand, it is also possible that, after radical formation, the addition step on the alkene precedes SO₂ incorporation. In addition to the mechanistic scenarios described above, the key sulfonyl radical can also be involved in further photocatalyst-mediated radical coupling reactions. For the sake of clarity, the discussion will focus on recent advances in the field, dividing the relevant examples per radical source utilized in the process.

4.1. Aryldiazonium salts

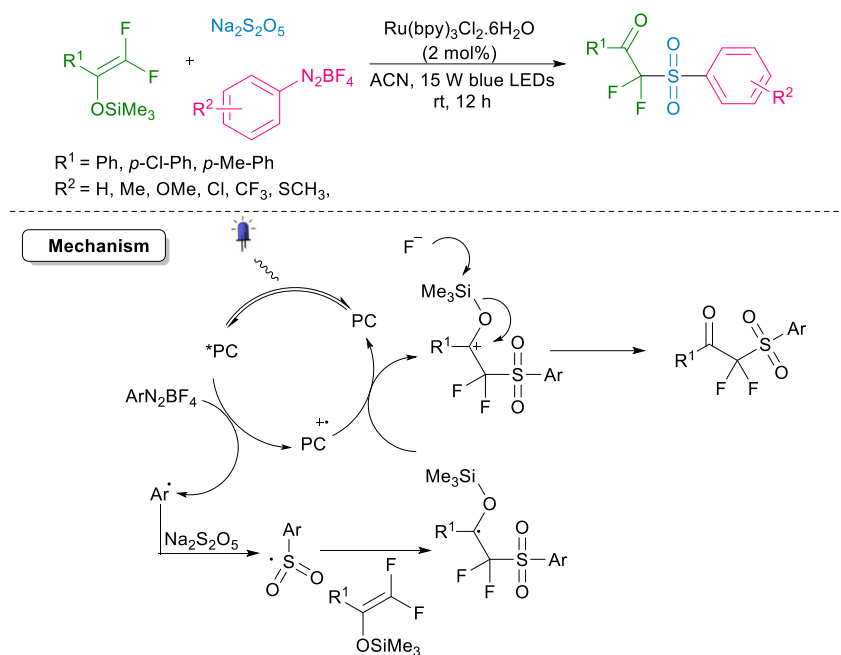
In 2017, Liu *et al.* combined photoredox catalysis with sulfonylation reactions, using aryldiazonium tetrafluoroborates in combination with *N*-(2-vinylphenyl) amides and *fac*-Ir(ppy)₃ with the aim to synthesize 4-(arylsulfonyl)methyl)-4*H* benzo[d][1,3] oxazines.²⁵⁰ Through mechanistic investigations, they postulated that arendiazonium tetrafluoroborates react with DABSO to form an aryl sulfonyl radical and DABCO⁺. The sulfonyl radical is then involved in the addition on the alkene, followed by a photocatalyst-assisted oxidation. In the presence of DABCO, an intramolecular attack of the amide to the cation finally generates the final product (Scheme 134).



Scheme 134: Synthesis of sulfonated benzo[d][1,3]oxazines.

Following this general mechanism, a diverse range of alkenes were remarkably functionalized, thus affording the generation of isobenzofuran-1(3*H*)-ones,²⁵¹ sulfonated 1-isindolinones,²⁵² 2,2-disubstituted tetrahydrofurans,²⁵³ coumarines.²⁵⁴

With the aim to synthesize α,α -difluoro- β -ketosulfones, He *et al.* also developed a photocatalyzed method to fix SO₂ on 2,2-difluoro enol silyl ethers, using arendiazonium salts and Na₂S₂O₅ as SO₂ source.²⁵⁵ With a similar functional group tolerability, the reaction followed a slightly different mechanism, where arendiazonium salts are first reduced by the excited state photocatalyst and then react with sodium metabisulfite to afford the arylsulfonyl radical intermediate. After the addition on difluoroenoxy silane and photocatalyst-mediated oxidation, the resulting cation then undergoes desilylation (with the assistance of F⁻ anions derived from tetrafluoroborate) to form the desired product (Scheme 135).



Scheme 135: Sulfonylation of difluoroenoxy silanes.

Recently, a similar strategy was employed by Zhou *et al.* to form polycyclic scaffolds that hold relevant importance in photochemistry, polymer chemistry, materials, and many other applications.²⁵⁶ In light of their utility, the authors sought to develop a straightforward strategy to form 4-sulfonated cyclopenta[gh] phenanthridines under mild conditions, exploiting, in this case, the reactivity of alkynes as radical traps. Following a mechanism similar to He's work (Scheme 135), the photocatalyst (eosin Y) is first responsible for the generation of an aryl radical from the arendiazonium salt, that subsequently forms the desired arylsulfonyl radical through the reaction with sodium metabisulfite. This ecofriendly reaction was tolerant to many functional groups, and electronic as well as steric factors did not influence with relevance the outcome of the reaction. The only limitation was the need for an aromatic substituent on the alkyne moiety. Indeed, both terminal and alkyl substituted alkynes failed to form the desired product (Scheme 136).



Scheme 136: Multicomponent synthesis of 4-sulfonated cyclopenta[gh] phenanthridines with SO₂ insertion.

Similarly, the multicomponent sulfonylation of alkynes allowed to generate sulfonylated dibenzazepine derivatives.²⁵⁷ The sulfonylation of alkynes was also accomplished by Ni *et al.* employing in this case a polymeric heterogeneous photocatalyst (p-g-C₃N₄).²⁵⁸ The reaction produced β -ketosulfones and proved to be tolerant to many functionalities. Steric effects played a role in the reaction outcome, affording lower yields in case of *ortho*-substitutions. The reaction was also conducted under sunlight, obtaining similar results. The reusability of the photocatalyst was also tested, and its efficiency confirmed up to six catalytic cycles (Scheme 137).



Scheme 137: Heterogeneous multicomponent hydrosulfonylation of alkynes.

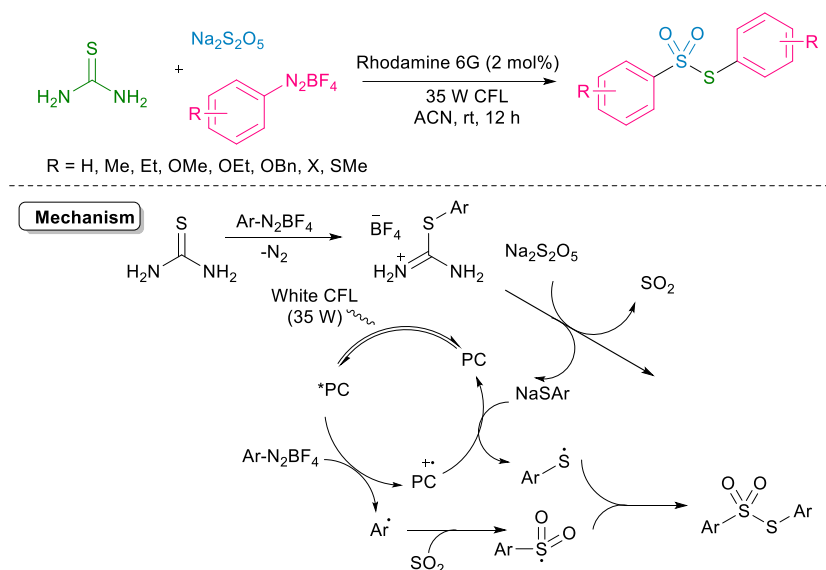
Recently, a four-component reaction manifold allowing the construction of complex sulfonylated quinoxalin-2(1*H*)-ones was presented by Lv *et al.*²⁵⁹ Upon addition of the key arylsulfonyl radical on the alkene, they were able to fine tune the reaction conditions to achieve the attack of the alkyl radical intermediate on quinoxalin-2(1*H*)-ones. The reaction was tolerant to both electro-donating and withdrawing groups on the aryl diazonium salts, while *ortho*-substituted styrenes only afforded lower yields. Notably,

aliphatic non-activated alkenes were also successfully employed. *N*-Substituted quinoxalinones could also be employed, while *N*-free quinoxalin-2(1*H*)-one was unreactive (Scheme 138).



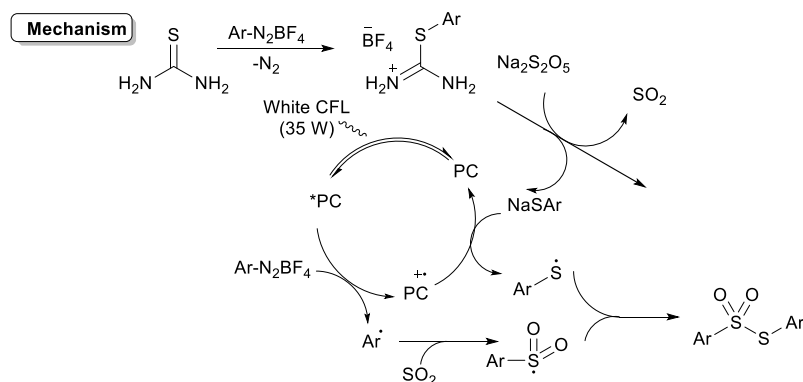
Scheme 138: Four component reaction for the construction of sulfone-containing quinoxalin-2(1*H*)-ones.

In situ formed diazo compounds were also employed in the synthesis of spiro[4,5]trienones, in a sulfonylation/ipso-cyclization reaction of *N*-arylpropiolamides and DABSO.²⁶⁰ In addition to the described methodologies, some interesting examples involving a radical coupling mechanism have appeared over the years. In 2018, Gong *et al.* disclosed a photoredox catalyzed benzylic sulfonylation of 4-methylphenols, using sodium metabisulfite as an SO₂ surrogate. In this report, aryl diazonium salts are first reduced to afford aryl radical formation.²⁶¹ Through the assistance of a photoredox catalyst (Rhodamine 6G), the authors proposed that an aryl radical is generated from aryl diazonium salts and then trapped by SO₂ to form an arylsulfonyl radical. To close the catalytic cycle, the authors next postulated the involvement of thiophenolate anions, derived from the reaction between aryl diazonium tetrafluoroborates and thiourea in the presence of sodium metabisulfite. After a radical coupling mechanism between the arylsulfonyl radical and the thiophenolate anion, the final product is therefore formed. The authors highlighted the utility of this strategy to form *S*-aryl thiosulfonates, without the need for additional oxidants or reductants. The reaction could only be applied to symmetrical thiosulfonates, as with the addition of two different aryl diazonium salts the reaction mixture became complex to analyze. Despite not being tolerant to *ortho*-substitution, the reaction was found to be easily applicable to many functionalities (Scheme 140).



Scheme 140: Synthesis of *S*-aryl thiosulfonates.

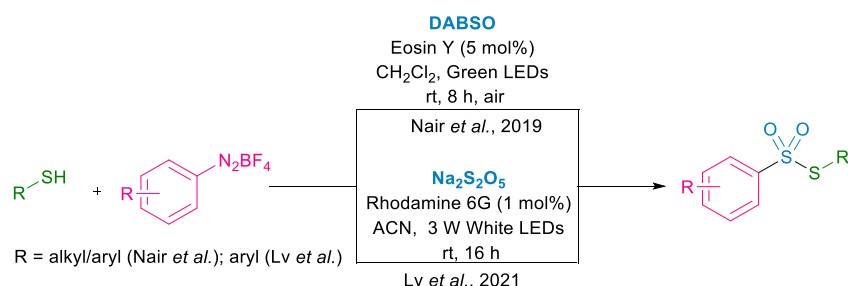
In the same year, Gong *et al.* presented the formation of unsymmetrical thiosulfonates, employing for this reaction arendiazonium salts, DABSO and thiols under photoredox catalyzed reaction conditions.²⁶² Through the assistance of a photoredox catalyst (Rhodamine 6G), the authors proposed that an aryl radical is generated from aryl diazonium salts and then trapped by SO₂ to form an arylsulfonyl radical. To close the catalytic cycle, the authors next postulated the involvement of thiophenolate anions, deriving from the reaction between aryl diazonium tetrafluoroborates and thiourea in the presence of sodium metabisulfite. After a radical coupling mechanism between the arylsulfonyl radical and the thiophenolate anion, the final product is therefore formed. The authors highlighted the utility of this strategy to form *S*-aryl thiosulfonates, without the need for additional oxidants or reductants. The reaction could only be applied to symmetrical thiosulfonates, as with the addition of two different aryl diazonium salts the reaction mixture became complex to analyze. Despite not being tolerant to *ortho*-substitution, the reaction was found to be easily applicable to many functionalities (Scheme 140).



Scheme 140: Synthesis of S-aryl thiosulfonates.

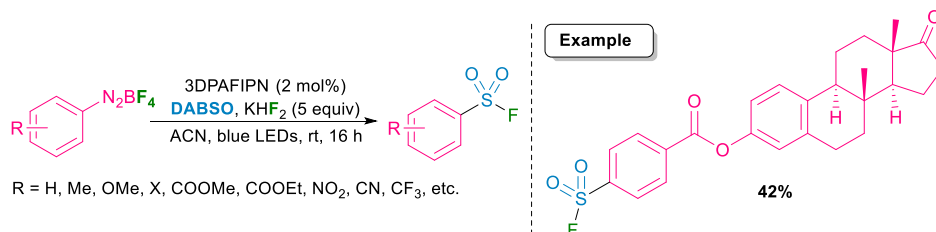
In the same year, Nair *et al.* presented the formation of unsymmetrical thiosulfonates, employing for this reaction aryl diazonium salts, DABSO and thiols under photoredox catalyzed reaction conditions.²⁶³ Worth mentioning is the synthesis *via* this strategy of glycosylated thiosulfonates, important precursors investigated in glycoprotein synthesis. The gram-scale reaction also afforded good yield (81% yield), demonstrating the robustness and scalability of the method.

This year, a similar approach to synthesize unsymmetrical thiosulfonates was developed by Lv *et al.*²⁶⁴ In order to avoid the expensive and harshly obtained DABSO, they opted for the use of sodium metabisulfite as a SO₂ surrogate, affording a wide range of sulfonylated products with high electronic and steric tolerability (Scheme 141).



Scheme 141: Synthesis of unsymmetrical thiosulfonates.

In the context of SuFex chemistry, the synthesis of arylsulfonyl fluorides with simple and mild conditions is highly desirable. Louvel *et al.* presented this year the employment of aryl diazonium salts, DABSO and KHF₂ as additive to achieve the photoredox catalyzed synthesis of these important synthons.²⁶⁵ The reaction features high tolerance to electronic and steric factors, therefore providing wide applicability (Scheme 142).



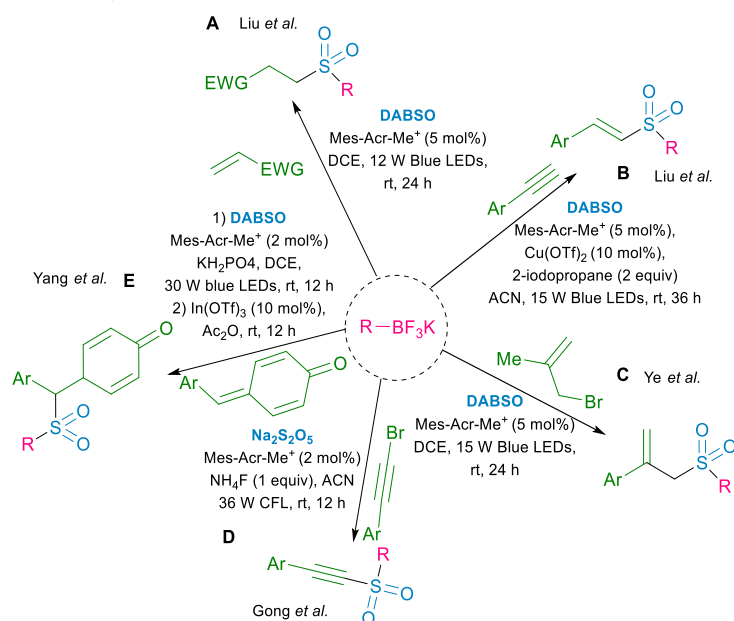
Scheme 142: Synthesis of arylsulfonyl fluorides.

4.2. Trifluoroborates

The first use of trifluoroborates in a reductive quenching cycle involving SO₂ incorporation was introduced by Liu *et al.* in 2018.²⁶⁶ These radicals were intercepted by SO₂ to generate the key sulfonyl radical intermediate. This transient species then engages in the addition on an electron-withdrawing alkene, following the traditional Giese-type reaction pathway. The highly oxidizing Mes-Acr-Me⁺ was used as the photocatalyst, while DABSO was employed as a SO₂ surrogate. The reaction tolerated several functional groups,

including free hydroxyl, nitro and halogen groups, and was applied to a broad variety of radical acceptors as well as trifluoroborates (Scheme 143, A). The same group also focused on the synthesis of vinyl sulfones, they are recently discovered active scaffolds for Parkinson's disease, employing the same radical source, but with a different choice of the unsaturated starting materials. Indeed, they unveiled the employment of alkynes as a radical trap that, with the assistance of copper(II) triflate, would lead to the regio- and stereoselective generation of (*E*)-allylsulfones (Scheme 143, B).²⁶⁷ Similar reaction conditions were also applied in allylation (Scheme 143, C)²⁶⁸ and alkynylation reactions as well. The latter is a recent example of the application of the sulfonylation reaction to the synthesis of alkylalkynyl sulfones (Scheme 143, D).²⁶⁹ The reaction pathway follows the previously described cycle, with the radical generation from alkyltrifluoroborates occurring upon excitation of Mes-Acr-Me⁺, followed by the addition on SO₂ (in this report, Na₂S₂O₅ was used as a SO₂ surrogate). The sulfonyl radical then attacks bromoalkynes, leading to the formation of a vinyl radical which is further reduced by the photocatalyst. After the elimination of Br⁻, the desired product is formed. The reaction was amenable to a wide variety of trifluoroborates, while for the alkyne counterpart, only aryl-substituted alkynes (bearing alkylic and electron-withdrawing substituents) could be employed.

This year, Yang *et al.* also presented the use of alkyl trifluoroborates as radical precursors to achieve the sulfonylation of *para*-quinone methides. Following the general mechanism delineated before, a wide range of *para*-quinone methides were successfully alkylated via 1,6-radical addition (Scheme 143, E).²⁷⁰

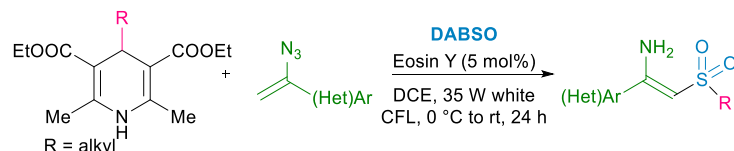


Scheme 143: Use of trifluoroborates in photoredox catalyzed sulfonylation reactions.

4.3. Hantzsch esters

SO₂ incorporation was also accomplished employing Hantzsch esters as a radical source. The general photoredox catalyzed mechanism follows a common pattern, where an alkyl radical is formed upon oxidation of the radical precursor by the excited photocatalyst. The radical then attacks SO₂, thus forming an alkyl sulfonyl radical. This key radical intermediate is then involved in the addition of unsaturated alkene moieties, following a Giese-type addition mechanism.

In 2019, Wang *et al.* employed vinyl azides as radical acceptors, generating (*Z*)-2-(alkylsulfonyl)-1-arylethen-1-amines.²⁷¹ The reaction was found to be amenable to the installation of primary and secondary alkyl groups, and no electronic and steric issues were observed in the substitution pattern of vinyl azides. Because of steric hindrance between the substituents on the vinyl azides and the sulfonyl radical, only the (*Z*)-product was formed (Scheme 144).



Scheme 144: Photoredox-catalyzed synthesis of (*Z*)-2-(alkylsulfonyl)-1-arylethen-1-amines.

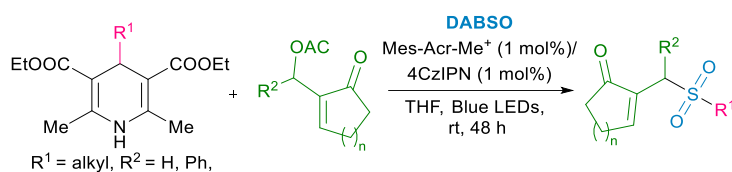
The same group also applied the sulfonylation strategy to the synthesis of (*E*)-chalcone derivatives, (vinylsulfonyl)benzene and 2-vinylpyridine derivatives, generating a range of interesting molecular scaffolds.²⁷² In particular, a cardamonin derivative could be prepared in 69% yield, a noticeable result considering the biological activity of this natural occurring chalcone (Scheme 145).



Scheme 145: Hydrosulfonylation reaction of electron-deficient alkenes with substituted Hantzsch esters.

Gong *et al.* also presented in 2020 a way to achieve the formation of alkynyl sulfones employing the same strategy delineated before with Hantzsch esters and using alkynyl bromides as radical acceptors.²⁷³

This year, an interesting method for the generation of allylic sulfones employing Morita–Baylis–Hillman (MBH) acetates, Hantzsch esters and DABSO as starting materials was developed.²⁷⁴ The synergism of photoredox and tertiary amine catalysis was the driving force to obtain the desired products. Indeed, the authors explain that, after radical generation and addition of SO₂, the released DABCO is both reacting with the MBH acetate and steering the reaction outcome. The reaction was also applied to trifluoroborates, and a range of primary and secondary alkyl radicals (both cyclic and acyclic) could be installed. Considering the reactivity of MBH acetates, better yields were obtained with electron-donating groups, while slightly lower yields arose from MBH acetates bearing electron-withdrawing groups (Scheme 146).



Scheme 146: Generation of allylic sulfones from Morita–Baylis–Hillman acetates.

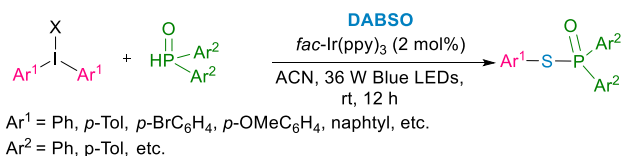
4.4. Diaryl iodonium salts and alkyl iodides

A limited number of examples involving diaryliodonium salts in combination with photoredox catalysis can also be found. In particular, Liu *et al.* in 2017 were able to form sulfonamides starting from diaryl iodonium salts, hydrazines and DABSO or Na₂S₂O₅ (in the presence of TFA for a slow SO₂ release) as SO₂ source.²⁷⁵ According to the insightful mechanistic studies, an *in situ* generated complex between hydrazine and SO₂ is first oxidized by the photocatalyst (perylene dye). The reduced state of the photocatalyst then reduces the aryl iodonium salt, leading to the generation of an aryl radical that then undergoes a free radical addition with the sulfonyl radical, forming the final product. The authors observed that, employing asymmetric aryl iodonium salts, selectivity could be achieved as only the more electron-poor aryl group was involved in the radical generation process. In particular, employing trimethoxybenzene as a dummy ligand, complete chemoselectivity could be achieved. Considering the hydrazine counterpart, while a discrete number of hydrazines was found to be reactive, anilines did not behave as suitable substrates (Scheme 147).



Scheme 147: Aminosulfonylation of diaryliodonium salts.

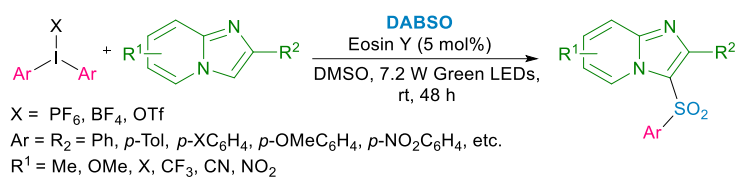
In the same year, Gong *et al.* also reported the use of diaryl iodonium tetrafluoroborates as a radical source in the synthesis of thiophosphates.²⁷⁶ The generation of the arylsulfonyl radical resembles the already described process, but the formation of the final product is enabled by the reduction of the arylsulfonyl radical by diarylphosphine oxide and the assistance of a tertiary amine cation (Scheme 148).



Scheme 148: Photoredox-catalyzed synthesis of thiophosphates.

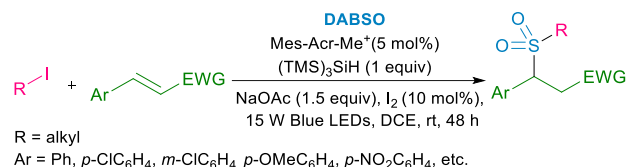
In 2020, the same radical source was applied to the synthesis of sulfonylated imidazoheterocycles.²⁷⁷ Despite the moderate yields for several examples, this remarkable synthetic procedure was usefully employed for the synthesis of interesting scaffolds for

medicinal chemistry purposes (2-phenylimidazo-[1,2-a]pyridine, 2-phenylimidazo[1,2-a]pyrimidine, benzo[d]imidazo[2,1-b]thiazole). The moderate yields were justified by the formation of two main side products, derived from the C3 bromination product of 2-phenylimidazo[1,2-a]pyridine, mediated by Eosin Y, and C-3 formylation of the 2-phenylimidazo[1,2-a]pyridine, derived from the involvement of DMSO used as solvent (Scheme 148).



Scheme 149: Synthesis of sulfonylated imidazoheterocycles.

Diaryliodonium salts also served as radical precursors in the formation of sulfonylated oxindoles from *N*-arylacrylamides and DABSO.²⁷⁸ Alkyl iodides were also employed as amenable radical precursors by Ye, Zheng *et al.*, that accomplished the sulfonylation of various substituted chalcones with good yields.²⁷⁹ Chalcones were the main substrates for this transformation, since acrylates, styrenes or Michael acceptors failed to deliver the desired product. Mechanistically, the authors postulated that the excited state of the photocatalyst can be involved in the formation of a trimethylsilyl radical, which is then responsible for the generation of an alkyl radical from the employed alkyl iodide. The sulfonyl radical resulting from the addition of the alkyl radical on SO₂ then attacks the electron-poor alkene. The next step can then follow two pathways: the radical intermediate can be reduced by the reduced photocatalyst and the resulting anion be protonated, or the trimethylsilyl silane can engage in a HAT step with this intermediate, thus forming the final product in both the scenarios (Scheme 150).



Scheme 150: Sulfonylation of chalcones with alkyl iodides.

4.5. *O*-Acyl oximes

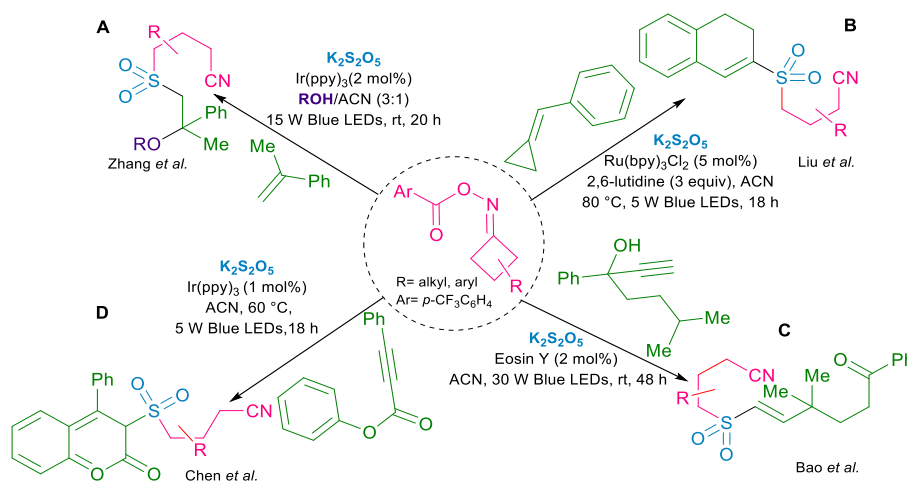
The installation of cyanoalkyl chains on molecular scaffolds holds great relevance, because of their prevalence on drug molecules and natural products, but also for the possibility to subject this skeleton to further transformations. A straightforward way to access cyanoalkyl chain-containing molecules relies on the photoredox catalyzed reduction of *O*-acyl oximes, which leads to the generation of an iminyl radical that further rearranges to deliver a cyanoalkyl radical. The combination of this radical generation strategy with SO₂ fixation has brought to the development of relevant methodologies.

In particular, Zhang *et al.* first presented the synthesis of β -alkoxy and β -hydroxy sulfones through the sulfonylation of *O*-acyl oximes.²⁸⁰ This multicomponent strategy was applied to a range of differently substituted alkenes and *O*-acyl oximes, showing tolerability to many functionalities, including heterocycles. Among alcohols, only primary alcohols (deuterated methanol as well) could be employed as nucleophiles. Water was also successfully introduced for the installation of hydroxyl groups. The mechanism described to explain this reactivity, starts with radical generation through reduction of the *O*-acyl oxime. After N-O bond dissociation and intramolecular rearrangement, a C-based radical is formed. SO₂ addition then follows, forming a sulfonyl radical involved in the attack on the alkene. Upon oxidation to achieve the catalyst turnover, a cation intermediate arises. After the reaction with alcohol or water, in the presence of a base, the product is finally formed (Scheme 151, A).

A similar mechanistic pathway was conceived to obtain 2-cyanoalkylsulfonated 3,4-dihydronaphthalenes from cycloketone oxime esters, methylenecyclopropanes (MCPs) and K₂S₂O₈ as a SO₂ source. Various substituents on MCPs were tolerated, but electronic and steric effects influenced the reactivity: *para*-substituted MCPs were more reactive than *ortho*- and *meta*-substituted ones. Electron-donating groups were also more effective than the electron-withdrawing ones. Both mono- and di-substituted cycloketone oxime esters were tolerated as well (Scheme 151, B).²⁸¹

Considering the relevance of vinylsulfones in medicinal chemistry, propargyl alcohols, together with cycloketone oximes and K₂S₂O₈ as SO₂ source were used as starting materials to form cyanoalkylated vinyl sulfones (Scheme 151, C).²⁸²

Similarly, Chen *et al.* applied this strategy to form 3-cyanoalkylsulfonylcoumarins. The generated cyanoalkylsulfonyl radicals engaged in a radical addition on alkyloates, a pathway that was still unexplored (Scheme 151, D).²⁸³

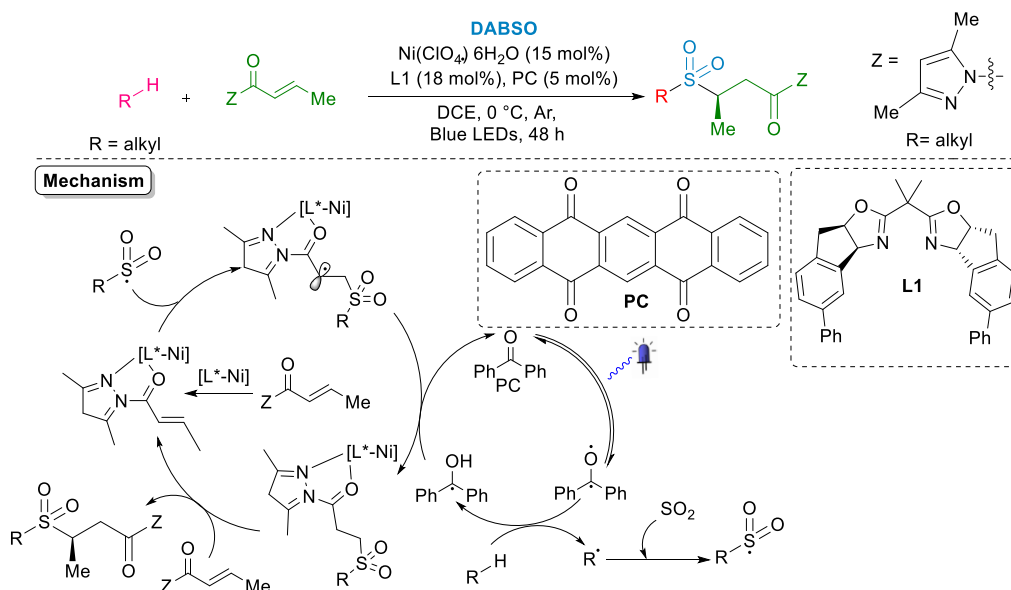


Scheme 151: Sulfonylation reactions for the installation of cyanoalkyl chains.

4.6. Miscellaneous

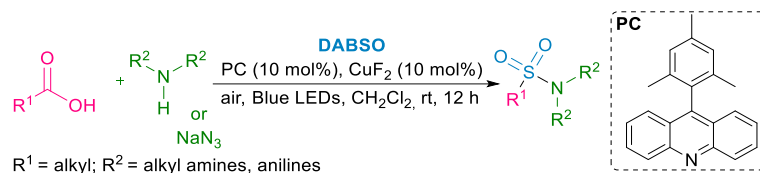
Recently, few innovative strategies for the SO₂ incorporation were developed, broadening the range of radical precursors and final molecular scaffolds obtained through mild and convenient reaction conditions.

This year, the three-component asymmetric radical sulfonylation of α,β -unsaturated carbonyl compounds employing cyclic and acyclic alkanes, toluene derivatives and ethers was accomplished.²⁸⁴ More than 50 examples were prepared, showing up to 50:1 rr and 95% ee. The radical generation was obtained through the use of 5,7,12,14-pentacenetetrone as a photocatalyst, DABSO as SO₂ surrogate and a nickel catalyst with a chiral bisoxazoline ligand. The nickel complex acted as a Lewis acid activator of the Michael acceptor. Indeed, the authors postulated that the chiral nickel catalyst ([L*-Ni]) first undergoes ligand exchange with the α,β -unsaturated *N*-acylpyrazole, forming the active complex then subjected to the radical sulfonylation. At the same time, the excited photocatalyst is able to abstract a hydrogen atom from the radical precursor. The radical is subsequently trapped by the *in situ* generated SO₂, leading to the formation of a sulfonyl radical that is involved in the outer sphere attack of the metal-coordinated α,β -unsaturated *N*-acylpyrazole, forming a further radical intermediate. To close the catalytic cycle, the involvement of photocatalyst and water present in the system in a SET and proton transfer steps was devised, but the involvement of DABCO could not be ruled out. The sulfonyl radical reacts with the less hindered face of the metal-Michael acceptor complex, forming *R* products with a high level of enantioselectivity. The authors also achieved high rates of regioselectivity, predictable if considering the bond dissociation energies of the C-H(sp³) bonds involved in the HAT. In particular, the adamantyl scaffold, whose tertiary C-H bond is difficult to functionalize regioselectively due to its high dissociation energy, was selectively sulfonylated under the presented reaction conditions. With even faster reaction times, toluene derivatives were functionalized as well, and drug molecules also succeeded in delivering the desired products. The authors hypothesized that radical stability and suppression of side reactions can be accounted by the presence of the SO₂ surrogate (Scheme 152).



Scheme 152: Asymmetric sulfonylation via direct C(sp³)-H functionalization.

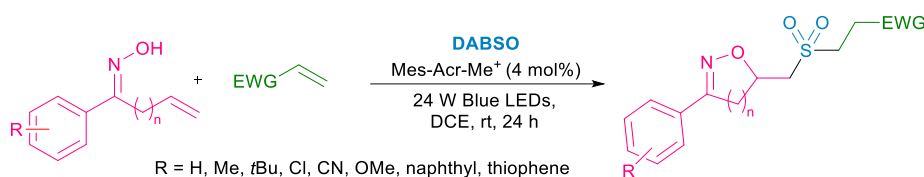
Nguyen *et al.* also presented a one-step generation of sulfonamides and sulfonyl azides, employing a multicomponent strategy involving aliphatic carboxylic acids, DABSO and *N*-centered coupling partners.²⁸⁵ Exploiting a proton-coupled electron transfer (PCET) mechanism to achieve decarboxylation and the use of a Cu co-catalyst, the authors were able to synthesize a wide range of aliphatic and aromatic sulfonamides and sulfonyl azides with good to excellent yields. Given the importance that the sulfonamide moiety holds as a bioisoster of carboxylic acids especially, this methodology stands out for the ability to generate this functionality in a one-step reaction under mild conditions. Among the scope, analogues of relevant drug molecules were functionalized, including aminoglutethimide, cholic acid and pinonic acid, underlining the wide applicability (Scheme 153).



Scheme 153: Synthesis of sulfonamides and sulfonyl azides.

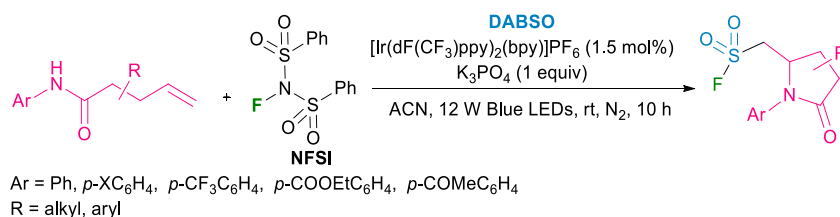
γ,δ -Unsaturated oximes were also employed as precursors for *N*-centered radicals that, upon visible light irradiation, underwent intramolecular cyclization, followed by SO₂-trapping and final addition of silyl enol ethers.²⁸⁶ A range of 3,4-dihydro-2*H*-pyrroles were generated under mild reaction conditions, enabling the synthesis of *N*-containing heterocycles.

In addition to this methodology, β,γ -unsaturated oximes/hydrazones were also employed in a radical cascade reaction by Chen *et al.* to afford sulfonylated isooxazoline/dihydropyrazole-substituted aliphatic sulfones.²⁸⁷ This multicomponent reaction involved the use of β,γ -unsaturated oximes/hydrazones as radical precursors. Upon photocatalyst mediated oxidation, the *O/N*-based radicals undergo 5-*exo-trig* cyclization, generating the alkyl radical intermediate able to attack SO₂. The reaction then follows the addition to electron-deficient alkenes previously described, giving rise to variously functionalized heterocycles. Six-membered heterocycles could also be successfully prepared under the optimal conditions, and an estrone-derived scaffold underwent the reaction as well (Scheme 154).



Scheme 154: Use of β,γ -unsaturated oximes/hydrazones in a photoredox-catalyzed sulfonylation.

With the ability to synthesize pyrrolidinone, oxazolidinone and imidazolidinone containing sulfonyl fluorides, Zhong *et al.* reported a straightforward strategy to form aliphatic sulfonyl fluorides in a multicomponent approach.²⁸⁸ A PCET mechanism is responsible for the generation of an amidyl radical that initiates the 5-*exo-trig* cyclization. DABSO and *N*-fluorobenzenesulfonamide (NFSI) are respectively the SO₂ surrogate and the fluorine source. The utility of the SO₂-F containing scaffolds was further demonstrated by SuFEX click reactions and metal-catalysed cross coupling reactions (Scheme 155).



Scheme 155: Synthesis of aliphatic sulfonyl fluorides.

An example of photoredox-catalyzed sulfonylation using Katritzky salts appeared in 2019, when Wang *et al.* utilized this radical source in the synthesis of dialkyl sulfones.²⁸⁹ They hypothesized and confirmed through mechanistic investigations that a radical mechanism is underlying the observed reactivity. Indeed, an alkyl radical can be formed through single-electron reduction of the pyridinium salt. Following the general pathway previously underlined, the radical then attacks SO₂ (sodium metabisulfite was employed as SO₂ surrogate), forming the key sulfonyl radical that is then captured by a silyl enol ether. After subsequent oxidation mediated by the photocatalyst, a base-assisted desilylation then occurs, forming the final ketone. The scope was tolerant to many functionalities, as halogen, trifluoromethyl, methoxy groups were all tolerated. Similarly, various alkyl radicals worked well under the optimized conditions, including free hydroxyl groups and heterocyclic scaffolds (Scheme 156).



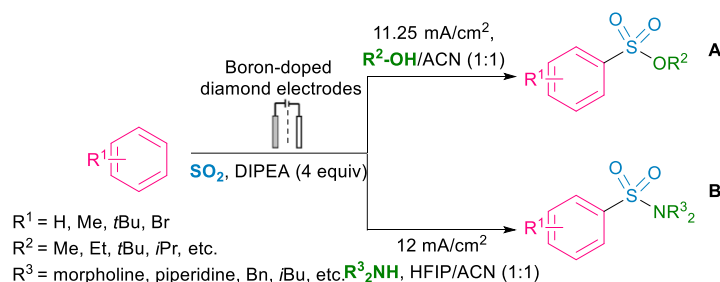
Scheme 156: Photoredox catalyzed sulfonylation using Katritzky salts.

4.7. SO₂ fixation through electrochemical methods

The introduction of sulfonyl groups by means of electrochemical methods has received increasing attention, but multicomponent electrochemical strategies for the incorporation of SO₂ are still elusive. Nevertheless, few recent examples have been developed. Due to the possible interference of DABCO (from DABSO), whose low oxidation potential would lead to competitive pathways, stock SO₂ solutions have been rather employed. It is indeed possible to accurately quantify SO₂ concentration through iodometry.

With respect to electrochemical processes, SO₂ can be easily reduced to SO₂^{•-}, but anodic oxidation of SO₂ is unachievable, therefore requiring the SO₂ fixation on electrochemically activated compounds.²⁴⁷

A multicomponent approach for the electrochemical synthesis of alkyl arylsulfonates was presented in 2020 by Blum *et al.*²⁹⁰ In this report, electron-rich arenes are functionalized in the presence of a primary or secondary alcohol and a stock solution of SO₂ in acetonitrile. The reaction was conducted in a divided cell set up to avoid the formation of complex ions between the SO₂ and the dithionite forming upon dimerization of SO₂ radical anion. On the other hand, the arene is oxidized at the anode. Noticeably, the reaction does not require the use of additional electrolytes, as the monoalkyl sulfite intermediate acts as both nucleophile and electrolyte itself. The same group implemented the reported procedure for the synthesis of sulfonamides.²⁹¹ Following the general mechanism explained above, electron-rich (hetero)arenes, SO₂ and amines can be incorporated in the final product in a one-step synthetic procedure. The scale-up of the reaction delineated was also successfully accomplished, employing a simple H-type glass cell, divided by a glass frit. A 13-fold increase of the reaction scale still afforded 85% of the desired product (Scheme 157).



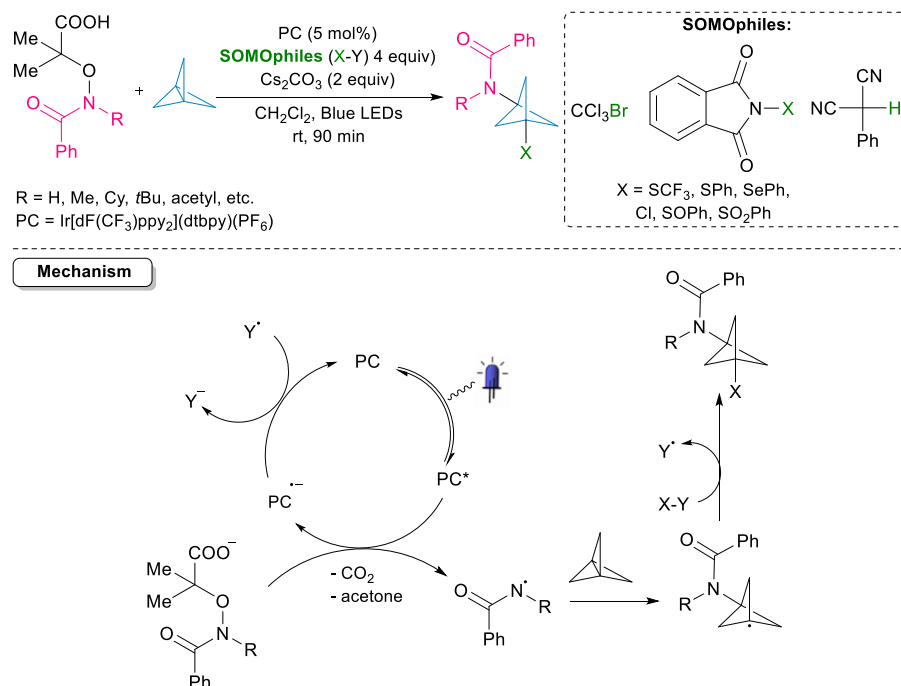
Scheme 157: Electrochemical multicomponent SO₂ fixation.

5. Installation of bicyclo[1.1.1]pentane (BCP)

Synthesized in 1964,²⁹² bicyclo[1.1.1]pentane (BCP) has been broadly studied for its chemical properties. In particular, innumerable applications in total synthesis, material science and medicinal chemistry among all, account for the utilization of these strained scaffold.²⁹³ The last field has been predominantly explored since the recognition of BCP and its derivatives as bioisoster of aromatic rings,²⁹⁴ tertbutyl group²⁹⁵ and internal alkynes.²⁹⁶ Indeed, the incorporation of BCP into drug candidates often offers advantages in terms of metabolic stability, water solubility and membrane permeability. The great interest in the employment of BCP into organic reactions relies on the reactivity of the central C-C σ -bond, whose involvement in polar and radical reactions can lead to the formation of variously 1,3-functionalized BCP derivatives. In the realm of photoredox catalysis, the increasing interest towards the functionalization of this versatile scaffold has enabled the development of innovative strategies in a multicomponent fashion. Recent reviews on the topic,^{297,298} highlight the relevance that these transformations are gaining, and we will therefore focus our attention on the description of the most relevant and recent procedures to achieve the difunctionalization of BCP using more than two starting materials in a one-pot reaction.

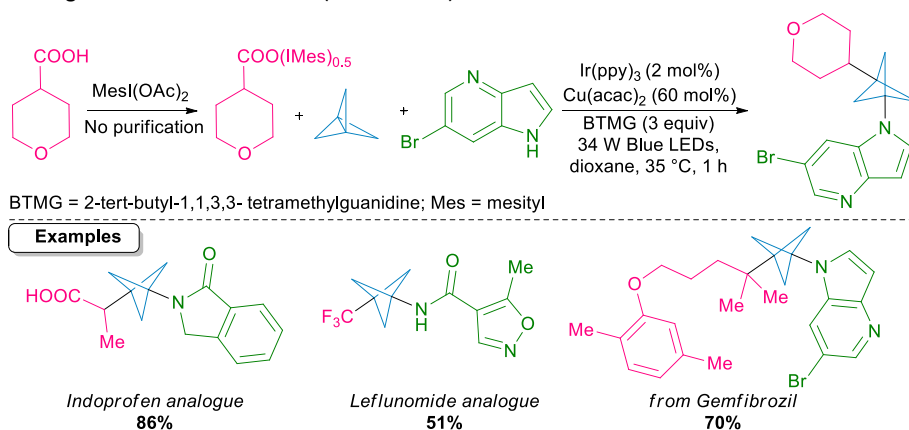
In 2020, Kim, Ruffoni *et al.* presented the first multicomponent strain release amino functionalization of BCP.²⁹⁹ The novelty of the work relies on the ability of the authors to develop an umpolung radical amination strategy, that would have been unfeasible under polar conditions due to the instability of the BCP cation. Aided by DFT studies, they proposed a mechanistic scenario that involves the oxidation of a carboxylate group, followed by rearrangement and elimination of CO₂ and acetone to deliver the formation of the electrophilic amidyl radical. This key radical is then able to intercept BCP, leading to a strain release step and central C-C bond cleavage. At this step, they reasoned that, despite its electrophilic character, this radical intermediate could undergo a group transfer

reaction with SOMOphiles to form the final difunctionalized product. SOMOphiles such as *N*-chlorosuccinimide, BrCCl₃, phthalimide-based reagents for the introduction of *S*- and *Se*- containing groups were found to suppress the oligomerization of BCP. The photocatalytic cycle is then ended by the reduction of radical Y• to Y⁻. Considering the amide groups installed, a wide range of functionalities were tolerated, including alkyl groups, heterocycles and commonly employed protecting groups. Only *N*-trifluoromethanesulfonyl, *N*-methyl radical required a solvent change to avoid the arylation of the amidyl radical. Overall, this strategy was able to deliver the formation of potentially useful aniline bioisosteres employing for the first time a multicomponent BCP amination reaction (Scheme 158).



Scheme 158: Strain-release amino-functionalization of [1.1.1] propellane with electrophilic nitrogen-radicals and SOMOphiles.

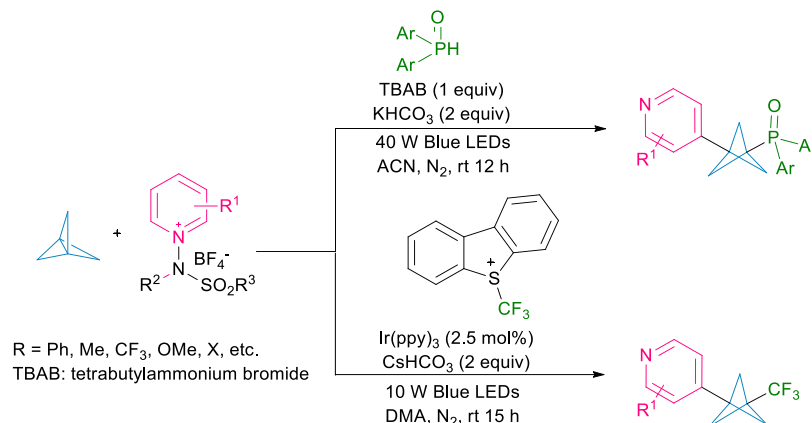
In the same year, Zhang, Smith *et al.* exploited BCP reactivity to install various functionalities on this moiety, with the aid of a photocatalyst (Ir(ppy)₃) and a Cu catalyst (Cu(acac)₂).³⁰⁰ This metallophotoredox catalyzed process proved to be extremely versatile, as different radical precursors could be utilized, including activated carboxylic acids, alkyl bromides, Togni's reagent, and thiosulfonates. On the other hand, various *N*-containing heterocycles, imines, anilines, sulfonamides, *S*- and *P*- containing functional groups could be installed as well, rendering this protocol adaptable to the synthesis of medicinally relevant synthons or amenable to the formation of drug analogues with similar or increased pharmacologic properties (*i.e.* Indoprofen and Leflunomide analogues). Mechanistically, a reductive quenching cycle is involved in this process. Similar to the previously presented mechanism, upon excitation, the photocatalyst was able to reduce the radical source, leading to the generation of a radical that was able to intercept BCP. The BCP radical intermediate was then trapped by a nucleophile ligated Cu(II) complex. The Cu(III) complex then generated underwent reductive elimination to give the desired difunctionalized product together with a Cu(I) complex. The fine-tuning of the conditions steered the reaction to the desired product, avoiding the two-component cross-coupling product with the exclusion of the BCP moiety or the oligomerization of BCP itself (Scheme 159).



Scheme 159: Copper-mediated synthesis of drug-like bicyclopentanes.

This year, a further multicomponent strategy developed by Shin *et al.* enabled the formation of diversified architectures,³⁰¹ in

particular phosphinoyl and pyridyl-functionalized BCPs, together with trifluoromethyl and pyridyl bearing BCPs. In this case, the formation of an electron donor-acceptor (EDA) complex between an *N*-aminopyridinium salt and tetrabutylammonium bromide (TBAB) in the presence of NaHCO₃ as base led to the formation, upon irradiation with blue LEDs, of an amidyl radical that could act as HAT reagent and generate a phosphinoyl radical from diphenylphosphine oxide. Similarly, employing Togni's reagent as trifluoromethylating agent, in the presence of Ir(ppy)₃, both a -CF₃ and differently functionalized pyridyl groups could be installed. Based on mechanistic investigations, the authors hypothesize a radical chain mechanism (Scheme 160).



Scheme 160: Visible-light-induced functionalization of [1.1.1]propellane.

6. Conclusions

In this review, we have focused on the vast development that multicomponent reactions have witnessed since the advent of photoredox catalysis and electrochemistry. In combination with the atom economy and the low waste production that typically characterize multicomponent reactions, we have underlined the benefits that these novel reaction platform offers. The use of photons or electrons as traceless reagents enhances the energy efficiency as reaction heating is rare and this is positively associated to a minor risk of byproduct formation and degradation. In addition, the possible utilization of enabling technologies such as flow chemistry allows the reaction scale-up, offering a valuable alternative to batch conditions, whose scaling-up can result in lower yields and sluggish reactions. Especially when considering photoredox catalyzed reactions, an increasing number of transformations has shown the potential to be applied under continuous-flow conditions. However, in many of the examples presented, the implementation of flow reactors has still not been widely adopted and circumscribed to a limited number of substrates. The translation of the batch reaction conditions in flow towards photo-/electro- MCRs appears more as a nice-to-have and not as a base for the investigation of novel reaction pathways.

Focusing on electrochemical multicomponent reactions, at first glance, it appears evident that its development is consistently inferior in a number of examples and in method development, in comparison to photoredox catalyzed reactions. A clear example is the overwhelming prevalence of anodic oxidations of the substrates as main activation method. The field therefore appears worth investigating, offering a complementary alternative to photoredox catalyzed reactions. As a matter of fact, if the employment of a photocatalyst offers obvious benefits in the design of redox-neutral reactions, electrochemistry has the advantage to allow for multiple sequential oxidation/reduction events and poses fewer limitations to the oxidation potential window that has to be considered if introducing a photocatalyst in the reaction mixture.

In both cases, the use of stoichiometric oxidants/reductants or of energetic but not selective and harmful UV irradiation is not required, offering greener approaches to achieve higher selectivity. This provides advantages in the functionalization of substrates otherwise impossible to transform with traditional thermal chemistry (*viz.* unactivated alkanes) under mild conditions. This directly results in the expansion of the scope of traditionally employed multicomponent reactions and opens the way to further exploration of novel reactivities.

Finally, it can also be noticed that only a few examples of enantioselective multicomponent transformations are currently reported in the literature. As the change in hybridization with the formation of saturated tetrasubstituted carbons is a common feature of most of the reactions here discussed, further method implementation appears to be fundamental in the development of the field. Overall, this review will serve as a useful tool to analyze the established efficiency of photoredox and electrochemical multicomponent processes and will offer a glimpse of the underinvestigated areas, forecasting further development in the upcoming years.

7. Author Contributions

GAC and SP wrote the manuscript. EVDE, S-LY, and UKS revised the manuscript. All authors contributed to the article and approved the submitted version.

8. Conflicts of interest

The authors declare that there is no conflict of interest.

9. Acknowledgements

SP is thankful to the FWO for obtaining a PhD scholarship (grant No. 11H0121N). This paper has been supported by the RUDN University Strategic Academic Leadership Program.

10. References

- 1 P. T. Anastas and M. M. Kirchhoff, *Accounts of Chemical Research*, 2002, **35**, 686-694.
- 2 P. T. Anastas and J. C. Warner, *Oxford University Press*.
- 3 <https://www.acs.org/content/acs/en/greenchemistry/principles/12-principles-of-green-chemistry.html>.
- 4 R. C. Cioc, E. Ruijter and R. V. A. Orru, *Green Chem.*, 2014, **16**, 2958-2975.
- 5 E. Ruijter, R. Scheffelaar and R. V. A. Orru, *Angewandte Chemie International Edition*, 2011, **50**, 6234-6246.
- 6 U. K. Sharma, N. Sharma, D. D. Vachhani and E. v. van der Eycken, *Chemical Society Reviews*, 2015, **44**, 1836-1860.
- 7 E. Ruijter and R. V. A. Orru, *Drug Discovery Today: Technologies*, 2013, **10**, e15-e20.
- 8 P. Slobbe, E. Ruijter and R. V. A. Orru, *MedChemComm*, 2012, **3**, 1189.
- 9 B. B. Touré and D. G. Hall, *Chemical Reviews*, 2009, **109**, 4439-4486.
- 10 A. Dömling, W. Wang and K. Wang, *Chemical Reviews*, 2012, **112**, 3083-3135.
- 11 J. C. Flores-Reyes, A. Islas-Jácome and E. González-Zamora, *Organic Chemistry Frontiers*, 2021, **8**, 5460-5515.
- 12 T. Zarganes-Tzitzikas, A. L. Chandgude and A. Dömling, *The Chemical Record*, 2015, **15**, 981-996.
- 13 U. K. Sharma, P. Ranjan, E. v. van der Eycken and S.-L. You, *Chemical Society Reviews*, 2020, **49**, 8721-8748.
- 14 X. Ma, S. Zhi and W. Zhang, *Molecules*, 2021, **26**, 1986.
- 15 V. A. Peshkov, O. P. Pereshivko and E. v. van der Eycken, *Chemical Society Reviews*, 2012, **41**, 3790.
- 16 I. Ugi, A. Dömling and W. Hörl, *Endeavour*, 1994, **18**, 115-122.
- 17 N. A. Romero and D. A. Nicewicz, *Chemical Reviews*, 2016, **116**, 10075-10166.
- 18 J. D. Bell and J. A. Murphy, *Chemical Society Reviews*, 2021, **50**, 9540-9685.
- 19 D. Leifert and A. Studer, *Angewandte Chemie International Edition*, 2020, **59**, 74-108.
- 20 L. Capaldo and D. Ravelli, *European Journal of Organic Chemistry*, 2017, **2017**, 2056-2071.
- 21 S. Garbarino, D. Ravelli, S. Protti and A. Basso, *Angewandte Chemie International Edition*, 2016, **55**, 15476-15484.
- 22 F. Lovering, J. Bikker and C. Humblet, *Journal of Medicinal Chemistry*, 2009, **52**, 6752-6756.
- 23 H. Yao, W. Hu and W. Zhang, *Molecules*, 2020, **26**, 105.
- 24 X.-W. Lan, N.-X. Wang and Y. Xing, *European Journal of Organic Chemistry*, 2017, **2017**, 5821-5851.
- 25 M.-Y. Cao, X. Ren and Z. Lu, *Tetrahedron Letters*, 2015, **56**, 3732-3742.
- 26 S. Purser, P. R. Moore, S. Swallow and V. Gouverneur, *Chem. Soc. Rev.*, 2008, **37**, 320-330.
- 27 D. A. Nagib, M. E. Scott and D. W. C. MacMillan, *Journal of the American Chemical Society*, 2009, **131**, 10875-10877.
- 28 D. A. Nagib and D. W. C. MacMillan, *Nature*, 2011, **480**, 224-228.
- 29 Y. Yasu, T. Koike and M. Akita, *Angewandte Chemie International Edition*, 2012, **51**, 9567-9571.
- 30 G. Levitre, G. Dagousset, E. Anselmi, B. Tuccio, E. Magnier and G. Masson, *Organic Letters*, 2019, **21**, 6005-6010.

- 31 L. Zhang, G. Zhang, P. Wang, Y. Li and A. Lei, *Organic Letters*, 2018, **20**, 7396-7399.
- 32 W. Jud, C. O. Kappe and D. Cantillo, *Chemistry - A European Journal*, 2018, **24**, 17234-17238.
- 33 Y. Huang, H. Hong, Z. Zou, C. Liao, J. Lu, Y. Qin, Y. Li and L. Chen, *Organic & Biomolecular Chemistry*, 2019, **17**, 5014-5020.
- 34 R. Tomita, Y. Yasu, T. Koike and M. Akita, *Angewandte Chemie International Edition*, 2014, **53**, 7144-7148.
- 35 L. Li, Q.-Y. Chen and Y. Guo, *Journal of Fluorine Chemistry*, 2014, **167**, 79-83.
- 36 Z.-H. Xia, Z.-H. Gao, L. Dai and S. Ye, *The Journal of Organic Chemistry*, 2019, **84**, 7388-7394.
- 37 L. Li, Y. Ma, M. Tang, J. Guo, Z. Yang, Y. Yan, X. Ma and L. Tang, *Advanced Synthesis & Catalysis*, 2019, **361**, 3723-3728.
- 38 X. Luo, Z. Fan, B. Zhang, C. Chen and C. Xi, *Chemical Communications*, 2019, **55**, 10980-10983.
- 39 Y. Arai, R. Tomita, G. Ando, T. Koike and M. Akita, *Chemistry - A European Journal*, 2016, **22**, 1262-1265.
- 40 Y. Ran, Q.-Y. Lin, X.-H. Xu and F.-L. Qing, *The Journal of Organic Chemistry*, 2016, **81**, 7001-7007.
- 41 P. Xiong, H.-H. Xu, J. Song and H.-C. Xu, *Journal of the American Chemical Society*, 2018, **140**, 2460-2464.
- 42 H. Xu, J. Song and H. Xu, *ChemSusChem*, 2019, **12**, 3060-3063.
- 43 M. Daniel, G. Dagousset, P. Diter, P.-A. Klein, B. Tuccio, A.-M. Goncalves, G. Masson and E. Magnier, *Angewandte Chemie International Edition*, 2017, **56**, 3997-4001.
- 44 X. Sun, H.-X. Ma, T.-S. Mei, P. Fang and Y. Hu, *Organic Letters*, 2019, **21**, 3167-3171.
- 45 X. Zhou, G. Li, Z. Shao, K. Fang, H. Gao, Y. Li and Y. She, *Organic & Biomolecular Chemistry*, 2019, **17**, 24-29.
- 46 Y. Yasu, T. Koike and M. Akita, *Organic Letters*, 2013, **15**, 2136-2139.
- 47 J. J. Ritter and P. P. Minieri, *Journal of the American Chemical Society*, 1948, **70**, 4045-4048.
- 48 N. Noto, T. Koike and M. Akita, *Chemical Science*, 2017, **8**, 6375-6379.
- 49 G. Dagousset, A. Carboni, E. Magnier and G. Masson, *Organic Letters*, 2014, **16**, 4340-4343.
- 50 Q. Yang, C. Li, Z.-C. Qi, X.-Y. Qiang and S.-D. Yang, *Chemistry - A European Journal*, 2018, **24**, 14363-14367.
- 51 L. Jarrige, A. Carboni, G. Dagousset, G. Levitre, E. Magnier and G. Masson, *Organic Letters*, 2016, **18**, 2906-2909.
- 52 Z.-B. Yin, J.-H. Ye, W.-J. Zhou, Y.-H. Zhang, L. Ding, Y.-Y. Gui, S.-S. Yan, J. Li and D.-G. Yu, *Organic Letters*, 2018, **20**, 190-193.
- 53 Q. Liu, L. Wu, R. Jackstell and M. Beller, *Nature Communications*, 2015, **6**, 5933.
- 54 A. Claraz, A. Djian and G. Masson, *Organic Chemistry Frontiers*, 2021, **8**, 288-296.
- 55 A. Carboni, G. Dagousset, E. Magnier and G. Masson, *Chem. Commun.*, 2014, **50**, 14197-14200.
- 56 Y. Duan, W. Li, P. Xu, M. Zhang, Y. Cheng and C. Zhu, *Organic Chemistry Frontiers*, 2016, **3**, 1443-1446.
- 57 Y.-Y. Liu, X.-Y. Yu, J.-R. Chen, M.-M. Qiao, X. Qi, D.-Q. Shi and W.-J. Xiao, *Angewandte Chemie International Edition*, 2017, **56**, 9527-9531.
- 58 F. Zhou, Y. Cheng, X.-P. Liu, J.-R. Chen and W.-J. Xiao, *Chemical Communications*, 2019, **55**, 3117-3120.
- 59 G. Fumagalli, S. Boyd and M. F. Greaney, *Organic Letters*, 2013, **15**, 4398-4401.
- 60 S. S. Babu, P. Muthuraja, P. Yadav and P. Gopinath, *Advanced Synthesis & Catalysis*, 2021, **363**, 1782-1809.
- 61 D. P. Hari and B. König, *Angewandte Chemie International Edition*, 2013, **52**, 4734-4743.
- 62 D. Prasad Hari, T. Hering and B. König, *Angewandte Chemie International Edition*, 2014, **53**, 725-728.
- 63 A. Tlahuext-Aca, R. A. Garza-Sanchez, M. Schäfer and F. Glorius, *Organic*

- Letters, 2018, **20**, 1546-1549.
- 64 Z.-H. Xia, C.-L. Zhang, Z.-H. Gao and S. Ye, *Organic Letters*, 2018, **20**, 3496-3499.
- 65 X.-H. Ouyang, Y. Li, R.-J. Song and J.-H. Li, *Organic Letters*, 2018, **20**, 6659-6662.
- 66 X.-X. Fang, P.-F. Wang, W. Yi, W. Chen, S.-C. Lou and G.-Q. Liu, *The Journal of Organic Chemistry*, 2019, **84**, 15677-15684.
- 67 M. Lux and M. Klussmann, *Organic Letters*, 2020, **22**, 3697-3701.
- 68 W. Zhang and S. Lin, *Journal of the American Chemical Society*, 2020, **142**, 20661-20670.
- 69 G. Fumagalli, P. T. G. Rabet, S. Boyd and M. F. Greaney, *Angewandte Chemie International Edition*, 2015, **54**, 11481-11484.
- 70 F. Cong, Y. Wei and P. Tang, *Chemical Communications*, 2018, **54**, 4473-4476.
- 71 K. Miyazawa, T. Koike and M. Akita, *Chemistry - A European Journal*, 2015, **21**, 11677-11680.
- 72 K. Miyazawa, T. Koike and M. Akita, *Tetrahedron*, 2016, **72**, 7813-7820.
- 73 J.-Q. Chen, W.-L. Yu, Y.-L. Wei, T.-H. Li and P.-F. Xu, *The Journal of Organic Chemistry*, 2017, **82**, 243-249.
- 74 J.-N. Mo, W.-L. Yu, J.-Q. Chen, X.-Q. Hu and P.-F. Xu, *Organic Letters*, 2018, **20**, 4471-4474.
- 75 Q. Qin, Y.-Y. Han, Y.-Y. Jiao, Y. He and S. Yu, *Organic Letters*, 2017, **19**, 2909-2912.
- 76 S. Govaerts, L. Angelini, C. Hampton, L. Malet-Sanz, A. Ruffoni and D. Leonori, *Angewandte Chemie International Edition*, 2020, **59**, 15021-15028.
- 77 Y. Yuan, Y. Chen, S. Tang, Z. Huang and A. Lei, *Science Advances*, , DOI:10.1126/sciadv.aat5312.
- 78 Y. Wang, L. Deng, H. Mei, B. Du, J. Han and Y. Pan, *Green Chemistry*, 2018, **20**, 3444-3449.
- 79 C. Liu, Y.-J. Yang, J.-Y. Dong, M.-D. Zhou, L. Li and H. Wang, *Organic Chemistry Frontiers*, 2019, **6**, 3944-3949.
- 80 Z.-P. Ye, J. Gao, X.-Y. Duan, J.-P. Guan, F. Liu, K. Chen, J.-A. Xiao, H.-Y. Xiang and H. Yang, *Chemical Communications*, 2021, **57**, 8969-8972.
- 81 M. Luo, B. Liu, Y. Li, M. Hu and J. Li, *Advanced Synthesis & Catalysis*, 2019, **361**, 1538-1542.
- 82 A. Barthelemy, B. Tuccio, E. Magnier and G. Dagousset, *Angewandte Chemie International Edition*, 2018, **57**, 13790-13794.
- 83 L. Sun, Y. Yuan, M. Yao, H. Wang, D. Wang, M. Gao, Y.-H. Chen and A. Lei, *Organic Letters*, 2019, **21**, 1297-1300.
- 84 L. Sun, L. Wang, H. Alhumade, H. Yi, H. Cai and A. Lei, *Organic Letters*, 2021, **23**, 7724-7729.
- 85 V. R. Yatham, Y. Shen and R. Martin, *Angewandte Chemie International Edition*, 2017, **56**, 10915-10919.
- 86 H.-T. Qin, S.-W. Wu, J.-L. Liu and F. Liu, *Chemical Communications*, 2017, **53**, 1696-1699.
- 87 Q. Fu, Z.-Y. Bo, J.-H. Ye, T. Ju, H. Huang, L.-L. Liao and D.-G. Yu, *Nature Communications*, 2019, **10**, 3592.
- 88 J. Hou, A. Ee, H. Cao, H. Ong, J. Xu and J. Wu, *Angewandte Chemie International Edition*, 2018, **57**, 17220-17224.
- 89 H. Wang, Y. Gao, C. Zhou and G. Li, *Journal of the American Chemical Society*, 2020, **142**, 8122-8129.
- 90 F.-D. Lu, G.-F. He, L.-Q. Lu and W.-J. Xiao, *Green Chemistry*, 2021, **23**, 5379-5393.
- 91 X. Yu, Q. Zhao, J. Chen, J. Chen and W. Xiao, *Angewandte Chemie International Edition*, 2018, **57**, 15505-15509.
- 92 J. Chen, B.-Q. He, P.-Z. Wang, X.-Y. Yu, Q.-Q. Zhao, J.-R. Chen and W.-J. Xiao, *Organic Letters*, 2019, **21**, 4359-4364.
- 93 D. Wu, S.-S. Cui, Y. Lin, L. Li and W. Yu, *The Journal of Organic Chemistry*, 2019, **84**, 10978-10989.
- 94 W. Sha, L. Deng, S. Ni, H. Mei, J. Han and Y. Pan, *ACS Catalysis*, 2018, **8**, 7489-7494.
- 95 B. Yang and Z. Lu, *ACS Catalysis*, 2017, **7**, 8362-8365.
- 96 B. Yang, X. Ren, X. Shen, T. Li and Z. Lu, *Chinese Journal of Chemistry*,

- 2018, **36**, 1017-1023.
- 97 Y. Yang, C.-H. Xu, Z.-Q. Xiong and J.-H. Li, *Chemical Communications*, 2020, **56**, 9549-9552.
- 98 J. Wu, Y. Zhang, X. Gong, Y. Meng and C. Zhu, *Organic & Biomolecular Chemistry*, 2019, **17**, 3507-3513.
- 99 S. Roy Chowdhury, D. Singh, I. U. Hoque and S. Maity, *The Journal of Organic Chemistry*, 2020, **85**, 13939-13950.
- 100 C. Dai, Y. Shen, Y. Wei, P. Liu and P. Sun, *The Journal of Organic Chemistry*, 2021, **86**, 13711-13719.
- 101 J.-H. Ye, M. Miao, H. Huang, S.-S. Yan, Z.-B. Yin, W.-J. Zhou and D.-G. Yu, *Angewandte Chemie International Edition*, 2017, **56**, 15416-15420.
- 102 B. Lipp, L. M. Kammer, M. Küçükdisli, A. Luque, J. Kühlbörn, S. Pusch, G. Matulevičiūtė, D. Schollmeyer, A. Šačkus and T. Opatz, *Chemistry - A European Journal*, 2019, **25**, 8965-8969.
- 103 S. Zhu, J. Qin, F. Wang, H. Li and L. Chu, *Nature Communications*, 2019, **10**, 749.
- 104 K.-Y. Ye, G. Pombar, N. Fu, G. S. Sauer, I. Keresztes and S. Lin, *Journal of the American Chemical Society*, 2018, **140**, 2438-2441.
- 105 N. Fu, Y. Shen, A. R. Allen, L. Song, A. Ozaki and S. Lin, *ACS Catalysis*, 2019, **9**, 746-754.
- 106 S. Tian, X. Jia, L. Wang, B. Li, S. Liu, L. Ma, W. Gao, Y. Wei and J. Chen, *Chemical Communications*, 2019, **55**, 12104-12107.
- 107 P. Xiong, H. Long, J. Song, Y. Wang, J.-F. Li and H.-C. Xu, *Journal of the American Chemical Society*, 2018, **140**, 16387-16391.
- 108 P. Xiong, H. Long and H. Xu, *Asian Journal of Organic Chemistry*, 2019, **8**, 658-660.
- 109 T.-T. Zhang, M.-J. Luo, Y. Li, R.-J. Song and J.-H. Li, *Organic Letters*, 2020, **22**, 7250-7254.
- 110 C. Wan, R.-J. Song and J.-H. Li, *Organic Letters*, 2019, **21**, 2800-2803.
- 111 T.-K. Xiong, X.-Q. Zhou, M. Zhang, H.-T. Tang, Y.-M. Pan and Y. Liang, *Green Chemistry*, 2021, **23**, 4328-4332.
- 112 F. Yuan, D. Yan, P. Gao, D. Shi, W. Xiao and J. Chen, *ChemCatChem*, 2021, **13**, 543-547.
- 113 X. Zhang, T. Cui, X. Zhao, P. Liu and P. Sun, *Angewandte Chemie International Edition*, 2020, **59**, 3465-3469.
- 114 T. Courant and G. Masson, *Chemistry - A European Journal*, 2012, **18**, 423-427.
- 115 F. Pettersson, G. Bergonzini, C. Cassani and C.-J. Wallentin, *Chemistry - A European Journal*, 2017, **23**, 7444-7447.
- 116 A. Carboni, G. Dagousset, E. Magnier and G. Masson, *Organic Letters*, 2014, **16**, 1240-1243.
- 117 X.-L. Yu, J.-R. Chen, D.-Z. Chen and W.-J. Xiao, *Chemical Communications*, 2016, **52**, 8275-8278.
- 118 J. Fang, Z.-K. Wang, S.-W. Wu, W.-G. Shen, G.-Z. Ao and F. Liu, *Chemical Communications*, 2017, **53**, 7638-7641.
- 119 W. Jin, M. Wu, Z. Xiong and G. Zhu, *Chemical Communications*, 2018, **54**, 7924-7927.
- 120 J. Ma, X. Xie and E. Meggers, *Chemistry - A European Journal*, 2018, **24**, 259-265.
- 121 L. Li, H. Luo, Z. Zhao, Y. Li, Q. Zhou, J. Xu, J. Li and Y.-N. Ma, *Organic Letters*, 2019, **21**, 9228-9231.
- 122 J. Sim, M. W. Campbell and G. A. Molander, *ACS Catalysis*, 2019, **9**, 1558-1563.
- 123 P. Wang, S. Zhu, D. Lu and Y. Gong, *Organic Letters*, 2020, **22**, 1924-1928.
- 124 Y. Guo, K. Wang, R. Wang, H. Song, Y. Liu and Q. Wang, *Advanced Synthesis & Catalysis*, 2021, **363**, 1651-1655.
- 125 J.-H. Choi and C.-M. Park, *Advanced Synthesis & Catalysis*, 2018, **360**, 3553-3562.
- 126 I. U. Hoque, S. R. Chowdhury and S. Maity, *The Journal of Organic Chemistry*, 2019, **84**, 3025-3035.
- 127 Y. Shen, M.-L. Shen and P.-S. Wang, *ACS Catalysis*, 2020, **10**, 8247-8253.
- 128 S. Sun, Y. Duan, R. S. Mega, R. J. Somerville and R. Martin, *Angewandte Chemie International Edition*, 2020, **59**, 4370-4374.

- 129 L. Guo, M. Yuan, Y. Zhang, F. Wang, S. Zhu, O. Gutierrez and L. Chu, *Journal of the American Chemical Society*, 2020, **142**, 20390-20399.
- 130 D. Zheng and A. Studer, *Angewandte Chemie International Edition*, 2019, **58**, 15803-15807.
- 131 T. Li, K. Liang, Y. Zhang, D. Hu, Z. Ma and C. Xia, *Organic Letters*, 2020, **22**, 2386-2390.
- 132 J. Q. Buquoi, J. M. Lear, X. Gu and D. A. Nagib, *ACS Catalysis*, 2019, **9**, 5330-5335.
- 133 J. Shen, J. Xu, L. He, Y. Ouyang, L. Huang, W. Li, Q. Zhu and P. Zhang, *Organic Letters*, 2021, **23**, 1204-1208.
- 134 S. Xu, H. Chen, Z. Zhou and W. Kong, *Angewandte Chemie International Edition*, 2021, **60**, 7405-7411.
- 135 L. Huang, C. Zhu, L. Yi, H. Yue, R. Kancherla and M. Rueping, *Angewandte Chemie International Edition*, 2020, **59**, 457-464.
- 136 P. Bellotti, M. Koy, C. Gutheil, S. Heuvel and F. Glorius, *Chemical Science*, 2021, **12**, 1810-1817.
- 137 D. Forster, W. Guo, Q. Wang and J. Zhu, *ACS Catalysis*, 2021, **11**, 10871-10877.
- 138 J. Ke, W. Liu, X. Zhu, X. Tan and C. He, *Angewandte Chemie International Edition*, 2021, **60**, 8744-8749.
- 139 R. Chinchilla and C. Nájera, *Chemical Reviews*, 2007, **107**, 874-922.
- 140 R. Chinchilla and C. Nájera, *Chemical Society Reviews*, 2011, **40**, 5084.
- 141 H. C. Kolb, M. G. Finn and K. B. Sharpless, *Angewandte Chemie International Edition*, 2001, **40**, 2004-2021.
- 142 M.-H. Huang, W.-J. Hao, G. Li, S.-J. Tu and B. Jiang, *Chemical Communications*, 2018, **54**, 10791-10811.
- 143 X. Ren and Z. Lu, *Chinese Journal of Catalysis*, 2019, **40**, 1003-1019.
- 144 F. Mohjer, P. Mofatehnia, Y. Rangraz and M. M. Heravi, *Journal of Organometallic Chemistry*, 2021, **936**, 121712.
- 145 A. Sagadevan, A. Ragupathi, C.-C. Lin, J. R. Hwu and K. C. Hwang, *Green Chemistry*, 2015, **17**, 1113-1119.
- 146 D. K. Das, V. K. Kumar Pampana and K. C. Hwang, *Chemical Science*, 2018, **9**, 7318-7326.
- 147 C. Wang, D. Ma, Y. Tu and C. Bolm, *Organic Letters*, 2020, **22**, 8937-8940.
- 148 A. Ragupathi, A. Sagadevan, C.-C. Lin, J.-R. Hwu and K. C. Hwang, *Chemical Communications*, 2016, **52**, 11756-11759.
- 149 A. Sagadevan, V. P. Charpe, A. Ragupathi and K. C. Hwang, *Journal of the American Chemical Society*, 2017, **139**, 2896-2899.
- 150 A. Ragupathi, A. Sagadevan, V. P. Charpe, C.-C. Lin, J.-R. Hwu and K. C. Hwang, *Chemical Communications*, 2019, **55**, 5151-5154.
- 151 S. Sultan, M. A. Rizvi, J. Kumar and B. A. Shah, *Chemistry - A European Journal*, 2018, **24**, 10617-10620.
- 152 N. Katta, M. Ojha, A. Murugan, S. Arepally and D. S. Sharada, *RSC Advances*, 2020, **10**, 12599-12603.
- 153 N. Chalotra, A. Ahmed, M. A. Rizvi, Z. Hussain, Q. N. Ahmed and B. A. Shah, *The Journal of Organic Chemistry*, 2018, **83**, 14443-14456.
- 154 N. Chalotra, M. A. Rizvi and B. A. Shah, *Organic Letters*, 2019, **21**, 4793-4797.
- 155 V. K. K. Pampana, A. Sagadevan, A. Ragupathi and K. C. Hwang, *Green Chemistry*, 2020, **22**, 1164-1170.
- 156 Y. R. Malpani, B. K. Biswas, H. S. Han, Y.-S. Jung and S. B. Han, *Organic Letters*, 2018, **20**, 1693-1697.
- 157 W. Lee, Y. Lee, M. Yoo, S. B. Han and H. J. Kim, *Organic Chemistry Frontiers*, 2020, **7**, 3209-3214.
- 158 Y. Xiang, Y. Li, Y. Kuang and J. Wu, *Chemistry - A European Journal*, 2017, **23**, 1032-1035.
- 159 T. Shang, J. Zhang, Y. Zhang, F. Zhang, X.-S. Li and G. Zhu, *Organic Letters*, 2020, **22**, 3667-3672.
- 160 S. Pelliccia, A. I. Alfano, P. Luciano, E. Novellino, A. Massarotti, G. C. Tron, D. Ravelli and M. Giustiniano, *The Journal of Organic Chemistry*, 2020, **85**, 1981-1990.
- 161 L. Guo, F. Song, S. Zhu, H. Li and L. Chu, *Nature Communications*, 2018, **9**, 4543.

- 162 C. C. Nawrat, C. R. Jamison, Y. Slutskyy, D. W. C. MacMillan and L. E. Overman, *Journal of the American Chemical Society*, 2015, **137**, 11270-11273.
- 163 H. Yue, C. Zhu, R. Kancherla, F. Liu and M. Rueping, *Angewandte Chemie*, 2020, **132**, 5787-5795.
- 164 C. Zhu, H. Yue, B. Maity, I. Atodiresei, L. Cavallo and M. Rueping, *Nature Catalysis*, 2019, **2**, 678-687.
- 165 A. K. Sahoo, A. Dahiya, B. Das, A. Behera and B. K. Patel, *The Journal of Organic Chemistry*, 2021, **86**, 11968-11986.
- 166 X. Kong, K. Yu, Q. Chen and B. Xu, *Asian Journal of Organic Chemistry*, 2020, **9**, 1760-1764.
- 167 X. Zhang, D. Lu and Z. Wang, *European Journal of Organic Chemistry*, 2021, **2021**, 4284-4287.
- 168 W.-B. Du, N.-N. Wang, C. Pan, S.-F. Ni, L.-R. Wen, M. Li and L.-B. Zhang, *Green Chemistry*, 2021, **23**, 2420-2426.
- 169 J. Zhou, W. Li, H. Zheng, Y. Pei, X. Liu and H. Cao, *Organic Letters*, 2021, **23**, 2754-2759.
- 170 Z. Yang, F. Lu, H. Li, Y. Zhang, W. Lin, P. Guo, J. Wan, R. Shi, T. Wang and A. Lei, *Organic Chemistry Frontiers*, 2020, **7**, 4064-4068.
- 171 D. Wang, Z. Wan, H. Zhang and A. Lei, *Advanced Synthesis & Catalysis*, 2021, **363**, 1022-1027.
- 172 K.-Y. Ye, Z. Song, G. S. Sauer, J. H. Harenberg, N. Fu and S. Lin, *Chemistry - A European Journal*, 2018, **24**, 12274-12279.
- 173 H.-D. Zuo, W.-J. Hao, C.-F. Zhu, C. Guo, S.-J. Tu and B. Jiang, *Organic Letters*, 2020, **22**, 4471-4477.
- 174 T.-S. Zhang, W.-J. Hao, R. Wang, S.-C. Wang, S.-J. Tu and B. Jiang, *Green Chemistry*, 2020, **22**, 4259-4269.
- 175 M. N. Elinson, S. K. Feducovich, A. N. Vereshchagin, S. v. Gorbunov, P. A. Belyakov and G. I. Nikishin, *Tetrahedron Letters*, 2006, **47**, 9129-9133.
- 176 M. N. Elinson, A. I. Ilovaisky, V. M. Merkulova, T. A. Zaimovskaya and G. I. Nikishin, *Mendeleev Communications*, 2011, **21**, 122-124.
- 177 M. N. Elinson, R. F. Nasybullin and G. I. Nikishin, *Journal of The Electrochemical Society*, 2013, **160**, G3053-G3057.
- 178 R. Kazemi-Rad, J. Azizian and H. Kefayati, *Journal of the Serbian Chemical Society*, 2016, **81**, 29-34.
- 179 M. N. Elinson, A. N. Vereshchagin and F. v. Ryzhkov, *The Chemical Record*, 2016, **16**, 1950-1964.
- 180 H. Kefayati, S. H. Amlashi, R. Kazemi-Rad and A. Delafrooz, *Comptes Rendus Chimie*, 2014, **17**, 894-898.
- 181 S. Makarem, A. A. Mohammadi and A. R. Fakhari, *Tetrahedron Letters*, 2008, **49**, 7194-7196.
- 182 S. Makarem, A. R. Fakhari and A. A. Mohammadi, *Industrial & Engineering Chemistry Research*, 2012, **51**, 2200-2204.
- 183 V. K. Singh, R. Dubey, A. Upadhyay, L. K. Sharma and R. K. P. Singh, *Tetrahedron Letters*, 2017, **58**, 4227-4231.
- 184 A. Upadhyay, L. K. Sharma, V. K. Singh, R. Dubey, N. Kumar and R. K. P. Singh, *Tetrahedron Letters*, 2017, **58**, 1245-1249.
- 185 Z. Vafajoo, N. Hazeri, M. T. Maghsoodlou and H. Veisi, *Chinese Chemical Letters*, 2015, **26**, 973-976.
- 186 L. Wang, J. Gao, L. Wan, Y. Wang and C. Yao, *Research on Chemical Intermediates*, 2015, **41**, 2775-2784.
- 187 R. Dubey, V. K. Singh, L. K. Sharma, A. Upadhyay, N. Kumar and R. K. P. Singh, *New Journal of Chemistry*, 2017, **41**, 7836-7839.
- 188 R. Sayyar, S. Makarem and B. Mirza, *Journal of Heterocyclic Chemistry*, 2019, **56**, 1839-1843.
- 189 H. Veisi, A. Maleki and S. Jahangard, *Tetrahedron Letters*, 2015, **56**, 1882-1886.
- 190 M.-N. Chen, J.-Q. Di, J.-M. Li, L.-P. Mo and Z.-H. Zhang, *Tetrahedron*, 2020, **76**, 131059.
- 191 N. Yang and G. Yuan, *The Journal of Organic Chemistry*, 2018, **83**, 11963-11969.
- 192 Z. Zhao, Y. He, M. Li, J. Xu, X. Li, L. Zhang and L. Gu, *Tetrahedron*, 2021, **87**, 132111.
- 193 L. Zeng, J. Li, J. Gao, X. Huang, W. Wang, X. Zheng, L. Gu, G. Li, S.

- Zhang and Y. He, *Green Chemistry*, 2020, **22**, 3416–3420.
- 194 C. Mannich and W. Krösche, *Archiv der Pharmazie*, 1912, **250**, 647–667.
- 195 A. Strecker, *Annalen der Chemie und Pharmacie*, 1850, **75**, 27–45.
- 196 L. Zhang, Y. Deng and F. Shi, *Tetrahedron Letters*, 2013, **54**, 5217–5219.
- 197 G. Lahm and T. Opatz, *The Journal of Organic Chemistry*, 2015, **80**, 12711–12717.
- 198 M. Rueping and C. Vila, *Organic Letters*, 2013, **15**, 2092–2095.
- 199 N. Pan, J. Ling, R. Zapata, J.-P. Pulicani, L. Grimaud and M. R. Vitale, *Green Chemistry*, 2019, **21**, 6194–6199.
- 200 J. Yi, S. O. Badir, R. Alam and G. A. Molander, *Organic Letters*, 2019, **21**, 4853–4858.
- 201 M. Chilamari, J. R. Immel and S. Bloom, *ACS Catalysis*, 2020, **10**, 12727–12737.
- 202 P. Ranjan, S. Pillitteri, G. Coppola, M. Oliva, E. v. van der Eycken and U. K. Sharma, *ACS Catalysis*, 2021, **11**, 10862–10870.
- 203 M. Oliva, P. Ranjan, S. Pillitteri, G. A. Coppola, M. Messina, E. v. van der Eycken and U. K. Sharma, *iScience*, 2021, **24**, 103134.
- 204 R. Kumar, N. J. Flodén, W. G. Whitehurst and M. J. Gaunt, *Nature*, 2020, **581**, 415–420.
- 205 J. H. Blackwell, R. Kumar and M. J. Gaunt, *Journal of the American Chemical Society*, 2021, **143**, 1598–1609.
- 206 K. Kolahdouzan, R. Kumar and M. J. Gaunt, *Chemical Science*, 2020, **11**, 12089–12094.
- 207 J. Yi, S. O. Badir, R. Alam and G. A. Molander, *Organic Letters*, 2019, **21**, 4853–4858.
- 208 X. Wang, B. Zhu, J. Dong, H. Tian, Y. Liu, H. Song and Q. Wang, *Chemical Communications*, 2021, **57**, 5028–5031.
- 209 X.-K. Qi, L. Guo, L.-J. Yao, H. Gao, C. Yang and W. Xia, *Organic Letters*, 2021, **23**, 4473–4477.
- 210 S. Pillitteri, P. Ranjan, L. G. Voskressensky, E. v. van der Eycken and U. K. Sharma, *Molecular Catalysis*, 2021, **514**, 111841.
- 211 A. L. Fuentes de Arriba, F. Urbitsch and D. J. Dixon, *Chemical Communications*, 2016, **52**, 14434–14437.
- 212 L. Qi and Y. Chen, *Angewandte Chemie International Edition*, 2016, **55**, 13312–13315.
- 213 T. Rossolini, J. A. Leitch, R. Grainger and D. J. Dixon, *Organic Letters*, 2018, **20**, 6794–6798.
- 214 A. Trowbridge, D. Reich and M. J. Gaunt, *Nature*, 2018, **561**, 522–527.
- 215 L. M. Kammer, M. Krumb, B. Spitzbarth, B. Lipp, J. Kühlbörn, J. Busold, O. M. Mulina, A. O. Terentev and T. Opatz, *Organic Letters*, 2020, **22**, 3318–3322.
- 216 H.-H. Zhang and S. Yu, *Organic Letters*, 2019, **21**, 3711–3715.
- 217 J.-X. Li, L. Li, M.-D. Zhou and H. Wang, *Organic Chemistry Frontiers*, 2018, **5**, 1003–1007.
- 218 S. Wang, B.-Y. Cheng, M. Sršen and B. König, *Journal of the American Chemical Society*, 2020, **142**, 7524–7531.
- 219 J.-B. Peng, H.-Q. Geng and X.-F. Wu, *Chem*, 2019, **5**, 526–552.
- 220 S. Sumino, A. Fusano, T. Fukuyama and I. Ryu, *Accounts of Chemical Research*, 2014, **47**, 1563–1574.
- 221 W. Guo, L.-Q. Lu, Y. Wang, Y.-N. Wang, J.-R. Chen and W.-J. Xiao, *Angewandte Chemie International Edition*, 2015, **54**, 2265–2269.
- 222 M. Majek and A. Jacobi von Wangelin, *Angewandte Chemie International Edition*, 2015, **54**, 2270–2274.
- 223 N. Micic and A. Polyzos, *Organic Letters*, 2018, **20**, 4663–4666.
- 224 L. Gu, C. Jin and J. Liu, *Green Chemistry*, 2015, **17**, 3733–3736.
- 225 H.-T. Zhang, L.-J. Gu, X.-Z. Huang, R. Wang, C. Jin and G.-P. Li, *Chinese Chemical Letters*, 2016, **27**, 256–260.
- 226 C. Gosset, S. Pellegrini, R. Jooris, T. Bousquet and L. Pelinski, *Advanced Synthesis & Catalysis*, 2018, **360**, 3401–3405.
- 227 Q.-Q. Zhou, W. Guo, W. Ding, X. Wu, X. Chen, L.-Q. Lu and W.-J. Xiao, *Angewandte Chemie International Edition*, 2015, **54**, 11196–11199.
- 228 X. Li, D. Liang, W. Huang, H. Zhou, Z. Li, B. Wang, Y. Ma and H. Wang, *Tetrahedron*, 2016, **72**, 8442–8448.

- 229 X. Jiang, M. Zhang, W. Xiong, L. Lu and W. Xiao, *Angewandte Chemie International Edition*, 2019, **58**, 2402-2406.
- 230 A. Cartier, E. Levernier, V. Corcé, T. Fukuyama, A. Dhimane, C. Ollivier, I. Ryu and L. Fensterbank, *Angewandte Chemie International Edition*, 2019, **58**, 1789-1793.
- 231 A. Cartier, E. Levernier, A. Dhimane, T. Fukuyama, C. Ollivier, I. Ryu and L. Fensterbank, *Advanced Synthesis & Catalysis*, 2020, **362**, 2254-2259.
- 232 S. Y. Chow, M. Y. Stevens, L. Åkerbladh, S. Bergman and L. R. Odell, *Chemistry - A European Journal*, 2016, **22**, 9155-9161.
- 233 A. M. Veatch and E. J. Alexanian, *Chemical Science*, 2020, **11**, 7210-7213.
- 234 G. M. Torres, Y. Liu and B. A. Arndtsen, *Science*, 2020, **368**, 318-323.
- 235 B. Lu, Y. Cheng, L.-Y. Chen, J.-R. Chen and W.-J. Xiao, *ACS Catalysis*, 2019, **9**, 8159-8164.
- 236 Z. Qi, L. Li, Y.-K. Liang, A.-J. Ma, X.-Z. Zhang and J.-B. Peng, *Organic Letters*, 2021, **23**, 4769-4773.
- 237 L. Zeng, H. Li, S. Tang, X. Gao, Y. Deng, G. Zhang, C.-W. Pao, J.-L. Chen, J.-F. Lee and A. Lei, *ACS Catalysis*, 2018, **8**, 5448-5453.
- 238 Y. Wu, L. Zeng, H. Li, Y. Cao, J. Hu, M. Xu, R. Shi, H. Yi and A. Lei, *Journal of the American Chemical Society*, 2021, **143**, 12460-12466.
- 239 M. Feng, B. Tang, S. H. Liang and X. Jiang, *Current Topics in Medicinal Chemistry*, 2016, **16**, 1200-1216.
- 240 S. Y. Woo, J. H. Kim, M. K. Moon, S.-H. Han, S. K. Yeon, J. W. Choi, B. K. Jang, H. J. Song, Y. G. Kang, J. W. Kim, J. Lee, D. J. Kim, O. Hwang and K. D. Park, *Journal of Medicinal Chemistry*, 2014, **57**, 1473-1487.
- 241 P. Devendar and G.-F. Yang, *Topics in Current Chemistry*, 2017, **375**, 82.
- 242 H. J. M. Gijzen, M. A. J. de Cleyn, M. Surkyn, G. R. E. van Lommen, B. M. P. Verbist, M. J. M. A. Nijsen, T. Meert, J. van Wauwe and J. Aerssens, *Bioorganic & Medicinal Chemistry Letters*, 2012, **22**, 547-552.
- 243 X. Jia, S. Kramer, T. Skrydstrup and Z. Lian, *Angewandte Chemie International Edition*, 2021, **60**, 7353-7359.
- 244 G. Qiu, K. Zhou, L. Gao and J. Wu, *Organic Chemistry Frontiers*, 2018, **5**, 691-705.
- 245 G. Qiu, K. Zhou and J. Wu, *Chemical Communications*, 2018, **54**, 12561-12569.
- 246 D. Joseph, M. A. Idris, J. Chen and S. Lee, *ACS Catalysis*, 2021, **11**, 4169-4204.
- 247 S. P. Blum, K. Hofman, G. Manolikakes and S. R. Waldvogel, *Chemical Communications*, 2021, **57**, 8236-8249.
- 248 S. Ye, M. Yang and J. Wu, *Chemical Communications*, 2020, **56**, 4145-4155.
- 249 S. Ye, X. Li, W. Xie and J. Wu, *European Journal of Organic Chemistry*, 2020, **2020**, 1274-1287.
- 250 T. Liu, D. Zheng, Z. Li and J. Wu, *Advanced Synthesis & Catalysis*, 2018, **360**, 865-869.
- 251 J. Zhang, K. Zhou and J. Wu, *Organic Chemistry Frontiers*, 2018, **5**, 813-816.
- 252 J. Zhang, F. Zhang, L. Lai, J. Cheng, J. Sun and J. Wu, *Chemical Communications*, 2018, **54**, 3891-3894.
- 253 F.-S. He, X. Cen, S. Yang, J. Zhang, H. Xia and J. Wu, *Organic Chemistry Frontiers*, 2018, **5**, 2437-2441.
- 254 D. Zheng, J. Yu and J. Wu, *Angewandte Chemie International Edition*, 2016, **55**, 11925-11929.
- 255 F.-S. He, Y. Yao, W. Xie and J. Wu, *Chemical Communications*, 2020, **56**, 9469-9472.
- 256 N. Zhou, M. Wu, K. Kuang, S. Wu and M. Zhang, *Advanced Synthesis & Catalysis*, 2020, **362**, 5391-5397.
- 257 Y. Yao, Z. Yin, F.-S. He, X. Qin, W. Xie and J. Wu, *Chemical Communications*, 2021, **57**, 2883-2886.
- 258 B. Ni, B. Zhang, J. Han, B. Peng, Y. Shan and T. Niu, *Organic Letters*, 2020, **22**, 670-674.
- 259 Y. Lv, J. Luo, M. Lin, H. Yue, B. Dai and L. He, *Organic Chemistry Frontiers*, 2021, **8**, 5403-5409.
- 260 Y. Liu, Q.-L. Wang, Z. Chen, Q. Zhou, B.-Q. Xiong, P.-L. Zhang and K.-W. Tang, *Chemical Communications*, 2019, **55**, 12212-12215.
- 261 X. Gong, J. Chen, L. Lai, J. Cheng, J. Sun and J. Wu, *Chemical*

- Communications*, 2018, **54**, 11172-11175.
- 262 X. Gong, X. Li, W. Xie, J. Wu and S. Ye, *Organic Chemistry Frontiers*, 2019, **6**, 1863-1867.
- 263 A. M. Nair, S. Kumar, I. Halder and C. M. R. Volla, *Organic & Biomolecular Chemistry*, 2019, **17**, 5897-5901.
- 264 Y. Lv, J. Luo, Y. Ma, Q. Dong and L. He, *Organic Chemistry Frontiers*, 2021, **8**, 2461-2467.
- 265 D. Louvel, A. Chelagha, J. Rouillon, P. Payard, L. Khrouz, C. Monnereau and A. Tlili, *Chemistry - A European Journal*, 2021, **27**, 8704-8708.
- 266 T. Liu, Y. Li, L. Lai, J. Cheng, J. Sun and J. Wu, *Organic Letters*, 2018, **20**, 3605-3608.
- 267 T. Liu, Y. Ding, X. Fan and J. Wu, *Organic Chemistry Frontiers*, 2018, **5**, 3153-3157.
- 268 S. Ye, X. Li, W. Xie and J. Wu, *Asian Journal of Organic Chemistry*, 2019, **8**, 893-898.
- 269 X. Gong, M. Yang, J.-B. Liu, F.-S. He and J. Wu, *Organic Chemistry Frontiers*, 2020, **7**, 938-943.
- 270 M. Yang, H. Han, H. Jiang, S. Ye, X. Fan and J. Wu, *Chinese Chemical Letters*, 2021, **32**, 3535-3538.
- 271 X. Wang, H. Li, G. Qiu and J. Wu, *Chemical Communications*, 2019, **55**, 2062-2065.
- 272 X. Wang, M. Yang, W. Xie, X. Fan and J. Wu, *Chemical Communications*, 2019, **55**, 6010-6013.
- 273 X. Gong, M. Yang, J.-B. Liu, F.-S. He, X. Fan and J. Wu, *Green Chemistry*, 2020, **22**, 1906-1910.
- 274 X. Wang, R. Liu, Q. Ding, W. Xiao and J. Wu, *Organic Chemistry Frontiers*, 2021, **8**, 3308-3313.
- 275 N.-W. Liu, S. Liang and G. Manolikakes, *Advanced Synthesis & Catalysis*, 2017, **359**, 1308-1319.
- 276 X. Gong, J. Chen, J. Liu and J. Wu, *Organic Chemistry Frontiers*, 2017, **4**, 2221-2225.
- 277 C. Breton-Patient, D. Naud-Martin, F. Mahuteau-Betzer and S. Piguel, *European Journal of Organic Chemistry*, 2020, **2020**, 6653-6660.
- 278 N.-W. Liu, Z. Chen, A. Herbert, H. Ren and G. Manolikakes, *European Journal of Organic Chemistry*, 2018, **2018**, 5725-5734.
- 279 S. Ye, D. Zheng, J. Wu and G. Qiu, *Chemical Communications*, 2019, **55**, 2214-2217.
- 280 J. Zhang, X. Li, W. Xie, S. Ye and J. Wu, *Organic Letters*, 2019, **21**, 4950-4954.
- 281 Y. Liu, Q.-L. Wang, Z. Chen, H. Li, B.-Q. Xiong, P.-L. Zhang and K.-W. Tang, *Chemical Communications*, 2020, **56**, 3011-3014.
- 282 P. Bao, F. Yu, F.-S. He, Z. Tang, W.-P. Deng and J. Wu, *Organic Chemistry Frontiers*, 2021, **8**, 4820-4825.
- 283 P. Chen, Z. Chen, B.-Q. Xiong, Y. Liang, K.-W. Tang, J. Xie and Y. Liu, *Organic & Biomolecular Chemistry*, 2021, **19**, 3181-3190.
- 284 S. Cao, W. Hong, Z. Ye and L. Gong, *Nature Communications*, 2021, **12**, 2377.
- 285 V. T. Nguyen, G. C. Haug, V. D. Nguyen, N. T. H. Vuong, H. D. Arman and O. v. Larionov, *Chemical Science*, 2021, **12**, 6429-6436.
- 286 R. Mao, Z. Yuan, Y. Li and J. Wu, *Chemistry - A European Journal*, 2017, **23**, 8176-8179.
- 287 J.-Q. Chen, N. Liu, Q. Hu, J. Liu, J. Wu, Q. Cai and J. Wu, *Organic Chemistry Frontiers*, 2021, **8**, 5316-5321.
- 288 T. Zhong, J.-T. Yi, Z.-D. Chen, Q.-C. Zhuang, Y.-Z. Li, G. Lu and J. Weng, *Chemical Science*, 2021, **12**, 9359-9365.
- 289 X. Wang, Y. Kuang, S. Ye and J. Wu, *Chemical Communications*, 2019, **55**, 14962-14964.
- 290 S. P. Blum, D. Schollmeyer, M. Turks and S. R. Waldvogel, *Chemistry - A European Journal*, 2020, **26**, 8358-8362.
- 291 S. P. Blum, T. Karakaya, D. Schollmeyer, A. Klapars and S. R. Waldvogel, *Angewandte Chemie International Edition*, 2021, **60**, 5056-5062.
- 292 G. M. Locke, S. S. R. Bernhard and M. O. Senge, *Chemistry - A European Journal*, 2019, **25**, 4590-4647.

- 293 J. M. Lopchuk, K. Fjelbye, Y. Kawamata, L. R. Malins, C.-M. Pan, R. Gianatassio, J. Wang, L. Prieto, J. Bradow, T. A. Brandt, M. R. Collins, J. Elleraas, J. Ewanicki, W. Farrell, O. O. Fadeyi, G. M. Gallego, J. J. Mousseau, R. Oliver, N. W. Sach, J. K. Smith, J. E. Spangler, H. Zhu, J. Zhu and P. S. Baran, *Journal of the American Chemical Society*, 2017, **139**, 3209-3226.
- 294 P. K. Mykhailiuk, *Organic & Biomolecular Chemistry*, 2019, **17**, 2839-2849.
- 295 M. v. Westphal, B. T. Wolfstädter, J.-M. Plancher, J. Gatfield and E. M. Carreira, *ChemMedChem*, 2015, **10**, 461-469.
- 296 I. S. Makarov, C. E. Brocklehurst, K. Karaghiosoff, G. Koch and P. Knochel, *Angewandte Chemie International Edition*, 2017, **56**, 12774-12777.
- 297 M. M. D. Pramanik, H. Qian, W.-J. Xiao and J.-R. Chen, *Organic Chemistry Frontiers*, 2020, **7**, 2531-2537.
- 298 F.-S. He, S. Xie, Y. Yao and J. Wu, *Chinese Chemical Letters*, 2020, **31**, 3065-3072.
- 299 J. H. Kim, A. Ruffoni, Y. S. S. Al-Faiyz, N. S. Sheikh and D. Leonori, *Angewandte Chemie International Edition*, 2020, **59**, 8225-8231.
- 300 X. Zhang, R. T. Smith, C. Le, S. J. McCarver, B. T. Shireman, N. I. Carruthers and D. W. C. MacMillan, *Nature*, 2020, **580**, 220-226.
- 301 S. Shin, S. Lee, W. Choi, N. Kim and S. Hong, *Angewandte Chemie International Edition*, 2021, **60**, 7873-7879.